INVESTIGATING THE ROLE OF MATRIX ARCHITECTURE ON VASCULARIZATION IN MMP-SENSITIVE PEG HYDROGELS

by

Marina Vigen

**A dissertation submitted in partial fulfillment
of the requirements for the degree of
Doctor of Philosophy
(Biomedical Engineering)
in the University of Michigan
2014**

Doctoral Committee:

Associate Professor Andrew J. Putnam, Chair
Assistant Professor Ariella Shikanov
Associate Professor Jan P. Stegemann
Professor Stephen J. Weiss

Acknowledgements

I am so appreciative of the support of so many mentors, friends, colleagues, and family- without your support and patience I would not be finishing my PhD. Thank you.

To start, I am deeply grateful for the guidance and support of my advisor, Professor Andrew Putnam. Your willingness to let me forge my own path- with the occasional correction- has taught me how to approach a problem and deal with setbacks. This, more than anything, is the most important lesson this journey has imparted. Beyond our discussions of science or research, thank you for your unquestioning support of my life outside of lab.

I would also like to articulate my deep appreciation to the other members of my dissertation committee, Professors Stephen Weiss, Jan Stegemann, and Ariella Shikanov. Thank you for asking the hard questions, and for the continuing collaboration and feedback.

I also gratefully acknowledge several funding sources which facilitated my research project and educational activities. This work was partially funded under award numbers R01HL085339 and R01HL118259 from the National Heart, Lung, and Blood Institute of the National Institutes of Health. Additionally, I acknowledge the University of Michigan first year BME fellowship, GAANN fellowship, and Rackham Graduate School travel award program for support.

Next, I have such respect and gratitude for everyone in the CSET lab. Thank you for making it nice to come in to work every day. To all of the more senior lab members (Stephanie, Jake, Bita, and Yen)- thank you for listening. You gave me confidence and support when I needed it. You taught by example and were wonderfully patient. To Rahul and Ana, thank you for your contributions to our intellectual discussions.

Of course, I would be remiss to exclusively thank my colleagues in the CSET lab- an additional thank you is owed to all of my collaborators. To Ram, Joan, and the Shikanov lab, your friendship and collaboration have been a bright point in my time at Michigan.

I also must thank my friends for their support and perspective. Thank you Layla- we have been through so much and you have been steadfast, patient, supportive, and constructive. Our friendship is what first made Ann Arbor feel like home for me, and I am so grateful. To Neha and Sibu, my lab neighbors- thank you for making every day wonderful and full of laughter (and lots of decaf coffee). To Lorenzo- thank you for helping me learn to find strength. To the rest of my friends, thank you for making my experience here so happy, and for keeping life interesting.

Lastly, thank you to my parents and older brother Kyle. You taught me the importance of learning how, and not what, to think. I am grateful for the love, support, friendship, and occasional criticism.

Table of Contents

List of Figures

List of Appendices

List of Abbreviations

(in alphabetical order)

3D- three-dimensional

AdSCs- adipose-derived stem cells

ANOVA- analysis of variance

BS-1- Bandeiraea Simplicifolia I lectin

CLI- critical limb ischemia

EC – endothelial cell

ECM – extracellular matrix

EGM-2 – Endothelial Growth Medium-2

EPCs – endothelial progenitor cells

FAL- femoral artery ligation

FDA- Food and Drug Administration

H&E- hematoxylin and eosin

HMVECs – human microvascular endothelial cells

HUVECs – human umbilical vein endothelial cells

iPSCs- induced pluripotent stem cells

LDPI- laser Doppler perfusion imaging

MMP- matrix metalloprotease

MRA- Magnetic resonance angiography

MSCs- mesenchymal stem cells

NHLFs- normal human lung fibroblasts

PAD- peripheral artery disease

PBS – phosphate-buffered saline

PCL- polycaprolactone)

PEG- polyethylene glycol

PLGA- poly(lactide-co-glycolide)

PDGF- platelet-derived growth factor

RBC- red blood cell

TGF-β – transforming growth factor-beta

UEA-1- Ulex Europaeus Agglutinin I lectin

VEGF – vascular endothelial growth factor

Z-fix- Zinc-buffered formalin

Abstract

The formation of functional blood vessels in engineered or ischemic tissues remains a significant scientific and clinical hurdle. Cell delivery, scaffold design, and growth factor delivery have been investigated to support neovascularization. This thesis focuses on a hybrid approach wherein cells are seeded within a biosynthetic scaffold. Our approach is motivated by the relatively poor performance of cells alone; cell engraftment is minimal (10%) in scaffold-free approaches. Natural and synthetic materials have been utilized to improve engraftment, but the biosynthetic scaffold presented here offers unique advantages to overcome limitations of natural materials and offers tunability of matrix properties and biological response.

A PEG hydrogel platform was adapted to investigate the roles of network crosslinking density and susceptibility to proteolysis on vascularization. Four-arm PEG vinyl sulfone (PEGVS) was polymerized by Michael-type addition with reactive cysteine groups on a slowly degraded matrix metalloprotease (MMP) susceptible peptide, GPQG↓IWGQ, or a peptide that is cleaved more rapidly, VPMS↓MRGG. Vascular networks formed *in vitro* from encapsulated endothelial cells and supportive stromal fibroblasts. Morphogenesis was robust to changes in cross-linking peptide identity, but significantly attenuated in more crosslinked gels. All gel types supported the *de novo* formation of perfused vasculature from transplanted cells in subcutaneous implants *in*

vivo; however, unlike the *in vitro* findings, vascularization was not decreased in the more cross-linked gels.

A mouse model of hindlimb ischemia was used to further assess the ability of PEG hydrogels to support revascularization in a model relevant for clinical translation. Cell-laden PEG hydrogel precursors and fibrin controls were delivered to SCID mice after femoral artery ligation. PEG hydrogels supported the formation of perfused vasculature irrespective of crosslinking-peptide identity. Hydrogel delivery improved reperfusion to the ischemic limb. Substantial loss of gel mechanical integrity and vessel regression were evident in fibrin gels, but not in PEG gels, 2 weeks post-implantation, suggesting PEG hydrogels are superior to fibrin with regards to vessel persistence. In sum, these findings demonstrate that structurally stable biomimetic PEG-based hydrogels direct vascularization in ischemic tissues via cell transplantation and hold promise in tissue regeneration and therapeutic angiogenesis.

Chapter 1

Introduction

1.1 Therapeutic Angiogenesis for Cardiovascular Disease

Cardiovascular disease (CVD) is the leading cause of mortality in the United States and globally, accounting for 25 and 30% of all deaths, respectively [1, 2]. Currently, approximately 1 in 3 Americans suffer from some form of CVD [3]. Additionally, in the US, the costs associated with CVD surpassed $300 billion in 2010 [4], and they are forecasted to double to over $600 billion by 2015 [4]. Despite improvements in therapeutic interventions for CVD patients, there is a persistent need for novel cardiovascular therapies and approaches to minimize costly interventions.

Atherosclerosis, the deposition of cholesterol and fibrous tissue into plaques on the interior of blood vessel walls, is a hallmark of chronic cardiovascular diseases such as coronary heart disease (CHD) and peripheral artery disease (PAD) [5, 6] (Figure 1-1B). In these conditions, chronic vascular insufficiency results in tissue ischemia and causes substantial mortality and morbidity in the form of tissue loss and diminished quality of life. In the 15.4 million Americans with CHD [4], atherosclerotic plaques develop in the coronary arteries, lead to vessel clogging, and often rupture, initiating

acute cardiovascular events. PAD is etiologically similar to CHD, but atherosclerosis and resulting complications occur in the extremities. PAD spans a spectrum in severity [7]. Some patients only suffer intermittent claudication, i.e. pain upon exertion, while others experience rest pain and tissue loss [8]. The latter patients are grouped into a separate condition, termed critical limb ischemia (CLI) based on the advanced disease stage. As of 2010, over 1 million Americans suffered from CLI [9], and 10-12 million suffered from PAD [7, 10] with the potential to progress to CLI. Current interventions for early-stage patients include lifestyle modification or pharmaceuticals [11]. These approaches are plagued by poor patient compliance and often do not adequately address disease etiology. Additionally, once PAD has progressed to CLI, lifestyle interventions are often insufficient to restore function to the ischemic tissue and endovascular approaches and

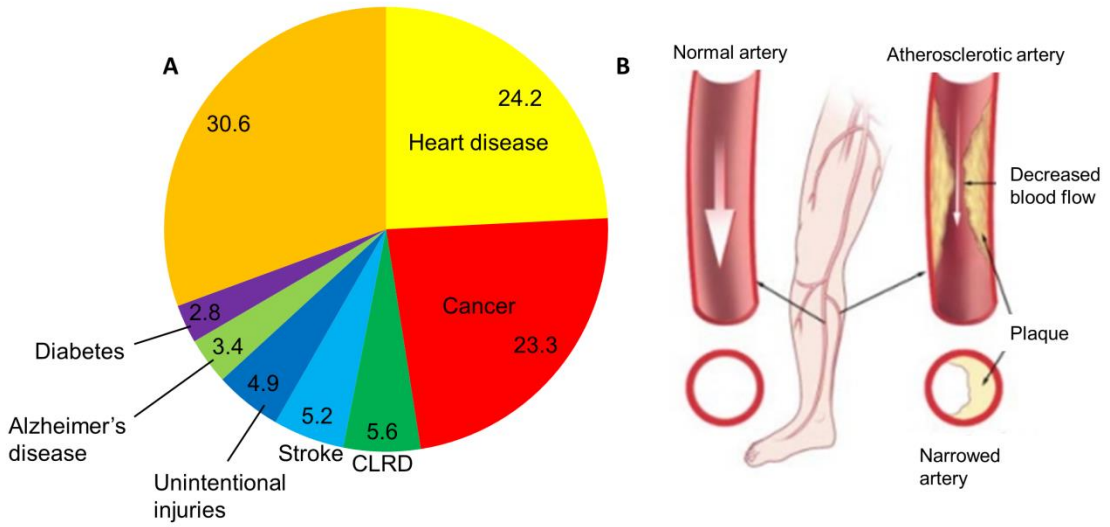

Figure 1-1. Cardiovascular disease in the United States.. Leading U.S. causes of death, 2010. Data from the National Vital Statistics System, CDC. B. Deposition of atherosclerotic plaques in peripheral vasculature leads to PAD and CLI. Adapted with permission [1].

invasive surgery are the standards of care [8]. However, surgical approaches suffer from limitations: certain patients are not candidates for these procedures, due to co-

morbidities [8, 11-13] and these procedures only improve perfusion through specific, major vessels. Within one year of diagnosis, 30 percent of CLI patients require limb amputation [14].

As such, substantial research has focused on the development of angiogenic therapies to treat the underlying ischemia. Gene or trophic factor delivery has been demonstrated to aid in re-perfusion in phase I and II trials [15], however these approaches do not fully recapitulate the complex milieu of soluble effectors secreted by cells. An alternate approach, which has not been as thoroughly vetted in the clinic, is to re-vascularize ischemic tissue via the delivery of vascular progenitor cells [16]. This approach has been somewhat successful; however, unresolved hurdles, cell source and cell survival post-implantation, for example, limit their adoption clinically.

1.2 Tissue Engineering and Current Limitations

End-stage organ failure is a notable cause of death in the United States, and organ transplantation is the current standard of care for these patients. Donated organs are sourced from living or deceased donors in accordance with stringent ethical and medical guidelines. There is a consistent and growing gap between the number of patients waiting for organs and those available. In 1991, 68% of patients on the waiting list received organs [17]. As of 2013, this number dropped to 24% of patients on the waiting list [17], highlighting the critical need for alternate approaches to generate functional replacement tissues. Additionally, data suggests time spent on the waiting list can adversely affect clinical outcomes. For example, the graft survival rate following

kidney transplantation is significantly attenuated in patients who spent longer on the organ waiting list [18].

Tissue engineering holds the potential to alleviate the organ gap through the development of hybrid biological substitutes that restore, maintain, or enhance tissue function [19]. Engineered tissues may be fabricated from autologous cells, mitigating the need for the suppression immunotherapies required following transplantation of donated organs. Nonetheless, in the 25 years since the field emerged, relatively few engineered tissues have reached the clinic. Vascularization is a key limiting challenge. Most cells in the body reside within 100-200 μm of a blood vessel [20]; at this distance diffusion is effective in delivering nutrients and oxygen to the tissue. Thus, extensive blood vessel networks are required for the creation of thick, metabolically active organs such as the heart, liver, or kidneys [21]. Current tissue engineering successes are confined to thin or avascular tissues [20]. Several approaches to vascularized engineered tissues have been utilized, and there is substantial overlap with the cell-based approaches utilized for therapeutic vascularization.

1.3 Vascularization in Development and Adult Physiology

The vascular system consists of an interconnected network of arteries, capillaries, and veins which sustain tissue viability via the delivery of oxygen and nutrients. The structure of these vessels corresponds to their function. Each class of vessel consists of an endothelial cell layer subtended by supportive periendothelial layers of varying complexity [22]. Capillaries are the most numerous [23] and are comprised of an endothelial cell layer circumscribed by supportive pericytes embedded

in a type IV collagen and laminin-rich basement membrane. The wall structure and relatively large surface area facilitate oxygen and nutrient transport to surrounding tissue [24]. Arteries have a more complex wall structure, with three specialized layers: the intima, media and adventitia, each separated by elastic lamina [23]. The smooth muscle cell-rich media and elastic lamina enable arteries to withstand high pressures and facilitate the transport of blood to smaller arterioles and capillaries [23, 25]. Veins consist of the same basic layers as arteries, but are thinner and less muscular. Here, again, function follows from structure: veins are exposed to lower pressures than arteries [25], and thus require less muscular subendothelial layers. The formation of a complex, highly specialized vascular network of arteries, capillaries, and veins is primarily controlled by developmental programs. Nonetheless, vascularization is additionally relevant in physiological and pathological processes in the adult organism.

Vascularization is highly regulated in adult organisms. To wit, disturbance of the complex equilibrium can trigger pathologies associated with either excessive vascularization, including cancer, inflammatory disorders, and several diseases of the eye [26]. By contrast, inadequate vascularization is seen in patients with ischemic diseases such as PAD and CHD. To understand these pathologies, it is critical to consider the mechanisms via which blood vessels form. Vascularization occurs through vasculogenesis, angiogenesis, or arteriogenesis [11, 26-28]. Vasculogenesis is typically considered to occur primarily in embryonic development, and refers to the organization of endothelial and hematopoietic progenitor cells into a primitive vascular plexus [11, 26, 28]. In contrast, in the adult, blood vessel growth occurs via either angiogenesis or arteriogenesis [26, 28]. In this work, I primarily focus on the latter two,

as my approach aims to address adult pathologies characterized by insufficient vascularization.

Angiogenesis is the sprouting of new vessels from pre-existing vasculature, and is evident both in development and the adult organism. In the adult, angiogenesis occurs during inflammation or wound healing and within tumors. This highly complex process is regulated by a series of spatially and temporally-defined stimuli which include soluble growth factors and cytokines [11, 25, 26, 29], signals presented by the extracellular matrix (ECM) [25, 30, 31], and interactions between endothelial and stromal or immune cells [29]. Prototypical sprouting angiogenesis *in vivo* is initiated with the release of numerous soluble pro-angiogenic signals, including factors such as VEGF, VEGF-C, ANG-2, FGFs, and others [11, 26], by inflammatory or tumor cells and in response to hypoxia. Pericytes then detach from the basement membrane, a specialized extracellular matrix rich in type IV collagen that subtends endothelial cells. Endothelial cell migration through the basement membrane and type I collagen-containing interstitial matrix is facilitated by a class of proteolytic enzymes termed matrix metalloproteases (MMPs) [32]. These migrating endothelial cells differentiate into tip and stalk cells, with respective roles to guide the direction of sprouting and to proliferate [11, 32] to form tubules. These tubules undergo maturation, a process encompassing lumen formation, basement membrane deposition, and pericytic stabilization [25, 32]. Numerous factors, including PDGF, TGF-β, and SDF-1α, are involved in pericyte recruitment and vessel stabilization.

Controlled proteolysis is critical through this entire process. Matrix degradation is required for migration and tubulogenesis (particularly, MT1-MMP is integral to this

process [33-35]), but excessive proteolysis leaves insufficient ECM to mechanically support the growing vasculature [36]. In addition to the role of proteases in degrading the basement membrane and interstitial matrix, they are critical to the release of growth factors sequestered within the ECM [25, 30, 31].

Arteriogenesis is a distinct process, and comprises the remodeling of pre-existing arterioles into large diameter arteries in response to increased blood flow [28, 37, 38]. In contrast to angiogenesis, ischemia and hypoxia are not driving forces in arteriogenesis. For instance, in animal models of femoral artery ligation (FAL), ischemia is evident in the lower leg and foot, yet collateralization is only evident in the upper leg muscles, which are not ischemic [37]. Instead, collateral vessel growth primarily occurs within normoxic tissues [37].

In the presence of arterial occlusion or stenosis, small arterioles that connect side branches proximal and distal to the area of reduced flow experience increased blood flow [39, 40]. Fluid shear stress (FSS) and circumferential wall stress (CWS) are increased in these arterioles [39]. In response to the changing shear stress, the endothelium is activated to produce cytokines, and recruits monocytes that release a milieu of additional cytokines, growth factors, and proteases [37, 39]. Other inflammatory cells- mast cells and T cells- also secrete pro-arteriogenic compounds [39]. SMCs are recruited to the remodeling arteriole and deposit new elastic lamina and rebuild the media and intima [39]. Tortuousity and a hallmark “corkscrew” appearance are characteristic of collateral vessels remodeled via arteriogenesis [39, 41].

As of yet, this section discusses angiogenesis and arteriogenesis as distinct, compensatory mechanisms for ameliorating ischemic disease. Recent studies,

however, suggest a more nuanced interplay exists between changes in flow to the distal capillary bed and in proximal arteries in an ischemic limb [38, 41, 42]. Reduced peripheral resistance may accompany angiogenesis in ischemic tissue, and thus potentiate blood flow through upstream collateral vessels. As outlined above, increased flow through collateral arterioles is a key trigger for arteriogenesis and mediates changes in FSS and CWS [39]. Thus, changes in the distal capillary bed can modulate more substantive increases in flow proximal to ischemic tissue. Based on these results, and on the importance of angiogenesis in comorbidities (e.g. diabetic ulcers) seen in patients, approaches to stimulate both angiogenesis and arteriogenesis should be considered relevant in the development of vascularization therapies.

1.4 Approaches to Engineer Blood Vessels

Several methods have been utilized to engineer vasculature for tissue engineering and therapeutic vascularization (Figure 1-2). Generally, methods fall into two categories: those wherein vasculature is formed *ex vivo* and then implanted, and those that facilitate vascularization *in vivo*. Both approaches aim to support rapid vascularization, which is critical to minimize necrosis at the interior of grafted tissues and to the restoration of function to ischemic host tissue. To date, cell delivery, scaffold design, growth factor delivery, and directed 3D fabrication have been used to facilitate vascularization.

Cell encapsulation in a scaffold, or delivery directly to a tissue of interest *in vivo,* results in the creation of vasculature that can restore flow to sites of ischemia and

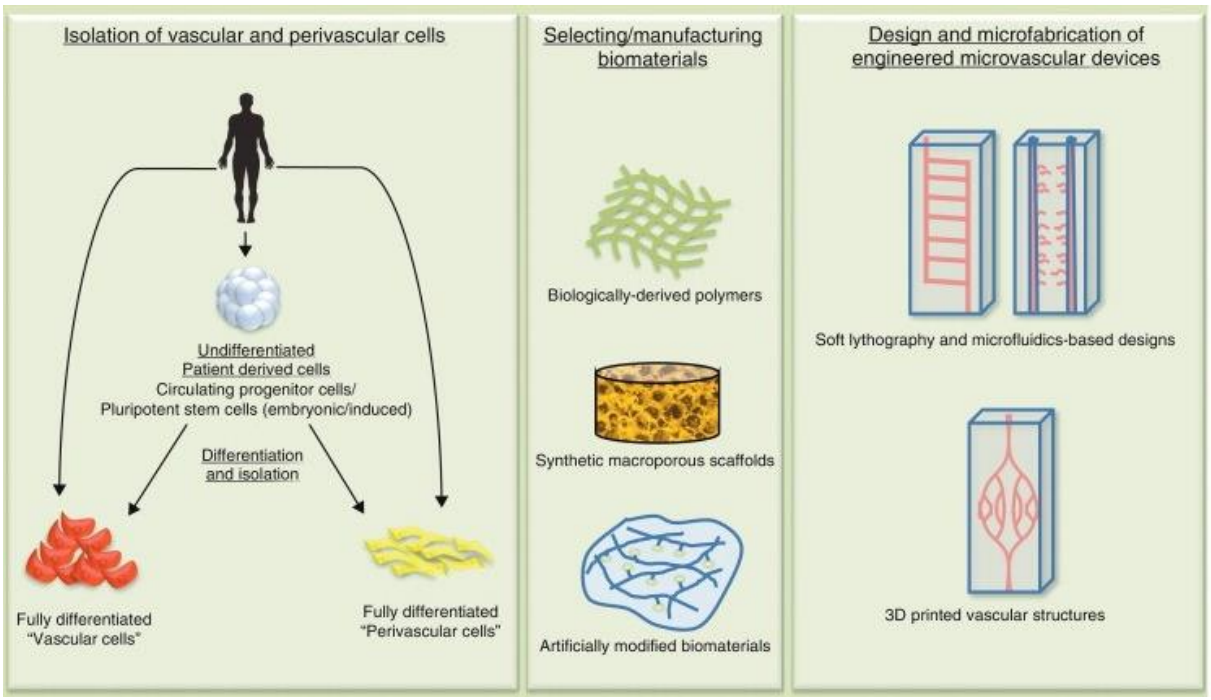

Figure1-2. Approaches to engineer vasculature. Three major avenues involve the isolation of relevant vascular and support cells, the design of scaffold materials, and, finally, various microfabrication approaches which allow for superior spatial control in 3D. Reproduced with permission [43].

sustain engineered tissue. A variety of cell types have been demonstrated to support vascularization, including cells that can differentiate into blood vessels as well as cells that recruit host vasculature *in vivo*. Endothelial cells from a variety of origins organize into vessel networks *in vitro* [44-47] and *in vivo* [48-53]. EC types used in these studies include human umbilical vein endothelial cells (HUVECs) [44, 47, 50, 52, 54-57], human microvascular endothelial cells (HMVECs) [46, 49, 53], endothelial progenitor cells (EPCs) [58-65], and ECs derived from induced pluripotent stem cells (iPSCs) [48, 51, 66]. Despite the widespread use of a variety of ECs for these studies, debate remains regarding the clinical relevance of various EC sources. In addition to cells that can directly organize into vasculature- i.e. ECs- pericyte-like support cells are critical to the formation of robust vascular networks. These cells are recruited to vasculature formed *in vivo*, and additionally may be seeded into engineered tissues [57, 67] or delivered to

ischemic tissue to enhance vascularization [51, 68, 69]. Various studies have investigated mesenchymal stem cells (MSCs) [64, 69-71], adipose-derived stem cells (ASCs) [72], and embryonic [47, 56, 57, 67, 73, 74] and adult [75] fibroblasts to potentiate vascularization. An in depth discussion of the role of various endothelial and support cells in vascularization can be found in chapter 2.

Substantial research has focused on the development of materials that support vascularization. Primarily, these efforts are motivated by the poor cell retention upon engraftment; >90% die rapidly when transplanted without a material carrier [11]. Studies from our lab and others have illustrated the efficacy of natural materials such as fibrin [70, 75-79], collagen [65, 79], and Matrigel [80] in facilitating vascularization. Additionally, composite matrices of fibrin and collagen have been demonstrated to support vascular network formation [71, 81]. Nonetheless, concerns remain regarding the purity, variability, and poorly defined composition of natural materials [82], which prompt efforts to develop pro-angiogenic synthetic materials. Ostensibly, these materials allow more careful tuning of matrix-presented cues in order to facilitate robust vascularization. Scaffolds based on poly(ethylene glycol) (PEG) [83-90], poly(D,L-lactide) (PLA) [91], poly(caprolactone) (PCL) [92], and alginate [93, 94] have been investigated as materials to facilitate vascularization from ECs *in vitro* and *in vivo.* Several variants of PEG-based systems support vascularization. Here, we focus on peptide-functionalized PEG hydrogels. In these systems, PEG is functionalized with an integrin-binding adhesive domain as well as with peptide sequences susceptible to cleavage by cell-derived MMPs or plasmin. Cell invasion and vascularization *in vitro* are substantially improved in protease-degradable gels as compared to controls [85,

86]. Additionally, variants of these gels support the recruitment of host vasculature upon implantation with growth factors *in vivo* [85, 87, 95-98].

Growth factor delivery has also been explored as an approach to engineer vasculature for tissue engineering and therapeutic angiogenesis. Several growth factors implicated in vascularization have been investigated for therapeutic vascularization, including VEGF-A, FGF-2, HGF, MCP-1, GM-CSF, PDGF-BB, and TGF-β [38]. Early pre-clinical studies of growth factors alone showed great promise to induce vascularization [38]. Based on these results, clinical trials were conducted. Despite promising results from initial, uncontrolled trials, the efficacy of growth factor delivery was not corroborated in the subsequent double-blind, randomized, controlled trials [99]. High rates of adverse events were documented for these trials, but these were comparable to those experienced in the baseline patient population [15], and thus, unlikely to result from the therapy itself. Although clinical trial results were underwhelming, substantial interest remains in developing more physiologically relevant approaches to use growth factors to induce vascularization. To date, growth factor therapies have utilized systemic delivery of a single factor or gene, which may limit efficacy [28]. Due to the complexity of spatial and temporal signals involved in mediating vascularization in vivo, recent research has re-focused on strategies to deliver factors locally, and with increased control. As suggested by several studies highlighted above, one approach to facilitate this is combination therapies of growth factor delivery with cell delivery [16] and materials-based approaches to vascularization. The kinetics of delivery and spatial presentation of growth factors can be tuned with appropriate scaffolds [53]. In PEG based hydrogels for instance, growth factor delivery

facilitates the recruitment of host vasculature following implantation in vivo [86, 95, 98, 100-102].

Finally, microfluidic approaches and other strategies allowing greater 3D control have been used to create organized vascular networks in pre-determined geometries. Microfluidics have been used to create spatially and temporally defined growth factor gradients[45, 46, 55], and have been used with natural and synthetic materials to create complex geometries for vascular applications [47, 73, 103]. The use of 3D printing [56] and modular microtissues [50] also show promise for the generation of vascular networks.

Overall, substantial progress has been made in the past decades in engineering vasculature for applications in therapeutic angiogenesis and tissue regeneration. Nonetheless, the dearth of commercial products in this area emphasizes the continued need for optimized systems to allow for the facile creation of robust engineered vessels. This thesis presents a hybrid system, inspired by several approaches described above, wherein cells are delivered in a bioengineered hydrogel to facilitate vascularization.

1.5 Hypothesis

We hypothesize that tailoring of the mechanical properties and degradation of a synthetic extracellular matrix mimetic will result in differing extents of vascularization. This hypothesis will be tested using a well-established *in vitro* model of vasculogenesis, and two *in vivo* models of vascularization.

1.6 Specific Aims

Aim 1: Construct and characterize PEG-based hydrogels with tailored proteolytic susceptibility and adhesive ligand density, and demonstrate their ability to support the adhesion, viability, and spreading of both endothelial cells (ECs) and normal human lung fibroblasts (NHLFs) in 3D. Our hypothesis is that synthetic PEG hydrogels presenting a cell-adhesive peptide and with tailored mechanical properties will support the viability and spreading of encapsulated endothelial cells and fibroblasts.

Aim 2: Using an established 3D *in vitro* model system, assess the ability of the PEG-based gels synthesized in aim 1 to support vasculogenesis from ECs and NHLFs. We hypothesize that the extent to which PEG-based hydrogels support vasculogenesis will depend on the proteolytic susceptibility of the hydrogels and on their mechanical properties.

Aim 3: Compare the neovascular response of PEG-based constructs containing ECs and NHLFs to that obtained with fibrin following implantation in a dorsal, subcutaneous location as well as intramuscularly in an ischemic hindlimb. We hypothesize that vascular organization will be evident in PEG gels implanted both subcutaneously and in an ischemic limb. Additionally, we anticipate the extent of vascularization of PEG hydrogels implanted in the model of hindlimb ischemia will be attenuated as compared to the fibrin gels.

1.7 Translational Potential

As mentioned previously, PAD and CLI result in morbidities of varying severity- from pain to tissue or limb loss- in approximately 10-12 million Americans [7]. Additionally, these patients often suffer comorbidities that complicate treatment of the primary cardiovascular disease. Specifically, PAD and CLI patients often also suffer from diabetes, and are at high risk for foot ulcers and gangrene, which further increase the risk of limb amputation [104-106].

The current standards of care- lifestyle interventions, pharmaceuticals, or surgery- are not effective in a subset of patients with advanced disease [8, 11]. This motivates the growth of therapeutic vascularization in pre-clinical and clinical research. Despite promising pre-clinical and early clinical results, many of the approaches to deliver genes or trophic factors to aid in reperfusion of ischemic tissue have not resulted in the restoration of function anticipated [99]. Less research, however, has investigated the delivery of cells for this purpose. Several larger clinical trials are currently in progress to assess the efficacy of cell-delivery approaches [8, 107]. Despite the qualified success of these approaches in pre-clinical and early clinical studies, questions of cell source and survival post-implantation remain.

To address these questions, we suggest the development of well-defined materials to enhance vascularization *in vivo* is of substantial clinical value. Scaffolds may act to stimulate vascularization by both increasing cell survival, as well as via the presentation of pro-angiogenic signals that can be intentionally tethered in the matrix. The material we utilized- a PEG-based hydrogel- presents a minimum of biological signals to create a well-defined scaffold that may be used to induce vascularization in several *in vitro* and *in vivo* models of vascularization. For distinct applications, the

scaffold presents the additional advantage of supporting chemical conjugation of other bioactive molecules. This research project studies the role of hydrogel material properties and degradation, with the aim of moving towards an engineered scaffold which facilitates cell survival and organization into vasculature upon implantation into ischemic tissue. These studies are of value for applications in therapeutic vascularization for CLI, PAD, and CHD, as well as for parenchymal tissue engineering.

1.8 Overview

In this chapter, we have discussed the motivation for the project, as well as given a high-level overview of the current understanding of vascularization in physiology. Chapter 2 gives an in-depth review of the role of stromal or mesenchymal support cells in the creation of engineered vasculature *in vitro* and *in vivo*. As briefly highlighted in this chapter, cell identity is critical in understanding the interplay between ECs and pericytes, as well as in translating research to clinically viable therapies for tissue engineering and ischemic disease. Next, Chapter 3 presents the PEG hydrogel system utilized in this work, assessment of the system's ability to support EC tubulogenesis *in vitro* and in a subcutaneous implant *in vivo*. This Chapter wraps up specific aims 1 and 2. In Chapter 4, the formation of vasculature in PEG hydrogels is investigated in a physiologically relevant model of hindlimb ischemia. This chapter examines a translational application of interest, and compares the PEG hydrogels to a well-established natural material with respect to support of re-vascularization of the ischemic tissue. Finally, the key findings of the thesis and translational implications are

summarized in Chapter 5. Experimental procedures and data investigating the role of fibronectin on vascularization in PEG hydrogels can be found in the appendices.

1.9 References

[1] CDC/NCHS, National Vital Statistics System.
[2] Cardiovascular diseases (CVDs). In: Organization WH, editor. Media centre. Geneva: World Health Organization; 2013.
[3] Heart Disease and Stroke Prevention, Addressing the Nation's Leading Killers: At a Glance 2011. In: Promotion NCfCDPaH, editor. Atlanta, GA: Centers for Disease Control and Prevention; 2011.
[4] Go AS, Mozaffarian D, Roger VL, Benjamin EJ, Berry JD, Blaha MJ, et al. Heart disease and stroke statistics--2014 update: a report from the American Heart Association. Circulation. 2014;129:e28-e292.
[5] Dzau VJ, Antman EM, Black HR, Hayes DL, Manson JE, Plutzky J, et al. The cardiovascular disease continuum validated: clinical evidence of improved patient outcomes: part I: Pathophysiology and clinical trial evidence (risk factors through stable coronary artery disease). Circulation. 2006;114:2850-70.
[6] US National Library of Medicine NIoH. Coronary Heart Disease. 2010.
[7] Facts about Peripheral Artery Disease (P.A.D.). In: Services USDoHaH, editor.2006.
[8] Lawall H, Bramlage P, Amann B. Treatment of peripheral arterial disease using stem and progenitor cell therapy. Journal of vascular surgery. 2011;53:445-53.
[9] Egorova NN, Guillerme S, Gelijns A, Morrissey N, Dayal R, McKinsey JF, et al. An analysis of the outcomes of a decade of experience with lower extremity revascularization including limb salvage, lengths of stay, and safety. Journal of vascular surgery. 2010;51:878-85, 85 e1.
[10] Selvin E, Erlinger T. Prevalence of and risk factors for peripheral artery disease in the United States. Circulation. 2004;110:738-4.
[11] Deveza L, Choi J, Yang F. Therapeutic angiogenesis for treating cardiovascular diseases. Theranostics. 2012;2:801-14.
[12] Brenes RA, Jadlowiec CC, Bear M, Hashim P, Protack CD, Li X, et al. Toward a mouse model of hind limb ischemia to test therapeutic angiogenesis. Journal of vascular surgery. 2012;56:1669-79; discussion 79.
[13] Lotfi S, Patel AS, Mattock K, Egginton S, Smith A, Modarai B. Towards a more relevant hind limb model of muscle ischaemia. Atherosclerosis. 2013;227:1-8.
[14] Feiring AJ, Krahn M, Nelson L, Wesolowski A, Eastwood D, Szabo A. Preventing leg amputations in critical limb ischemia with below-the-knee drug-eluting stents: the PaRADISE (PReventing Amputations using Drug eluting StEnts) trial. Journal of the American College of Cardiology. 2010;55:1580-9.
[15] Tongers J, Roncalli JG, Losordo DW. Therapeutic angiogenesis for critical limb ischemia: microvascular therapies coming of age. Circulation. 2008;118:9-16.
[16] Losordo DW, Dimmeler S. Therapeutic angiogenesis and vasculogenesis for ischemic disease: part II: cell-based therapies. Circulation. 2004;109:2692-7.

[17] United States Organ Transplantation, OPTN & SRTR 2011 Annnual Data Report. In: Services USDoHaH, editor.2012.
[18] Meier-Kriesche H, Kaplan B. Waiting Time on Dialysis as the Strongest Modifiable Risk Factor for Renal Transplant Outcomes. Transplantation. 2002;74:1377-81.
[19] Hubbell JA. Biomaterials in Tissue Engineering. Nature biotechnology. 1995;13:565-76.
[20] Jain RK, Au P, Tam J, Duda DG, Fukumura D. Engineering vascularized tissue. Nature biotechnology. 2005;23:821-3.
[21] L'Heureux N, Dusserre N, Konig G, Victor B, Keire P, Wight TN, et al. Human tissue-engineered blood vessels for adult arterial revascularization. Nat Med. 2006;12:361-5.
[22] L'Heureux N, Germain L, Labbé R, Auger FA. In vitro construction of a human blood vessel from cultured vascular cells: A morphologic study. Journal of vascular surgery. 1993;17:499-509.
[23] Jain RK. Molecular regulation of vessel maturation. Nature Medicine. 2003;9:685-93.
[24] Aird WC. Phenotypic heterogeneity of the endothelium: II. Representative vascular beds. Circ Res. 2007;100:174-90.
[25] Potente M, Gerhardt H, Carmeliet P. Basic and therapeutic aspects of angiogenesis. Cell. 2011;146:873-87.
[26] Carmeliet P, Jain RK. Molecular mechanisms and clinical applications of angiogenesis. Nature. 2011;473:298-307.
[27] Lloyd PG, Yang HT, Terjung RL. Arteriogenesis and angiogenesis in rat ischemic hindlimb: role of nitric oxide. American journal of physiology Heart and circulatory physiology. 2001;281:H2528-H38.
[28] Semenza GL. Vasculogenesis, angiogenesis, and arteriogenesis: mechanisms of blood vessel formation and remodeling. Journal of cellular biochemistry. 2007;102:840-7.
[29] Davis GE, Kim DJ, Meng CX, Norden PR, Speichinger KR, Davis MT, et al. Control of vascular tube morphogenesis and maturation in 3D extracellular matrices by endothelial cells and pericytes. Methods in molecular biology. 2013;1066:17-28.
[30] Barker TH. The role of ECM proteins and protein fragments in guiding cell behavior in regenerative medicine. Biomaterials. 2011;32:4211-4.
[31] Chen TT, Luque A, Lee S, Anderson SM, Segura T, Iruela-Arispe ML. Anchorage of VEGF to the extracellular matrix conveys differential signaling responses to endothelial cells. The Journal of cell biology. 2010;188:595-609.
[32] Ghajar CM, George SC, Putnam AJ. Matrix Metalloproteinase Control of Capillary Morphogenesis. Crit Rev Eukaryot Gene Expr. 2008;18:251-78.
[33] Kachgal S, Carrion B, Janson IA, Putnam AJ. Bone marrow stromal cells stimulate an angiogenic program that requires endothelial MT1-MMP. Journal of cellular physiology. 2012.
[34] Chun TH, Sabeh F, Ota I, Murphy H, McDonagh KT, Holmbeck K, et al. MT1-MMP-dependent neovessel formation within the confines of the three-dimensional extracellular matrix. The Journal of cell biology. 2004;167:757-67.
[35] Hiraoka N, Allen E, Apel IJ, Gyetko MR, Weiss SJ. Matrix metalloproteinases regulate neovascularization by acting as pericellular fibrinolysins. Cell. 1998;95:365-77.

[36] Blasi F, Carmeliet P. uPAR: a versatile signalling orchestrator. Nature reviews Molecular cell biology. 2002;3:932-43.
[37] Scholz D, Cai W, Schaper W. Arteriogenesis, a new concept of vascular adaptation in occlusive disease. 4. 2001.
[38] Cao Y, Hong A, Schulten H, Post MJ. Update on therapeutic neovascularization. Cardiovasc Res. 2005;65:639-48.
[39] Schaper W, Scholz D. Factors regulating arteriogenesis. Arterioscler Thromb Vasc Biol. 2003;23:1143-51.
[40] Madeddu P, Emanueli C, Spillmann F, Meloni M, Bouby N, Richer C, et al. Murine models of myocardial and limb ischemia: diagnostic end-points and relevance to clinical problems. Vascular pharmacology. 2006;45:281-301.
[41] Greve JM, Chico TJ, Goldman H, Bunting S, Peale FV, Jr., Daugherty A, et al. Magnetic resonance angiography reveals therapeutic enlargement of collateral vessels induced by VEGF in a murine model of peripheral arterial disease. Journal of magnetic resonance imaging : JMRI. 2006;24:1124-32.
[42] Lindner V, Macaig T. The Putative Convergent and Divergent Natures of Angiogenesis and Arteriogenesis. Circulation Research. 2001;89:747-9.
[43] Blinder YJ, Mooney DJ, Levenberg S. Engineering approaches for inducing blood vessel formation. Current Opinion in Chemical Engineering. 2014;3:56-61.
[44] Sasagawa T, Shimizu T, Sekiya S, Haraguchi Y, Yamato M, Sawa Y, et al. Design of prevascularized three-dimensional cell-dense tissues using a cell sheet stacking manipulation technology. Biomaterials. 2010;31:1646-54.
[45] Farahat WA, Wood LB, Zervantonakis IK, Schor A, Ong S, Neal D, et al. Ensemble analysis of angiogenic growth in three-dimensional microfluidic cell cultures. PloS one. 2012;7:e37333.
[46] Chung S, Sudo R, Zervantonakis IK, Rimchala T, Kamm RD. Surface-treatment-induced three-dimensional capillary morphogenesis in a microfluidic platform. Advanced materials. 2009;21:4863-7.
[47] Cuchiara MP, Gould DJ, McHale MK, Dickinson ME, West JL. Integration of Self-Assembled Microvascular Networks with Microfabricated PEG-Based Hydrogels. Advanced functional materials. 2012;22:4511-8.
[48] Samuel R, Daheron L, Liao S, Vardam T, Kamoun WS, Batista A, et al. Generation of functionally competent and durable engineered blood vessels from human induced pluripotent stem cells. Proceedings of the National Academy of Sciences of the United States of America. 2013;110:12774-9.
[49] Gibot L, Galbraith T, Huot J, Auger FA. A preexisting microvascular network benefits in vivo revascularization of a microvascularized tissue-engineered skin substitute. Tissue engineering Part A. 2010;16:3199-206.
[50] Gupta R, Van Rooijen N, Sefton MV. Fate of Endothelialized Modular Constructs Implanted in an Omental Pouch in Nude Rats. Tissue engineering Part A. 2009;15:2875-87.
[51] Rufaihah AJ, Huang NF, Jame S, Lee JC, Nguyen HN, Byers B, et al. Endothelial cells derived from human iPSCS increase capillary density and improve perfusion in a mouse model of peripheral arterial disease. Arterioscler Thromb Vasc Biol. 2011;31:e72-9.

[52] Baranski JD, Chaturvedi RR, Stevens KR, Eyckmans J, Carvalho B, Solorzano RD, et al. Geometric control of vascular networks to enhance engineered tissue integration and function. Proceedings of the National Academy of Sciences of the United States of America. 2013;110:7586-91.
[53] Chen RR, Silva EA, Yuen WW, Brock AA, Fischbach C, Lin AS, et al. Integrated approach to designing growth factor delivery systems. FASEB journal : official publication of the Federation of American Societies for Experimental Biology. 2007;21:3896-903.
[54] Moon JJ, Hahn MS, Kim I, Nsiah BA, West JL. Micropatterning of Poly(Ethylene Glycol) Diacrylate Hydrogels with Biomolecules to Regulate and Guide Endothelial Morphogenesis. Tissue engineering Part A. 2009;15:579-85.
[55] Baker BM, Trappmann B, Stapleton SC, Toro E, Chen CS. Microfluidics embedded within extracellular matrix to define vascular architectures and pattern diffusive gradients. Lab Chip. 2013;13:3246-52.
[56] Miller JS, Stevens KR, Yang MT, Baker BM, Nguyen Duc T, Cohen DM, et al. Rapid casting of patterned vascular networks for perfusable engineered three-dimensional tissues. Nat Mat. 2012;11:768-74.
[57] Lesman A, Habib M, Caspi O, Gepstein A, Arbel G, Levenberg S, et al. Transplantation of a Tissue-Engineered Human Vascularized Cardiac Muscle. Tissue engineering Part A. 2010;16:115-25.
[58] Rafii S, Lyden D. Therapeutic stem and progenitor cell transplantation for organ vascularization and regeneration. Nature Medicine. 2003;9:702-12.
[59] Asahara T, Murohara T, Sullivan A, Silver M, van der Zee R, Li T, et al. Isolation of Putative Progenitor Endothelial Cells for Angiogenesis. Science. 1997;275:964-7.
[60] Asahara T, Masuda H, Takahashi T, Kalka C, Pastore C, Silver M, et al. Bone Marrow Origin of Endothelial Progenitor Cells Responsible for Postnatal Vasculogenesis in Physiological and Pathological Neovascularization. Circulation Research. 1999;85:221-8.
[61] Suuronen EJ, Veinot JP, Wong S, Kapila V, Price J, Griffith M, et al. Tissue-engineered injectable collagen-based matrices for improved cell delivery and vascularization of ischemic tissue using CD133+ progenitors expanded from the peripheral blood. Circulation. 2006;114:I138-44.
[62] Kalka C, Masuda H, Takahashi T, Kalka-Moll WM, Silver M, Kearney M, et al. Transplantation of ex vivo expanded endothelial progenitor cells for therapeutic neovascularization. Proceedings of the National Academy of Sciences of the United States of America. 2000;97:3422-7.
[63] Takahashi T, Kalka C, Masuda H, Chen D, Silver M, Kearney M, et al. Ischemia- and cytokine-induced mobilization of bone marrow-derived endothelial progenitor cells for neovascularization. Nat Med. 1999;5:434-8.
[64] Au P, Tam J, Fukumura D, Jain RK. Bone marrow-derived mesenchymal stem cells facilitate engineering of long-lasting functional vasculature. Blood. 2008;111:4551-8.
[65] Critser PJ, Kreger ST, Voytik-Harbin SL, Yoder MC. Collagen matrix physical properties modulate endothelial colony forming cell-derived vessels in vivo. Microvascular research. 2010;80:23-30.
[66] Margariti A, Winkler B, Karamariti E, Zampetaki A, Tsai TN, Baban D, et al. Direct reprogramming of fibroblasts into endothelial cells capable of angiogenesis and

reendothelialization in tissue-engineered vessels. Proceedings of the National Academy of Sciences of the United States of America. 2012;109:13793-8.
[67] Levenberg S, Rouwkema J, Macdonald M, Garfein ES, Kohane DS, Darland DC, et al. Engineering vascularized skeletal muscle tissue. Nature biotechnology. 2005;23:879-84.
[68] Planat-Benard V, Silvestre JS, Cousin B, Andre M, Nibbelink M, Tamarat R, et al. Plasticity of human adipose lineage cells toward endothelial cells: physiological and therapeutic perspectives. Circulation. 2004;109:656-63.
[69] Kinnaird T, Stabile E, Burnett MS, Lee CW, Barr S, Fuchs S, et al. Marrow-derived stromal cells express genes encoding a broad spectrum of arteriogenic cytokines and promote in vitro and in vivo arteriogenesis through paracrine mechanisms. Circ Res. 2004;94:678-85.
[70] Ghajar CM, Blevins KS, Hughes CC, George SC, Putnam AJ. Mesenchymal Stem Cells Enhance Angiogenesis in Mechanically Viable Prevascularized Tissues via Early Matrix Metalloproteinase Upregulation. Tissue engineering. 2006;12:2875-88.
[71] Rao RR, Peterson AW, Ceccarelli J, Putnam AJ, Stegemann JP. Matrix composition regulates three-dimensional network formation by endothelial cells and mesenchymal stem cells in collagen/fibrin materials. Angiogenesis. 2012;15:253-64.
[72] Rehman J, Traktuev D, Li J, Merfeld-Clauss S, Temm-Grove CJ, Bovenkerk JE, et al. Secretion of angiogenic and antiapoptotic factors by human adipose stromal cells. Circulation. 2004;109:1292-8.
[73] Baranski JD, Chaturvedi R, Stevens KR, Eyckmans J, Carvalho B, Solorzano RD, et al. Geometric control of vascular networks to enhance engineered tissue integration and function. Proceedings of the National Academy of Sciences of the United States of America. 2013;110:7586-91.
[74] Koike N, Fukumura D, Gralla O, Au P, Schechner JS, Jain RK. Creation of long-lasting blood vessels. Nature. 2004;428:138-9.
[75] Chen X, Aledia AS, Ghajar CM, Griffith CK, Putnam AJ, Hughes CC, et al. Prevascularization of a Fibrin-Based Tissue Construct Accelerates the Formation of Functional Anastomosis with Host Vasculature. Tissue engineering Part A. 2009;15:1363-71.
[76] Nehls V, Drenckhahn D. A microcarrier-based cocultivation system for the investigation of factors and cells involved in angiogenesis in three-dimensional fibrin matrices in vitro. Histochem Cell Biol. 1995;104:459-66.
[77] Ghajar CM, Chen X, Harris JW, Suresh V, Hughes CC, Jeon NL, et al. The effect of matrix density on the regulation of 3-D capillary morphogenesis. Biophysical journal. 2008;94:1930-41.
[78] Ghajar CM, Kachgal S, Kniazeva E, Mori H, Costes SV, George SC, et al. Mesenchymal cells stimulate capillary morphogenesis via distinct proteolytic mechanisms. Experimental cell research. 2010;316:813-25.
[79] Allen P, Melero-Martin J, Bischoff J. Type I collagen, fibrin and PuraMatrix matrices provide permissive environments for human endothelial and mesenchymal progenitor cells to form neovascular networks. Journal of tissue engineering and regenerative medicine. 2011;5:e74-86.

[80] Nor JE, Peters MC, Christensen JB, Sutorik MM, Linn S, Khan MK, et al. Engineering and Characterization of Functional Human Microvessels in Immunodeficient Mice. Laboratory Investigation. 2001;81:453-63.
[81] Kroon ME, van Schie MLJ, van der Vecht B, van Hinsbergh VWM, Koolwijkm P. Collagen type 1 retards tube formation by human microvascular endothelial cells in a fibrin matrix. Angiogenesis. 2002;5:257-65.
[82] Patterson J, Martino MM, Hubbell JA. Biomimetic materials in tissue engineering. Materials today. 2010;13:14-22.
[83] Chiu YC, Cheng MH, Engel H, Kao SW, Larson JC, Gupta S, et al. The role of pore size on vascularization and tissue remodeling in PEG hydrogels. Biomaterials. 2011;32:6045-51.
[84] Kraehenbuehl TP, Ferreira LS, Zammaretti P, Hubbell JA, Langer R. Cell-responsive hydrogel for encapsulation of vascular cells. Biomaterials. 2009;30:4318-24.
[85] Moon JJ, Saik JE, Poche RA, Leslie-Barbick JE, Lee SH, Smith AA, et al. Biomimetic hydrogels with pro-angiogenic properties. Biomaterials. 2010;31:3840-7.
[86] Miller JS, Shen CJ, Legant WR, Baranski JD, Blakely BL, Chen CS. Bioactive hydrogels made from step-growth derived PEG-peptide macromers. Biomaterials. 2010;31:3736-43.
[87] Phelps EA, Landazuri N, Thule PM, Taylor WR, Garcia AJ. Bioartificial matrices for therapeutic vascularization. Proceedings of the National Academy of Sciences of the United States of America. 2010;107:3323-8.
[88] Phelps EA, Headen DM, Taylor WR, Thule PM, Garcia AJ. Vasculogenic bio-synthetic hydrogel for enhancement of pancreatic islet engraftment and function in type 1 diabetes. Biomaterials. 2013;34:4602-11.
[89] Sokic S, Papavasiliou G. Controlled Proteolytic Cleavage Site Presentation in Biomimetic PEGDA Hydrogels Enhances Neovascularization In Vitro. Tissue engineering Part A. 2012.
[90] Sokic S, Christenson MC, Larson JC, Appel AA, Brey EM, Papavasiliou G. Evaluation of MMP substrate concentration and specificity for neovascularization of hydrogel scaffolds. Biomaterials Science. 2014;2:1343.
[91] Leong MF, Rasheed MZ, Lim TC, Chian KS. In vitro cell infiltration and in vivo cell infiltration and vascularization in a fibrous, highly porous poly(D,L-lactide) scaffold fabricated by cryogenic electrospinning technique. Journal of biomedical materials research Part A. 2009;91:231-40.
[92] Santos MI, Tuzlakoglu K, Fuchs S, Gomes ME, Peters K, Unger RE, et al. Endothelial cell colonization and angiogenic potential of combined nano- and micro-fibrous scaffolds for bone tissue engineering. Biomaterials. 2008;29:4306-13.
[93] Silva EA, Mooney DJ. Spatiotemporal control of vascular endothelial growth factor delivery from injectable hydrogels enhances angiogenesis. J Thromb Haemost. 2007;5.
[94] Silva EA, Kim ES, Kong HJ, Mooney DJ. Material-based deployment enhances efficacy of endothelial progenitor cells. Proceedings of the National Academy of Sciences of the United States of America. 2008;105:14347-52.
[95] Leslie-Barbick JE, Saik JE, Gould DJ, Dickinson ME, West JL. The promotion of microvasculature formation in poly(ethylene glycol) diacrylate hydrogels by an immobilized VEGF-mimetic peptide. Biomaterials. 2011;32:5782-9.

[96] Zisch AH, Lutolf MP, Ehrbar M, Raeber GP, Rizzi SC, Davies N, et al. Cell-demanded release of VEGF from synthetic, biointeractive cell-ingrowth matrices for vascularized tissue growth. FASEB journal : official publication of the Federation of American Societies for Experimental Biology. 2003.
[97] Saik JE, Gould DJ, Watkins EM, Dickinson ME, West JL. Covalently immobilized platelet-derived growth factor-BB promotes angiogenesis in biomimetic poly(ethylene glycol) hydrogels. Acta biomaterialia. 2011;7:133-43.
[98] Saik JE, Gould DJ, Keswani AH, Dickinson ME, West JL. Biomimetic hydrogels with immobilized ephrinA1 for therapeutic angiogenesis. Biomacromolecules. 2011;12:2715-22.
[99] Simons M, Ware JA. Therapeutic angiogenesis in cardiovascular disease. Nature reviews Drug discovery. 2003;2:863-71.
[100] Raeber GP, Lutolf MP, Hubbell JA. Mechanisms of 3-D migration and matrix remodeling of fibroblasts within artificial ECMs. Acta biomaterialia. 2007;3:615-29.
[101] Leslie-Barbick JE, Shen C, Chen C, West JL. Micron-scale spatially patterned, covalently immobilized vascular endothelial growth factor on hydrogels accelerates endothelial tubulogenesis and increases cellular angiogenic responses. Tissue engineering Part A. 2011;17:221-9.
[102] Phelps EA, Templeman KL, Thulé PM, García AJ. Engineered VEGF-releasing PEG–MAL hydrogel for pancreatic islet vascularization. Drug Delivery and Translational Research. 2013.
[103] Chiu LLY, Montgomery M, Liang Y, Liu H, Radisic M. Perfusable branching microvessel bed for vascularization of engineered tissues. PNAS. 2012:E3414-E23.
[104] Association AD. Peripheral Arterial Disease in People with Diabetes. Diabetes care. 2003;26:3333-41.
[105] Leibson CL, Ransom JE, Olson W, Zimmerman BR, O'Fallon WM, Palumbo PJ. Peripheral Arterial Disease, Diabetes, and Mortality. Diabetes care. 2004;27:2843-9.
[106] Criqui MH. Peripheral arterial disease - epidemiological aspects. Vascular Medicine. 2001;6:3-7.
[107] Fadini GP, Agostini C, Avogaro A. Autologous stem cell therapy for peripheral arterial disease meta-analysis and systematic review of the literature. Atherosclerosis. 2010;209:10-7.

Chapter 2

Literature Review: Mesenchymal Support Cells in the Assembly of Functional Vessel Networks

2.1 Introduction

The field of regenerative medicine has witnessed impressive advances over the past 25-30 years, progressing ever closer to the goal of translating engineered tissue constructs into human patients. However, despite an expanding literature documenting advances in biomaterials and stem cell biology, the two major factors limiting the clinical applicability of engineered tissues 20 years ago continue to present significant hurdles today: the ability to generate tissues that function equivalently to the native tissues they are intended to replace, and the ability to vascularize these tissues to sustain their metabolic demands. With respect to the latter of these two hurdles, an improved fundamental understanding of the process of blood vessel assembly in development and disease is leading to new strategies to vascularize tissues.

Blood vessels are responsible for the convective delivery of oxygen, nutrients, and other large macromolecules, as well as immune cells, to all tissues in the human

body. Vessels form primarily via two morphogenetic programs: vasculogenesis and angiogenesis (Figure 2-1). Vasculogenesis involves the *de novo* assembly of vessels from progenitor cells, and primarily occurs in development. Angiogenesis involves the sprouting and growth of new capillaries from existing vessels into a previously avascular tissue. Both are complex and dynamic processes that depend on the interplay of soluble factors and insoluble cues from the extracellular matrix (ECM) [1]. Fundamental studies of these processes have led to the identification of numerous pro-angiogenic factors, the delivery of which has been explored to promote the development of new blood vessels to restore blood supply to ischemic tissue. However, clinical trials relying on bolus injection of individual factors have been disappointing [2], perhaps due to the limited half-life of most protein growth factors, the lack of temporal and spatial control over growth factor release, and the inability of single factors to properly regulate neovascularization [3, 4]. Newer strategies involving sustained delivery of pro-angiogenic factors or genes from biodegradable scaffolds to overcome protein stability issues [5-8], as well as delivery of multiple pro-angiogenic factors in a time-dependent fashion to mimic the process of natural vessel development [4, 9], have been shown to induce formation of vascular networks. However even combinations of multiple factors may not fully recapitulate the complex mileiu of pro-angiogenic signals presented to cells *in vivo*.

Cell-based therapies have also been explored to more completely mimic the cascade of signals needed to promote stable vasculogenesis. These approaches involve delivering (an) appropriate cell type(s) that can directly differentiate into capillary structures or provide a physiologic mixture of pro-angiogenic cues to accelerate the

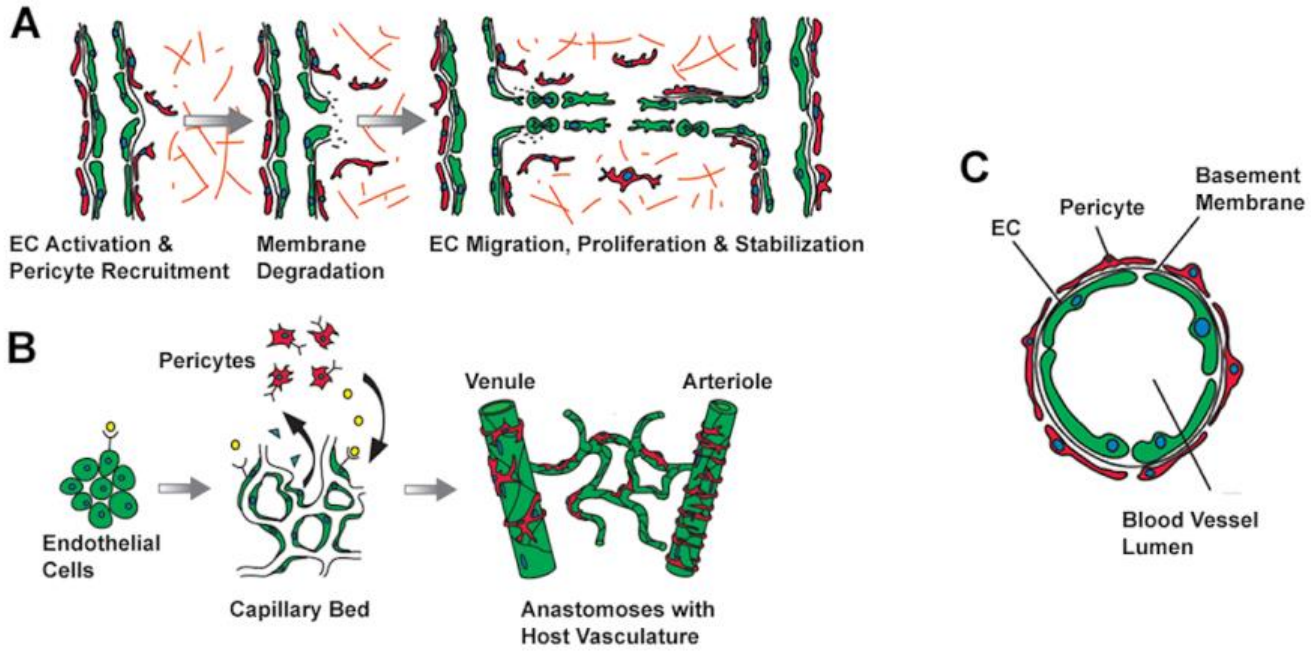

Figure 2-1. Formation of new blood vessels and the role of pericytes. A. Angiogenesis is the process by which new blood vessels sprout from preexisting blood vessels. Pericytes (red) are key players from the beginning. Dissociation of the pericytes from the vessel wall coincides with EC activation, followed by degradation of the vascular basement membrane. The ECs then migrate into the surrounding interstitial ECM, proliferate, and organize into immature vessels. Nascent vessels are stabilized via the deposition of basement membrane and association of pericytes with these tubules. B. In development, ECs originate from angioblasts or hemangioblasts in the embryo, while pericytes are derived from mesenchymal stem cells or neural crest cells. These two populations of cells then cooperate to form a primitive vascular plexus via a process known as vasculogenesis. Many tissue engineering approaches to vascularization have attempted to recreate this process either by prevascularizing a scaffold or via the direct injection of the cells within a carrier matrix. Networks formed via this method have been demonstrated to inosculate with host vasculature following implantation in vivo. C. Mature vasculature is characterized by the presence of a basement membrane and a pericyte coat surrounding the endothelial cell tubule. (Adapted from Bergers, G. and Song, S. 2005. The role of pericytes in blood-vessel formation and maintenance. Neuro Oncol, 7, 452–64, with permission from Oxford University Press.).

recruitment of host vessels. A variety of cell types have been shown to form new capillary networks and/or induce collateral blood vessel development *in vivo* [10-13]. In addition, cells have been implanted using scaffold materials and extracellular matrix proteins to improve cell retention and engraftment [14, 15]. However, delivery of endothelial cells (ECs) alone within a scaffold has led to mixed results, with some reports of leaky unstable vessels [16]. There is now general consensus that co-delivery

of an appropriate supporting cell type can stabilize nascent capillaries [17], and that these cells are essential for the formation of mature and functional vessel networks [18]. Despite the consensus regarding this paradigm, the choice of which cells to co-deliver with ECs remains an open question. This chapter will focus primarily on the use of mesenchymal support cells, and discuss key studies that document their potential roles in vascular assembly.

2.2 Initial Vascular Engineering Approaches Focused on Endothelial Cell Delivery

Early cell-based approaches to vascularize tissues *in vivo* concentrated primarily on the implantation of ECs without a supportive cell type, and yielded variable success. One of the first studies to report the formation of functional vasculature *in vivo* used genetically modified human umbilical vein endothelial cells (HUVECs) and assessed their ability to assemble into vascular structures in a subcutaneous mouse model [19]. HUVECs over-expressing Bcl-2 (to enhance their survival) supported the formation of a dense vascular network in collagen-fibronectin gels, while wild-type HUVECs did not. Host erythrocytes were found within the HUVEC-derived vessels, indicating their functional perfusion. Furthermore, mouse-derived mural cells positive for smooth muscle α-actin (αSMA) associated with the nascent vasculature within the implant region only in constructs containing Bcl-2 transduced HUVECs. While the use of viral gene delivery approaches to over-express Bcl-2 and enhance EC survival upon implantation presents translational limitations, there is no doubt that this study spawned greater interest in cell transplantation approaches to promote vascularization.

Another study from about the same time showed that functional new vasculature can also be created by seeding human dermal microvascular endothelial cells (HDMECs) in PLLA/Matrigel scaffolds and subsequently implanting these tissue constructs in subcutaneous pockets in SCID mice [20]. Host erythrocytes were found to perfuse the implant vasculature within 7 to 10 days, indicating functional inosculation with host vessels. However, association of mouse-derived cells positive for αSMA with the HDMEC tubules did not occur until 21 days post-implantation; after 4 weeks, some HDMECs apoptosed, presumably due to the lack of perivascular support from mural cells. This apoptosis could be partially overcome by over-expressing Bcl-2 in the HDMECs, which also led to increased vessel density in the constructs. Collectively, these results suggest that delivery of ECs alone can lead to the formation of functional blood vessels, but the stability of these vessel networks depends on the survival of the ECs.

2.3 Pericytes Support the Formation and Maturation of Capillary Blood Vessels

In the body, supporting cells of mesenchymal origin known as pericytes (also termed Rouget cells or mural cells) closely encircle endothelial cells in capillaries and microvessels and are believed to be responsible for stabilizing capillary blood vessels (Figure 2-1C) [21]. Pericytes are generally described as perivascular cells embedded within the basement membrane of microvasculature where they closely associate with endothelial cells [22]. While no single marker identifies all pericytes, common markers include αSMA, desmin, neuron-glial antigen 2 (NG-2), platelet-derived growth factor

receptor (PDGF)-β, aminopeptidase A & N, and RGS5 [22]. Not all pericytes display these markers, and their expression patterns change with the tissue and stage of development. This ambiguity has confounded a unifying and consistent definition of a pericyte.

Despite this ambiguity in their identity, the general consensus from two decades of research is that pericytic stabilization of EC lined vessel structures is critical both in development as well as in physiological and pathological processes in the adult organism [23]. Pericytes associate with EC tubules *in vivo* and this association modulates pruning of the vasculature, vessel permeability, and basement membrane deposition [24], suggesting that their predominant function is to mediate vascular stabilization and maturation. A number of recent studies utilizing *in vitro* co-cultures of bovine retinal pericytes and ECs in 3D collagen gels have revealed important new mechanistic insights regarding the reciprocal interactions between these two cell types. In one such study, ECs were shown to remodel existing ECM and create guidance tunnels that served as conduits for the recruitment and motility of pericytes [25]. These recruited pericytes then induced ECs to produce basement membrane components involved in extracellular matrix (ECM) crosslinking, including fibronectin, nidogen-1/2, perlecan, and laminin. Pericytes also induced ECs to upregulate integrins capable of binding to the basement membrane, including $\alpha_5\beta_1$, $\alpha_3\beta_1$, $\alpha_6\beta_1$, and $\alpha_1\beta_1$. Inhibiting these integrins, disrupting fibronectin assembly, or suppressing pericyte TIMP-3 expression all decreased basement membrane deposition and led to pathological, increased lumenal diameter [25]. Furthermore, the recruitment of the pericytes to the nascent vasculature has been shown to result from EC-derived platelet-derived growth factor (PDGF)–BB

and heparin-binding EGF-like growth factor (HB-EGF); disrupting these signals in quail embryogenesis results in vascular pathologies that may have relevance for human congenital abnormalities as well [26]. However, because of the still ambiguous definition of a pericyte, many investigators have utilized a variety of different supporting mesenchymal cell types capable of supporting capillary morphogenesis. A great deal of mechanistic information about their ability to regulate angiogenesis has now been documented in the literature. Although the remainder of this chapter will primarily focus on the use of mesenchymal stem cells (MSCs) as perivascular support cells, we will also briefly discuss insights from studies that have utilized fibroblasts or vascular smooth muscle cells to compare and contrast the mechanistic similarities and differences.

2.4 Mesenchymal Stem/Stromal/Support Cells (MSCs)

Mesenchyme refers to a type of undifferentiated loose connective tissue derived from the mesoderm during development. The term stroma is used almost interchangeably with mesenchyme, though strictly speaking stroma refers to the supportive framework of adult tissues in which functional (parenchymal) cells reside, and mesenchyme is used more often in a developmental context. Regardless, mesenchymal stem cells (MSCs) are a population of adult tissue-derived adherent cells that were first discovered in the bone marrow by Friedenstein, et al., who described them as “osteogenic stem cells” [27]. These cells were initially identified based on their ability to form clonal adherent colonies of fibroblastic cells (“colony forming unit-fibroblast”), and later shown to possess the capacity to differentiate into bone, cartilage,

and fat [28]. This latter capability is why they were initially dubbed “stem” cells by Caplan [29]. MSCs from bone marrow and a variety of other adult tissues are already the focus of numerous human clinical trials [30, 31], and have shown enormous promise in preclinical studies to facilitate bone regeneration [32], promote tissue neovascularization [11, 33, 34], and reduce inflammation [35]. Much of their therapeutic benefit seems to be related to their trophic effects, i.e. through the secretion of numerous growth factors [35], and thus many in the literature now refer to them as mesenchymal stromal cells, marrow stromal cells, or (more recently) “medicinal signaling cells” [29].

MSCs reside within a perivascular niche *in vivo* and can support vascular stability and development. *In vivo [36]*, MSCs have been identified in multiple human organs and tissues, including bone marrow, skeletal muscle, pancreas, placenta, white adipose tissue, and others (Figure 2-2) [21]. In each of these tissues, MSCs reside next to capillaries larger than 10 μm in diameter and arterioles ranging from 10-100 μm in diameter [21]. Further studies suggest that the perivascular niche for MSCs may aid in their ability to home to sites of stroke [37] and cancer [38] and to produce paracrine effectors [39]. In response to injury, MSCs localize to the injured tissue and produce factors that destabilize existing vessels, promote angiogenesis, and contribute to the maturation and stabilization of nascent capillaries [40]. Despite the increasing evidence that all MSCs may in fact be pericytes, their exact location(s) and function(s) *in vivo* remain open questions [36]. Nevertheless, both *in vitro* and *in vivo* studies of MSCs and ECs have revealed promising clues as to their roles in vascular support.

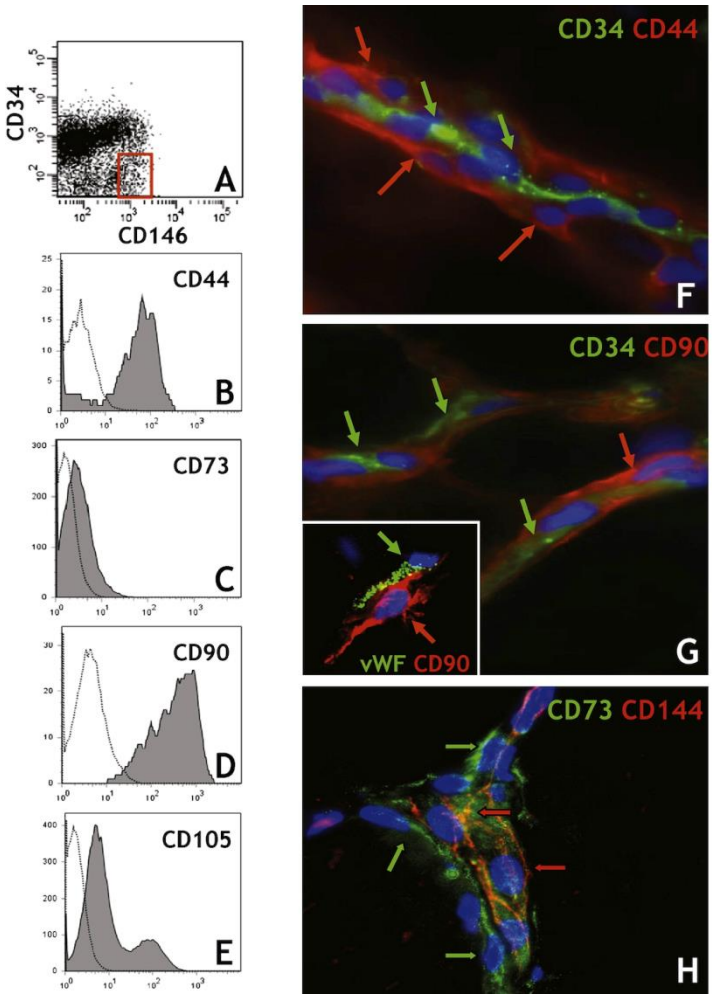

Figure 2-2. Perivascular cells natively express MSC markers. The stromal vascular fraction isolated from human white adipose tissue was stained simultaneously with antibodies to perivascular cells and MSCs and analyzed by flow cytometry. Cells negative for CD45, CD56, and CD34 and high for CD146 expression were gated (A) and analyzed for coexpression of CD44 (B), CD73 (C), CD90 (D), and CD105 (E). Clear histograms in B-E represent control cells incubated with unrelated isotype-matched antibodies. F-H. Frozen sections of human white adipose tissue were costained with antibodies to CD34 (green) or von Willebrand factor (vWF, green) to reveal endothelial cells (green arrows) and either CD44 (red, [F]) or CD90 (red, [G]). Pericytes lining small blood vessels express both CD44 (F) and CD90 ([G], main) (red arrows). Pericytes surrounding capillaries also strongly express CD90 ([G], inset ×1000) (red arrow). (H) Frozen sections of adult human muscle were costained with antibodies to CD144 (red) to reveal endothelial cells (red arrows) and CD73 (green). Pericytes lining the small blood vessel express CD73 ([H], ×600, green arrows). (Adapted from *Cell Stem Cell*, 3, Crisan, M. et al., A perivascular origin for mesenchymal stem cells in multiple human organs, 301–13. Copyright 2008, with permission from Elsevier.)

2.4.1 Angiogenic Factors Secreted by MSCs

To induce angiogenesis, MSCs secrete numerous soluble factors that modulate the behavior of normally quiescent ECs. Of note are the factors: VEGF, IGF-1, PlGF,

MCP-1, bFGF, and IL-6 [40]. VEGF (Vascular Endothelial Growth Factor) is a crucial promoter of angiogenesis, and the most widely studied of the pro-angiogenic growth factors. Through binding to its receptor tyrosine kinase, VEGFR-2, VEGF is able to trigger signaling cascades that induce endothelial tubulogenesis. Further, VEGF induces tip cell migration and proliferation of ECs, while through NOTCH activation it leads to down regulation of VEGFR-2 on stalk cells thereby providing spatial regulation of angiogenesis [41]. Levels of VEGF also modulate vascular permeability, with higher levels leading to fenestrations and leaky vessels [41, 42]. VEGF receptors can also be activated by PlGF (Placental Growth Factor) which binds to and activates VEGF-R1. Further, PlGF enhances the effects of VEGF in promoting angiogenesis [43]. However, it is not normally found in adult tissues, but rather is found in ischemic tissues and is associated with pathological recruitment of vasculature [43].

Other factors capable of modulating the proliferation of ECs include IGF-1 (Insulin-like Growth Factor)-1 that binds to its corresponding receptor, IGF1R, which is highly expressed on microvascular endothelial cells [44]. IGF-1 plays a key role in the formation of new vasculature in adult tissues [45] and is found on proliferating endothelial cells. While an overabundance of IGF-1 is often implicated in tumorogenesis. Inadequate IGF-1 has been associated with diabetic retinopathy and impaired dermal wound healing [46]. IL-6 (interleukin 6) has also been implicated in angiogenic effects, mediated through binding to its corresponding receptor IL-6R on ECs to activate ERK1/2 and STAT pathways, thereby inducing proliferation, migration and tube formation. Although this factor acts in a dose-dependent manner, ECs have a

high threshold for IL-6 and require high levels of the factor, suggesting it largely has a localized role [47].

bFGF (basic Fibroblast Growth Factor) was the first pro-angiogenic factor identified and promotes vascular stability [48]. It binds with high affinity to heparin sulfate proteoglycans, facilitating subsequent binding to its associated cell-surface receptor FGFR. bFGF is crucial to vascular maintenance and may serve as a trophic factor for ECs [48]. Finally, MCP-1/CCL2 (monocyte chemotactic protein-1, also known as CCL2) binds to CCR2 on ECs and can induce migration and angiogenic invasion *in vitro*. The addition of MCP-1 increases angiogenic invasion *in vivo*, but knockouts of MCP-1 or CCR2 form normal vasculature suggesting only a modulatory role [49].

Presumably, these key angiogenic factors (VEGF, IGF-1, PlGF, MCP-1, bFGF, and IL-6) represent a major component of MSCs ability to modulate vascular assembly. While this collection of MSC-derived or pro-angiogenic factors is not exhaustive, these six factors provide a means by which MSCs can drive the proliferation, migration, and organization of ECs towards the production of vasculature.

2.4.2 Hypoxia-Induced Activation of MSCs

Soluble factors play central roles in the inducement of vasculature in a hypoxic environment. These factors provide a means for MSCs to communicate over a distance to recruit ECs for re-vascularization. The loss of vasculature leads to a hypoxic environment within a tissue, and re-vascularization approaches have investigated hypoxia as a cue for the recruitment of vasculature. Microarray analysis of 2232 genes revealed changes in MSC gene expression during hypoxic culture, with notable

changes in the levels of VEGF, IGF, HGF, and other factors implicated in angiogenesis [50]. In comparison to mononuclear cells, which upregulate inflammatory and chemotactic genes, MSCs responded to hypoxia through genes involved in development, morphogenesis, cell adhesion, and proliferation [50].

A separate study evaluated secretion of VEGF, HGF, and TGF-β from MSCs derived from adipose tissue. It was found that only secretion of VEG-F increased significantly under hypoxia. Further, conditioned media from these hypoxic MSCs increased EC proliferation and decreased apoptosis [51]. A later study assessed the molecular pathways activated in EC by conditioned medium from MSC cultured under hypoxic conditions. The medium decreases hypoxic EC apoptosis, increases survival, and increases tube formation and has higher levels of pro-angiogenic factors IL-6 and MCP-1 in addition to VEG-F. These were shown to activate the PI3K-Akt pathway in EC which regulates apoptosis. Blocking this pathway with inhibitors of PI3KT or expression of dominant negative genes for PI3K attenuated the pro-angiogneic effect. While IL-6 promoted angiogenesis in a dose-dependent manner and activated the ERK1/2 pathway, inhibition of this pathway did not attenuate angiogenesis, suggesting that these factors promote angiogenesis via the PI3K pathway [52].

In response to hypoxic stress, MSCs have been shown to upregulate the expression of hypoxia inducible factor-1α (HIF-1α), which drives increased expression of VEGFR1 [53]. This increased the migration response of MSC to VEGF, and provides a feedback mechanism wherein MSC not only secrete VEGF but are also more sensitive to VEGF gradients, thereby enabling MSCs to efficiently home to hypoxic regions. In addition to immediate responses to hypoxia, MSCs can also be

preconditioned to a hypoxic environment. This was found to drives changes in the Wnt signaling pathway, which is responsible for self-renewal and morphogenesis in stem cells. Preconditioned MSCs were more potent at restoring vasculature to an ischemic limb *in vivo* [54], highlighting the role of hypoxia in inducing the production of factors that reduce cell death and promote re-vascularization.

2.4.3 Interactions with the Extracellular Matrix

Although soluble cues from MSCs can signal ECs to initiate angiogenesis, insoluble cues from the ECM- both chemical and mechanical- can also influence MSCs and their pro-angiogenic capacity [55]. Chemical cues modulating interactions between MSCs and the endothelial basement membrane are likely to be important, consistent with published evidence for other adult stem cell populations that can interact with the vasculature [56]. It has previously been reported that the recruitment of pericytes stimulates EC basement membrane assembly [25], and that MSCs utilize the $\alpha_6\beta_1$ integrin to bind to it [57]. Whether this adhesive mechanism influences the secretion of pro-angiogenic cues from the MSCs or not remains to be seen, but that seems to be a plausible hypothesis given the evidence in the literature.

The intrinsic mechanical properties of the ECM are also known to affect cell phenotypes in general [58], and MSC behavior specifically [59]. A 2009 study by Mammoto, et al. showed that ECs modulate the expression of their VEGF receptor (VEGF-R2) in response to the elastic properties of their substrate, and that this mechanism is critical in ECM-based control of angiogenesis [60]. Another study investigated the secretome of MSCs cultured on soft versus rigid substrates. By

monitoring the levels of >90 angiogenic proteins, they found that MSC secrete higher levels of IL-8, uPA and VEGF on stiff substrates as opposed to soft substrates [61].

Externally-applied mechanical forces provide an additional means to influence the pro-angiogenic potential of MSCs. In one study, MSCs cultured in a fibrin gel compressed in a bioreactor responded to mechanical loading by changing the profile of secreted growth factors [62]. Application of conditioned medium from compressed MSCs to ECs enhanced 2D tubulogenesis and 3D spheroid sprouting assays via a mechanism that depends on FGF and VEGF receptor activation in ECs. Analysis of the MSC-conditioned media revealed increased soluble MMP-2, TGFβ1, and bFGF, but not VEGF, as a result of the mechanical stimulation [62]. In a later study, the same group demonstrated that cyclic strain disrupted endothelial organization on 2D Matrigel assays, with elevated levels of VEGF and unchanged levels of MMP-2 and -9 in response to stretching [63]. By repeating the assay with the addition of conditioned media from MSCs cultivated in similarly dynamic mechanical conditions, paracrine stimuli were shown to increase network lengths, but not to alter the negative effect of cyclic stretching [63]. Collectively, these findings suggest that changes in MSCs in response to altered mechanical stimuli may influence their abilities to induce angiogenesis.

2.4.4 Stromal Cell Control of ECM Remodeling

ECs must break through their basement membrane and invade the surrounding interstitial matrix to sprout a new blood vessel. Essential to this process is proteolytic remodeling of the extracellular matrix (ECM). It is now well-established that capillary

invasion in type I collagen matrices depends critically on membrane-bound MMP14 (also known as MT1-MMP) [64, 65], while invasion of the provisional clot (composed primarily of the plasma protein fibrinogen in its cleaved form, fibrin) present in wounds, sites of inflammation, and tumors may depend less on MMPs and more on the serine proteases that comprise the plasminogen activator (PA)/plasmin axis [66, 67]. However, in more complex tissue explant cultures, capillary invasion in fibrin matrices proceeds independent of the PA/plasmin axis and relies instead on MT-MMP activity [68]. These results imply that in addition to the ECM, stromal cell types have the potential to bias the proteases utilized by ECs to undergo capillary morphogenesis.

Research from our own laboratory has utilized a 3D angiogenic model in which ECs invade a fibrin clot in co-culture with stromal cells to investigate the influence of stromal cell identity on ECM remodeling [69]. When MSCs from the bone marrow were used as the stromal cell type, we found that ECM proteolysis during angiogenesis requires MMPs, and that new sprout formation was almost completely inhibited in the presence of small molecule inhibitors of MMPs [70]. By contrast, when fibroblasts were used as the supporting cell type, angiogenic sprouting could only be inhibited when both plasmin-mediated and MMP-mediated fibrinolysis were blocked, suggesting a proteolytic plasticity dictated by the identity of the supporting cells [70]. When adipose-derived MSCs (ASCs) were used instead, angiogenic sprouting could be achieved when either MMPs or plasmin were inhibited individually, but not when both proteolytic axes were inhibited simultaneously [71]. In this fashion, angiogenesis induced by ASCs mirrored that induced by fibroblasts, despite their similar multipotency to bone marrow-derived MSCs. Furthermore, both fibroblasts and ASCs produced higher levels of HGF

and TNFα while inducing EC to upregulate urokinase plasminogen activator (uPA) when compared to co-cultures containing ECs and MSCs from bone marrow [71]. A more definitive study used RNA interference to demonstrate that ECs require MT1-MMP, but not MMP-2 or MMP-9, to form new sprouts in the presence of bone marrow-derived MSCs in a fibrin matrix [72]. These data suggest that the mechanism(s) by which ECs form new vessel networks depend(s) not only on the ECs and the matrix, but also on the identity of supporting stromal cells present in the interstitial matrix.

Several studies now also suggest that pericytes regulate the expression of MT1-MMP in endothelial tips cells at the leading ends of sprouting capillaries. Among these, Lafleur, et al. used co-cultures of ECs with smooth muscle cells or pericytes to first show that the perivascular support cells regulate the activity of MT1-MMP and subsequent MMP-2 activation in ECs via the secretion of tissue inhibitor of metalloproteinase-2 (TIMP-2) [73]. Saunders, et al. then showed that EC-pericyte interactions in 3D collagen gels induced TIMP-3 expression by the pericytes and TIMP-2 expression by the ECs [74], while Yana, et al. showed that the mural cells limit the expression of MT1-MMP to endothelial tip cells by restricting its expression in stalk cells [75]. By controlling the specification of ECs into tip cells and stalk cells via local control of proteolysis, these mechanisms can potentially explain one possible way in which pericytes stabilize nascent capillaries.

2.4.5 Differentiation of MSCs to SMCs Supports Vascular Stability

After recruitment of ECs, MSCs begin to display vascular smooth muscle cell (SMC) markers and take on a new role in the maintenance of EC structures. *In vitro*,

MSCs can be induced to differentiate directly into SMCs by exposure to transforming growth factor beta (TGF-β). TGF-β acts by induction of Jagged 1 (JAG1), a ligand for Notch and causes MSCs to express SMC markers such as αSMA, calponin 1, and myocardin. Additionally, the direct activation of the Notch signaling pathway induced differentiation of MSCs to SMCs [76]. Further, ECs express the Notch ligand delta-like-4 (DLL4) and are themselves modulated by Notch signaling, providing a means for reciprocal interaction between ECs and SMCs [77].

Another means of driving MSC differentiation towards an SMC is through interactions with ECs. Using 10T½ cells (a mouse multipotent cell line widely used as a model mural cell type), Hirschi, et al. controlled their interactions with ECs *in vitro* using a co-culture system in which the two cell types could interact directly through cell-cell junctions or indirectly through soluble, paracrine factors [78]. When plated in adjacent agarose wells to permit only soluble communication, the 10T½ cells migrated towards the ECs mediated by PDGF-BB, while the ECs produced TGF-β that induced the 10T½s to express several SMC markers (i.e., SM-myosin, SM22α, and calponin) [78]. In the absence of heterotypic cell-cell contacts, the ECs were found to secrete PDGF-B that increased 10T½ cell proliferation. However, co-culture with direct cell-cell contact decreased proliferation of both cell types independent of TGF-β and PDGF [79].

In another study, direct contact co-culture between ECs and 10T½s was shown to upregulate SM22α to a greater extent than direct TGF-β treatment alone [80]. Likewise, in a transwell co-culture system, MSCs were shown to migrate in response to PDGF signaling from ECs [81]. When placed in direct contact with the ECs, the MSCs upregulated the SMC marker myocardin, that could not be induced in separated co-

cultures or by TGF-β alone. Together, these studies suggest that ECs utilize soluble cues to induce MSC proliferation and migration towards EC; once the MSCs come into contact with the ECs, they terminate proliferation and differentiate to the SMC lineage.

2.5 Stimulation of Capillary Morphogenesis by Other Supporting Cell Types

Up to this point, this chapter has focused primarily on the use of MSCs with multilineage potential as a source of stromal cells capable of supporting the formation of vascular networks. However, valuable mechanistic insights have been achieved through the use of other terminally differentiated mesenchymal cell types, most notably fibroblasts and smooth muscle cells [82, 83]. The use of fibroblasts is justified based on their known roles in wound healing, and the argument that nearly every tissue in the body contains resident fibroblasts that are likely to influence vessel morphogenesis. Like MSCs, fibroblasts can occupy a perivascular location proximal to blood vessels, both *in vitro* and *in vivo*, and attain some characteristics of pericytes (Figure 2-3) [82]. A justification for using SMCs is also clear, given their roles in maintaining vessel tone and contractility in arterioles and arteries, and the fact that pericytes are widely considered to be primitive SMCs. Early studies focused on the development of model systems to study the paracrine induction of angiogenic sprouting by fibroblasts [84, 85]. Hughes and colleagues have published extensively on the control of angiogenic sprouting by fibroblasts [86-89]. This group has recently and exhaustively investigated the

"secretome" of fibroblasts for factors that enhance the angiogenic activity of ECs,

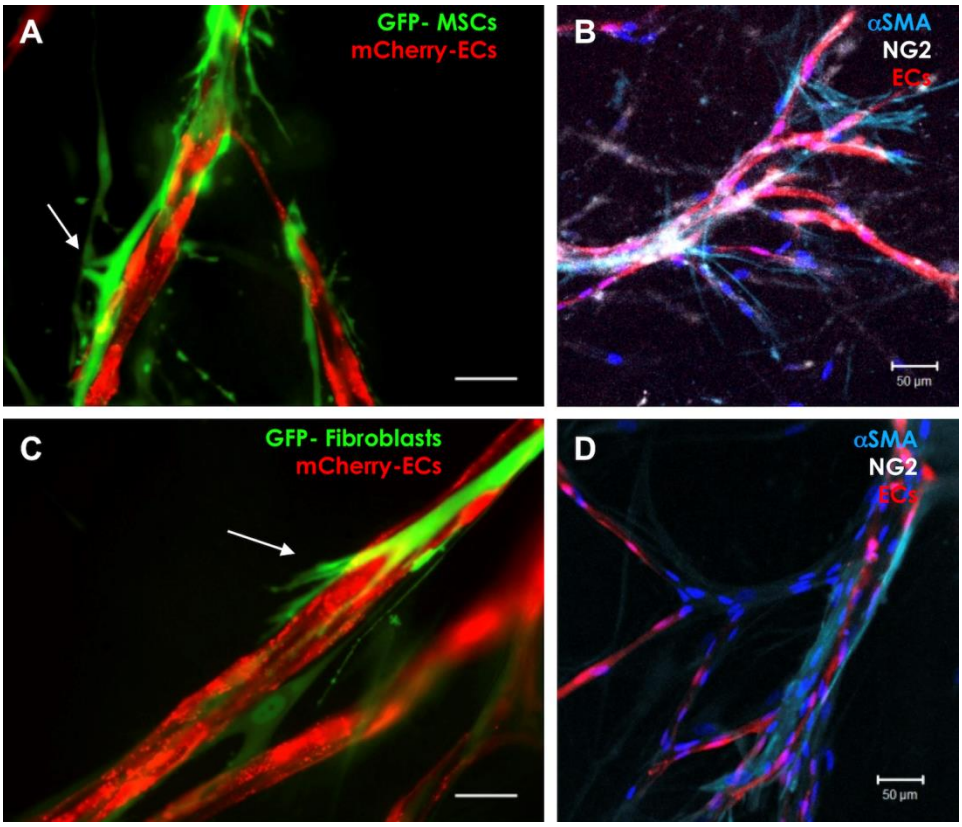

Figure 2-3. MSCs and fibroblasts both stimulate ECs to form mature capillary networks in model 3D cultures. MSCs (A,B) or fibroblasts (C,D) interspersed throughout fibrin ECMs in the presence of mCherry-transduced ECs induce capillary formation and occupy perivascular locations (white arrows in A and C). Cultures containing mCherry-transduced ECs and either MSCs (B) or fibroblasts (D) were fixed and IF stained for pericyte markers α SMA (aqua) and NG2 (white). Both MSCs and fibroblasts expressed α SMA, but only the MSCs expressed NG2. Nuclei (DAPI) are visible in the blue channel. In panels A and C, scale = 25 μm; in panels B and D, scale = 50 μm. (Adapted from Experimental Cell Research, 316, Ghajar, C. M. et al., Mesenchymal cells stimulate capillary morphogenesis via distinct proteolytic mechanisms, 813–25. Copyright 2010, with permission from Elsevier.)

and demonstrated the role of high fibronectin and hepatocyte growth factor (HGF) [90].

To further understand the influence of stromal fibroblasts on capillary formation, Newman et al. performed a series of experiments to determine the relative importance of fibroblast-derived soluble factors and insoluble factors [91]. They identified a cocktail of soluble factors- angiopoietin-1, angiogenin, HGF, transforming growth factor-α (TGF-α), and tumor necrosis factor (TNF)- that could induce sprouting, but not lumen development, in the absence of stromal support cells. Further studies revealed that the

addition of fibroblast-conditioned medium restored the lumenogenesis. The authors showed that five genes expressed in fibroblasts - collagen I, procollagen C endopeptidase enhancer 1, secreted protein acidic and rich in cysteine (SPARC), transforming growth factor-β-induced protein IG-h3, and insulin growth factor-binding protein 7 (IGFBP7) – were necessary for lumen formation. When purified collagen I, SPARC and IGFBP7 were added back to cultures containing fibroblasts deficient in the production of these proteins, lumen formation was recovered and the matrix became stiffer [91]. This loss-of-function/gain-of-function approach provides some of the most compelling mechanistic evidence to date to explain how supporting fibroblasts regulate the formation of vascular network, and is consistent with a prior study implicating ECM deposition in neovascularization [92]. It remains to be seen if multipotent MSCs or fully committed SMCs facilitate capillary growth and development via the same mechanisms as fibroblasts, but it seems likely that at least some of the mechanisms will be conserved.

2.6 Delivery of Stromal Cells with ECs Enhances Vessel Formation and Stability *In Vivo*

2.6.1 Terminally-differentiated adult cells

In the past 10 years, a number of studies have focused on the potential of terminally-differentiated adult cell types, particular the afore-mentioned fibroblasts and SMCs, to promote vessel formation and stabilization upon implantation *in vivo*. Building on the numerous contributions in the literature demonstrating the ability of fibroblasts to support angiogenic sprouting *in vitro* (discussed above), a 2009 study by Chen, et al.

demonstrated that pre-formed vessel networks assembled in fibrin gels from HUVECs and normal human lung fibroblasts (NHLFs) *in vitro* prior to implantation *in vivo* could successfully inosculate with host vessels and become perfused with red blood cells [93]. Increased EC proliferation and perfusion was dependent on the presence of NHLFs. A subsequent study comparing endothelial progenitor cells (EPCs) with HUVECs demonstrated that pre-vascularized constructs containing an order of magnitude higher density of NHLFs (2 million/mL) yielded more mature vessels that inosculated with host vessels 2-3 days more quickly than those with a lower density of support cells (0.2 million/mL) [94].

Smooth muscle cells (SMCs), commonly found *in vivo* in the medial layer of larger diameter vessels, are another adult cell type that has been used in several studies to support implanted endothelial networks. In one study, human saphenous vein SMCs (HSVSMCs) were shown to promote vascularization when encapsulated in Matrigel constructs with umbilical cord blood-derived EPCs or adult peripheral blood-derived EPCs (termed cb- and adult-EPCs, respectively) and then implanted subcutaneously in nude mice [95]. Vessel density depended on EPC source, as seen from sections stained for hCD31 and αSMA. Constructs containing EPCs alone did not vascularize, a finding consistent with prior work from others [96]. Robust αSMA staining was seen both around vessel lumens as well as throughout the Matrigel in implants with SMCs, suggesting that a percentage of these cells co-localize with the EPC-derived vasculature [95].

Human aortic SMCs (HASMCs) have also been shown to accelerate vessel formation *in vivo* when co-implanted with Bcl-2-transduced HUVECs within a 3D PGA-

collagen-fibronectin scaffold in a SCID mouse model [97]. Grafts incorporating both HUVECs and HASMCs had more αSMA positive cells associated with the vasculature compared to grafts containing either cell type alone at all time points. By 60 days, grafts incorporating both cell types had vessels of significantly larger caliber than grafts containing either cell type alone [97]. Similar observations have been reported with Matrigel-enriched PLLA scaffolds containing human microvascular endothelial cells (HMVECs) and human pulmonary artery SMCs (hPASMCs) implanted subcutaneously in NOD/SCID mice [98]. Co-localization of structures staining positive for hCD31 and αSMA increased from 7 to 21 days post-implantation in constructs containing both cell types, suggesting SMCs assume a perivascular location over time. Fluorescence angiography using systemically injected FITC-labeled lectin demonstrated perfusion of implant vasculature and successful inosculation with host vessels. SMC association with the vascular network was confirmed by multiphoton fluorescence microscopy with labeled SMCs and UEA-1 stained human microvessels.

Collectively, these studies demonstrate that delivering fibroblasts or SMCs with ECs is more effective than ECs alone at creating stable vasculature capable of inosculating with host-derived vessels over time, supporting the general consensus that co-delivery of a supporting cell type can yield better results. However, the feasibility of acquiring fibroblasts from the lung or SMCs from the walls of large vessels may limit the clinical translatability of these cells types, which thus motivates investigation of alternate stromal cell sources. Furthermore, new evidence (discussed below) suggests that fibroblasts may not regulate vessel quality and quantity to the same degree as other populations of supporting cells, perhaps because they are not truly bona fide pericytes.

2.6.2 Multipotent Cells Enhance Vessel Network Functionality In Vivo

Endothelial cells have the capacity to support formation of functional, mature vasculature *in vivo* when co-delivered with human embryonic stem cells (hESCs) and mesenchymal stem cells derived from either cord blood, bone marrow, or adipose tissue [16]. This area of research has prompted significant interest, as stem cells from various sources function as pericytes *in vivo* [99]. Additionally, they may be a more clinically viable option for therapeutic vascularization as many of these cell types can be derived autologously [100] and easily manipulated *in vitro* [101].

One of the earliest and most influential studies to use a supporting mesenchymal cell type to drive the formation of functional vasculature *in vivo* involved the co-implantation of HUVECs with mouse embryonic fibroblasts, termed 10T½s, in a fibronectin-collagen gel in a SCID mouse cranial window [102]. Vasculature in constructs containing HUVECs alone regressed within 60 days, likely due to delays in the recruitment of mouse-derived mural cells. In contrast, vasculature formed via the co-delivery approach was functional for up to one year, a result that was hypothesized to result from the pericytic support. Several metrics were used to assess functionality. Fluorescent dextran was delivered systemically to mice, allowing visual confirmation via intravital microscopy of the inosculation of implant vasculature with host-derived vessels. Engineered vessels were more permeable than quiescent vasculature, but less permeable than tumor vasculature. Further, like native vasculature, the implant's vessels responded to the vasoconstrictor endothelin-1. Overall, this study demonstrated

that the addition of stromal cells improved vessel functionality, and highlighted the importance of pericytic support for engineering vasculature *in vivo*.

In a later paper, the same investigators compared the ability of umbilical cord blood (CB)-derived and peripheral blood (PB)-derived EPCs to form functional, long-lasting vasculature when combined with 10T½s *in vivo* [96]. In addition to the metrics of functionality used in their previous work, red blood cell velocity and leukocyte rolling in response to cytokine stimulation were monitored. Vasculature derived from PB-EPCs underwent regression within 3 weeks, regardless of the presence of 10T½s, while the stability of the vasculature derived from the CB-EPCs was dependent on the presence of 10T½s, a result which highlights the importance of pairing appropriate endothelial and stromal cell sources to develop engineered vascular networks.

Numerous studies have also explored combinations of bone marrow-derived MSCs with ECs in vascularization strategies. In one such study, HUVECs were co-encapsulated with MSCs in a collagen-fibronectin gel and implanted into SCID mice in a cranial window [101]. The resultant engineered vasculature was stable and perfused for >130 days *in vivo*. In this work, both 10T½s and MSCs were used as support cells to assess the ability of each to support vascular development. While both cell types supported vascular networks of comparable length, it was not clear if both supporting cell types yielded vasculature with similar functional properties *in vivo*. Nevertheless, in constructs containing MSCs, systemically administered dextran localized to the lumens of the engineered vessel networks, demonstrating functional inosculation with host vessels. Further, MSCs localized to a periendothelial location and expressed αSMA, SM22α, and desmin. Furthermore, the nascent vessels circumscribed by the MSCs

were capable of vasoconstriction in response to endothelin-1. Taken together, these data suggest MSCs differentiate into perivascular cells. Contrary to reports from other research groups [103], the MSCs contributed to vascularization *in vivo,* but did not directly differentiate into ECs.

Recent work from another leading team investigated the pericytic capacity of mesenchymal progenitor cells (MPCs) derived from bone marrow or umbilical cord blood [100]. It is unclear if these cells are similar to MSCs used by other investigators or not, since there are no consensus markers to prospectively isolate progenitors from the bone marrow. Regardless, like MSCs, these MPCs appeared to act like pericytes when combined with cord blood-derived EPCs in Matrigel and subsequently implanted subcutaneously in immunocompromised mice [100]. Vascularization was apparent using both bone marrow and umbilical cord MPC sources one week after implantation, and was maintained for more than four weeks *in vivo*, as evidenced by the perfusion of vasculature with host erythrocytes. Additionally, αSMA and hCD31 staining confirmed that EPCs remained on the lumenal side of the tubule while the MPCs assumed a periendothelial location consistent with pericytes. Perfusion through the implant was assessed using a bioluminescent assay, in which luciferin delivered via intraperitoneal injection was detected in samples containing luciferase-expressing EPCs and unlabeled MPCs, but not in those samples containing EPCs alone. These data suggest inosculation with host vasculature depends on the presence of stromal cells, which corroborates previous data suggesting that functional perfusion is compromised in the absence of mesenchymal support cells [93, 95, 97, 102].

In an approach that distinguishes itself from the use of adult stem cells, vascular progenitor cells were isolated from human embryoid bodies and differentiated into endothelial-like (EL) or smooth muscle-like (SML) cells [104]. Subsequent transplantation of either EL cells alone or a combination of EL and SML cells in a Matrigel scaffold into nude mice resulted in microvessel formation. Microvessel density did not differ substantially between the EL only and EL and SML-containing scaffolds, which deviates somewhat from previous studies that emphasize co-delivery for robust vascularization. However, these data are confounded by the use of heterogeneous cell populations and ill-defined assessment of the functionality of the luminal structures that were quantified to determine vessel density.

ASCs are seen as a particularly attractive clinical source for vascular therapies since they can be easily harvested in large numbers from liposuction procedures [99]. ASCs associate with capillaries *in vivo* and have been demonstrated to assume a pericytic role both *in vitro* and *in vivo* [99]. In one important study, collagen constructs containing EPCs and ASCs, alone and in combination, were implanted into NOD-SCID mice [105]. The density of perfused vessels increased in constructs containing both EPCs and ASCs with multi-layered structures found more frequently in implants containing both cell types. To investigate other clinical applications, the constructs were implanted with either pancreatic islets or adipocytes and the organization of the parenchymal cells into neo-organs was demonstrated [105.

2.6.3 Comparing the Vasculature Formed with Distinct Mesenchymal Support Cells

Thus far, the studies reviewed provide strong support for the proposition that co-delivery of a supporting mesenchymal cell type with ECs can yield stable vascular networks that inosculate with host vessels. However, the choice of stromal cell type has varied widely over these studies, and have included MSCs from bone marrow, adipose tissue, cord blood, as well as fibroblasts (from human lung) and both venous and arterial SMCs. It is clear that despite the consensus that delivery of two cell types is better than one in terms of building vasculature, there is still no consensus as to which population of mesenchymal support cells will be the “winner” in terms of a viable clinical strategy.

Recent work from our own laboratory aimed to partially address this issue. Building prior *in vitro* observations, and the pioneering work of other investigative teams highlighted earlier in this chapter, we set out to systematically compare the functionality of vasculature formed *in vivo* using various mesenchymal support cells [16]. In our study, HUVECs suspended in fibrin were injected subcutaneously with one of three stromal cell types: NHLFs, bone marrow-derived MSCs, or adipose-derived MSCs (ASCs). The formation of vasculature was monitored over 14 days via laser Doppler perfusion imaging and standard histological assessments, while vessel 'leakiness' was assessed using a modified dextran tracer assay. Previous studies assayed for tracer in the lumens of engineered vessels, but we also quantified the fraction of dye outside the capillary lumen as a metric of permeability. As expected, vessels formed via delivery of ECs alone were of a fairly poor quality and showed signs of leakiness via the presence of fluorescent dextran in the interstitial matrix (Figure 2-4). Interestingly, despite the fact that the EC-NHLF implants yielded the highest vessel density, the vessels generated

from this combination of cells were also of a rather poor quality. By contrast, vessels formed via co-delivery of ECs with MSCs from either the bone marrow or adipose tissue exhibited decreased vessel leakiness (Figure 2-4) and increased expression of mature smooth muscle markers. These data suggest that the multipotent stromal cells yield vasculature of superior quality because they may differentiate into pericytes and eventually into SMCs.

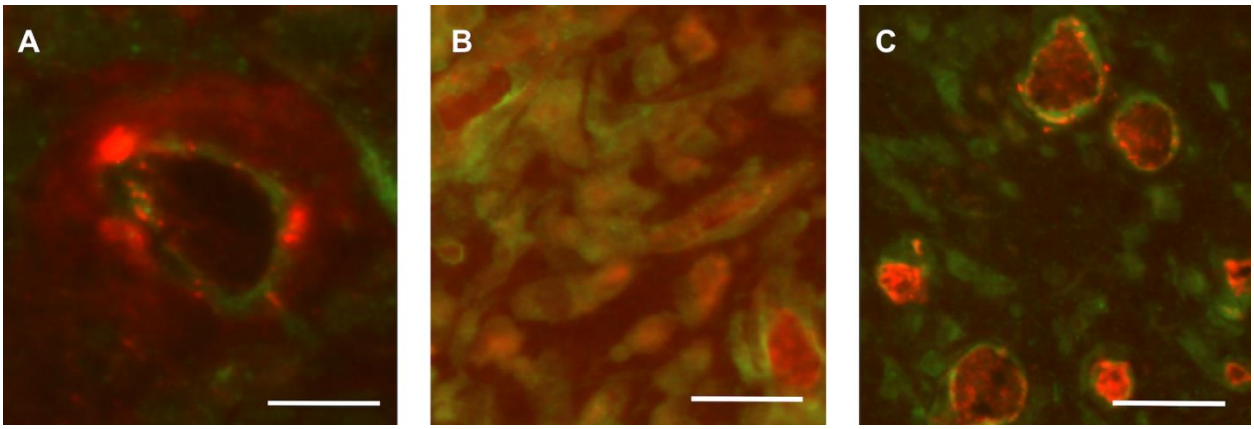

Figure 2-4. Coinjection of ECs with MSCs yields neovasculature with superior functional properties. SCID mice bearing implants containing only (A) ECs, (B) ECs + fibroblasts, or (C) ECs + MSCs were subjected to tail vein injections of a 70-kDa Texas Red–dextran (red) tracer to visualize inosculation and characterize vessel leakiness. Tissues were counterstained with antihuman CD31 antibodies (green) to verify the human origins of the vessels. The red tracer was found in the interstitial matrix outside of the new vessels when ECs were delivered alone (A) or with fibroblasts (B), but was contained within the vessels formed from ECs + MSCs (C). Scale bars = 20 μm. (Adapted from Grainger, S. J. et al. 2013. Stromal cell identity influences the *in vivo* functionality of engineered capillary networks formed by co-delivery of endothelial cells and stromal cells. *Tissue Engineering. Part A,* 19, 1209–22, with permission from Mary Ann Liebert, Inc.)

In translational therapies, it will be critical to determine the appropriate combination of cells and matrix that optimizes the re-vascularization of ischemic tissues. While the studies presented are pivotal in reaching this end, gaps in the current data highlight the need for additional work in the field. In particular, vascular elements do not exist in isolation within the body, but rather function in concert with parenchymal tissues. As a result, there is significant interest in studying vascularization in the presence of other tissues.

2.7 Vascularization in the Context of Complex Engineered Tissues

Vascularization is of substantial clinical value for cardiovascular therapies and is a key step in the formation of large, complex engineered tissues. Towards that goal, researchers seeking to create tissue constructs with complex functions have begun to combine parenchymal cells with vascular and stromal cells to facilitate construct vascularization. One such demonstration of this approach created vascularized skeletal muscle *in vitro* by combining myoblasts, mouse embryonic fibroblasts (MEFs), and HUVECs in an oriented PLLA-PLGA scaffold, which was then implanted in SCID mice *in vivo* [106]. Human CD31 and vWF staining of histological sections confirmed the human origin of implant vasculature. Additionally, fluorescent lectin was administered systemically and localized to the lumen of construct vasculature, suggesting the successful inosculation of host and implant tissue. Both vascularization and differentiation of muscle tissue were shown to be optimal in constructs combining all three cell types.

A similar combination strategy has also been utilized to create vascularized cardiac tissue constructs, formed from hESC-derived cardiomyocyes, human umbilical vein and hESC-derived ECs, and MEFs [107]. Vessel number, contractile force, collagen content, and β-myosin heavy chain (β-MHC) positive cells increased in constructs containing all three cell types as compared with constructs composed of cardiomyocytes alone. Constructs lacking the vascular element did not display

physiologically appropriate active contraction, electrical pacing, and mechanical properties, suggesting the pro-vascular milieu facilitates both vascular and cardiac development. Although many challenges remain, these two examples demonstrate that successful vascularization of engineered tissues requires not only the ECs, but also a supporting stromal cell type that serves as a stabilizing pericyte-like population.

2.8 Conclusions and Future Directions

Consensus within the research community suggests that the vascularization of engineered constructs is significantly enhanced when endothelial cells are not delivered alone, but rather, in combination with mesenchymal support cells. This finding has been confirmed across several murine models as well as with various mesenchymal support cells. Nevertheless, the most appropriate choice of mesenchymal support cell for eventual therapeutic applications remains unclear due both to concerns about cell sourcing and to the current gaps in understanding regarding the manner in which vessel quality and function vary with the identity of the support cells. Though the data remain incomplete, multiple studies suggest that multipotent mesenchymal stem cells from various sources provide vascular support in a manner similar to native pericytes. Further research is needed to justify the choice of cells for any eventual cell therapy to treat ischemic diseases or for the creation of robust engineered tissues, and to accelerate the translation of these research cell-based approaches to the clinic.

2.9 References

[1] Ingber DE, Folkman J. How does extracellular matrix control capillary morphogenesis? Cell. 1989;58:803-5.
[2] Simons M, Ware JA. Therapeutic angiogenesis in cardiovascular disease. Nature reviews Drug discovery. 2003;2:863-71.
[3] Chen RR, Silva EA, Yuen WW, Brock AA, Fischbach C, Lin AS, et al. Integrated approach to designing growth factor delivery systems. Faseb J. 2007.
[4] Sun Q, Silva EA, Wang A, Fritton JC, Mooney DJ, Schaffler MB, et al. Sustained release of multiple growth factors from injectable polymeric system as a novel therapeutic approach towards angiogenesis. Pharm Res. 2010;27:264-71.
[5] Lee KY, Peters MC, Anderson KW, Mooney DJ. Controlled growth factor release from synthetic extracellular matrices. Nature. 2000;408:998-1000.
[6] Murphy WL, Mooney DJ. Controlled delivery of inductive proteins, plasmid DNA and cells from tissue engineering matrices. J Periodontal Res. 1999;34:413-9.
[7] Sun Q, Chen RR, Shen Y, Mooney DJ, Rajagopalan S, Grossman PM. Sustained vascular endothelial growth factor delivery enhances angiogenesis and perfusion in ischemic hind limb. Pharmaceutical research. 2005;22:1110-6.
[8] Zisch AH, Lutolf MP, Ehrbar M, Raeber GP, Rizzi SC, Davies N, et al. Cell-demanded release of VEGF from synthetic, biointeractive cell ingrowth matrices for vascularized tissue growth. Faseb J. 2003;17:2260-2.
[9] Richardson TP, Peters MC, Ennett AB, Mooney DJ. Polymeric system for dual growth factor delivery. Nat Biotechnol. 2001;19:1029-34.
[10] Iba O, Matsubara H, Nozawa Y, Fujiyama S, Amano K, Mori Y, et al. Angiogenesis by implantation of peripheral blood mononuclear cells and platelets into ischemic limbs. Circulation. 2002;106:2019-25.
[11] Kinnaird T, Stabile E, Burnett MS, Shou M, Lee CW, Barr S, et al. Local delivery of marrow-derived stromal cells augments collateral perfusion through paracrine mechanisms. Circulation. 2004;109:1543-9.
[12] Pesce M, Orlandi A, Iachininoto MG, Straino S, Torella AR, Rizzuti V, et al. Myoendothelial differentiation of human umbilical cord blood-derived stem cells in ischemic limb tissues. Circ Res. 2003;93:e51-62.
[13] Rehman J, Traktuev D, Li J, Merfeld-Clauss S, Temm-Grove CJ, Bovenkerk JE, et al. Secretion of angiogenic and antiapoptotic factors by human adipose stromal cells. Circulation. 2004;109:1292-8.
[14] Nor JE, Christensen J, Mooney DJ, Polverini PJ. Vascular endothelial growth factor (VEGF)-mediated angiogenesis is associated with enhanced endothelial cell survival and induction of Bcl-2 expression. Am J Pathol. 1999;154:375-84.
[15] Nor JE, Peters MC, Christensen JB, Sutorik MM, Linn S, Khan MK, et al. Engineering and characterization of functional human microvessels in immunodeficient mice. Lab Invest. 2001;81:453-63.
[16] Grainger SJ, Carrion B, Ceccarelli J, Putnam AJ. Stromal Cell Identity Influences the In Vivo Functionality of Engineered Capillary Networks Formed by Co-delivery of Endothelial Cells and Stromal Cells. Tissue engineering Part A. 2013.
[17] Koike N, Fukumura D, Gralla O, Au P, Schechner JS, Jain RK. Tissue engineering: creation of long-lasting blood vessels. Nature. 2004;428:138-9.

[18] Au P, Tam J, Fukumura D, Jain RK. Bone marrow-derived mesenchymal stem cells facilitate engineering of long-lasting functional vasculature. Blood. 2008;111:4551-8.
[19] Schechner JS, Nath AK, Zheng L, Kluger MS, Hughes CC, Sierra-Honigmann MR, et al. In vivo formation of complex microvessels lined by human endothelial cells in an immunodeficient mouse. Proceedings of the National Academy of Sciences of the United States of America. 2000;97:9191-6.
[20] Nor JE, Peters MC, Christensen JB, Sutorik MM, Linn S, Khan MK, et al. Engineering and Characterization of Functional Human Microvessels in Immunodeficient Mice. Laboratory Investigation. 2001;81:453-63.
[21] Crisan M, Yap S, Casteilla L, Chen C-W, Corselli M, Park TS, et al. A Perivascular Origin for Mesenchymal Stem Cells in Multiple Human Organs. Cell Stem Cell. 2008;3:301-13.
[22] Armulik A, Abramsson A, Betsholtz C. Endothelial/Pericyte Interactions. Circulation Research. 2005;97:512-23.
[23] Bergers G, Song S. The role of pericytes in blood-vessel formation and maintenance. Neuro Oncol. 2005;7:452-64.
[24] Thurston G. Complementary actions of VEGF and angiopoietin-1 on blood vessel growth and leakage. J Anat. 2002;200:575-80.
[25] Stratman AN, Malotte KM, Mahan RD, Davis MJ, Davis GE. Pericyte recruitment during vasculogenic tube assembly stimulates endothelial basement membrane matrix formation. Blood. 2009;114:5091-101.
[26] Stratman AN, Schwindt AE, Malotte KM, Davis GE. Endothelial-derived PDGF-BB and HB-EGF coordinately regulate pericyte recruitment during vasculogenic tube assembly and stabilization. Blood. 2010;116:4720-30.
[27] Friedenstein AJ, Petrakova KV, Kurolesova AI, Frolova GP. Heterotopic of bone marrow. Analysis of precursor cells for osteogenic and hematopoietic tissues. Transplantation. 1968;6:230-47.
[28] Pittenger MF, Mackay AM, Beck SC, Jaiswal RK, Douglas R, Mosca JD, et al. Multilineage potential of adult human mesenchymal stem cells. Science. 1999;284:143-7.
[29] Caplan AI. What's in a name? Tissue Eng Part A. 2010;16:2415-7.
[30] Giordano A, Galderisi U, Marino IR. From the laboratory bench to the patient's bedside: an update on clinical trials with mesenchymal stem cells. J Cell Physiol. 2007;211:27-35.
[31] Wagner J, Kean T, Young R, Dennis JE, Caplan AI. Optimizing mesenchymal stem cell-based therapeutics. Curr Opin Biotechnol. 2009;20:531-6.
[32] Simmons CA, Alsberg E, Hsiong S, Kim WJ, Mooney DJ. Dual growth factor delivery and controlled scaffold degradation enhance in vivo bone formation by transplanted bone marrow stromal cells. Bone. 2004;35:562-9.
[33] Nagaya N, Kangawa K, Itoh T, Iwase T, Murakami S, Miyahara Y, et al. Transplantation of mesenchymal stem cells improves cardiac function in a rat model of dilated cardiomyopathy. Circulation. 2005;112:1128-35.
[34] Silva GV, Litovsky S, Assad JA, Sousa AL, Martin BJ, Vela D, et al. Mesenchymal stem cells differentiate into an endothelial phenotype, enhance vascular density, and improve heart function in a canine chronic ischemia model. Circulation. 2005;111:150-6.

[35] Caplan AI. Adult mesenchymal stem cells for tissue engineering versus regenerative medicine. J Cell Physiol. 2007.
[36] da Silva Meirelles L, Caplan AI, Nardi NB. In search of the in vivo identity of mesenchymal stem cells. Stem cells. 2008;26:2287-99.
[37] Kokovay E, Li L, Cunningham LA. Angiogenic recruitment of pericytes from bone marrow after stroke. J Cereb Blood Flow Metab. 2005;26:545-55.
[38] Beckermann BM, Kallifatidis G, Groth A, Frommhold D, Apel A, Mattern J, et al. VEGF expression by mesenchymal stem cells contributes to angiogenesis in pancreatic carcinoma. Br J Cancer. 2008;99:622-31.
[39] Doorn J, Moll G, Le Blanc K, van Blitterswijk C, de Boer J. Therapeutic applications of mesenchymal stromal cells: paracrine effects and potential improvements. Tissue Engineering Part B: Reviews. 2011;18:101-15.
[40] da Silva Meirelles L, Fontes AM, Covas DT, Caplan AI. Mechanisms involved in the therapeutic properties of mesenchymal stem cells. Cytokine & Growth Factor Reviews. 2009;20:419-27.
[41] Carmeliet P, Jain RK. Molecular mechanisms and clinical applications of angiogenesis. Nature. 2011;473:298-307.
[42] Olsson A-K, Dimberg A, Kreuger J, Claesson-Welsh L. VEGF receptor signalling ? in control of vascular function. Nat Rev Mol Cell Biol. 2006;7:359-71.
[43] Carmeliet P, Moons L, Luttun A, Compernolle V, Wu Y, Bono F, et al. Synergism between vascular endothelial growth factor and placental growth factor contributes to angiogenesis and plasma extravasation in pathological conditions. Nature medicine. 2001;7.
[44] Chisalita SI, Arnqvist HJ. Insulin-like growth factor I receptors are more abundant than insulin receptors in human micro- and macrovascular endothelial cells. American Journal of Physiology - Endocrinology And Metabolism. 2004;286:E896-E901.
[45] Aghdam SY, Eming SA, Willenborg S, Neuhaus B, Niessen CM, Partridge L, et al. Vascular endothelial insulin/IGF-1 signaling controls skin wound vascularization. Biochemical and Biophysical Research Communications. 2012;421:197-202.
[46] Shaw LC, Pan H, Afzal A, Calzi SL, Spoerri PE, Sullivan SM, et al. Proliferating endothelial cell-specific expression of IGF-I receptor ribozyme inhibits retinal neovascularization. Gene Ther. 2006;13:752-60.
[47] Fan Y, Ye J, Shen F, Zhu Y, Yeghiazarians Y, Zhu W, et al. Interleukin-6 stimulates circulating blood-derived endothelial progenitor cell angiogenesis in vitro. J Cereb Blood Flow Metab. 2007;28:90-8.
[48] Cross MJ, Claesson-Welsh L. FGF and VEGF function in angiogenesis: signalling pathways, biological responses and therapeutic inhibition. Trends in Pharmacological Sciences. 2001;22:201-7.
[49] Salcedo R, Ponce ML, Young HA, Wasserman K, Ward JM, Kleinman HK, et al. Human endothelial cells express CCR2 and respond to MCP-1: direct role of MCP-1 in angiogenesis and tumor progression. Blood. 2000;96:34-40.
[50] Ohnishi S, Yasuda T, Kitamura S, Nagaya N. Effect of Hypoxia on Gene Expression of Bone Marrow-Derived Mesenchymal Stem Cells and Mononuclear Cells. STEM CELLS. 2007;25:1166-77.

[51] Rehman J, Traktuev D, Li J, Merfeld-Clauss S, Temm-Grove CJ, Bovenkerk JE, et al. Secretion of Angiogenic and Antiapoptotic Factors by Human Adipose Stromal Cells. Circulation. 2004;109:1292-8.
[52] Hung S-C, Pochampally RR, Chen S-C, Hsu S-C, Prockop DJ. Angiogenic Effects of Human Multipotent Stromal Cell Conditioned Medium Activate the PI3K-Akt Pathway in Hypoxic Endothelial Cells to Inhibit Apoptosis, Increase Survival, and Stimulate Angiogenesis. STEM CELLS. 2007;25:2363-70.
[53] Okuyama H, Krishnamachary B, Zhou YF, Nagasawa H, Bosch-Marce M, Semenza GL. Expression of Vascular Endothelial Growth Factor Receptor 1 in Bone Marrow-derived Mesenchymal Cells Is Dependent on Hypoxia-inducible Factor 1. Journal of Biological Chemistry. 2006;281:15554-63.
[54] Leroux L, Descamps B, Tojais NF, Seguy B, Oses P, Moreau C, et al. Hypoxia Preconditioned Mesenchymal Stem Cells Improve Vascular and Skeletal Muscle Fiber Regeneration After Ischemia Through a Wnt4-dependent Pathway. Mol Ther. 2010;18:1545-52.
[55] Discher DE, Mooney DJ, Zandstra PW. Growth factors, matrices, and forces combine and control stem cells. Science. 2009;324:1673-7.
[56] Shen Q, Wang Y, Kokovay E, Lin G, Chuang SM, Goderie SK, et al. Adult SVZ stem cells lie in a vascular niche: a quantitative analysis of niche cell-cell interactions. Cell Stem Cell. 2008;3:289-300.
[57] Carrion B, Huang CP, Ghajar CM, Kachgal S, Kniazeva E, Jeon NL, et al. Recreating the perivascular niche ex vivo using a microfluidic approach. Biotechnology and Bioengineering. 2010;107:1020-8.
[58] Discher DE, Janmey P, Wang YL. Tissue cells feel and respond to the stiffness of their substrate. Science. 2005;310:1139-43.
[59] Engler AJ, Sen S, Sweeney HL, Discher DE. Matrix Elasticity Directs Stem Cell Lineage Specification. Cell. 2006;126:677-89.
[60] Mammoto A, Connor KM, Mammoto T, Yung CW, Huh D, Aderman CM, et al. A mechanosensitive transcriptional mechanism that controls angiogenesis. Nature. 2009;457:1103-8.
[61] Seib FP, Prewitz M, Werner C, Bornhäuser M. Matrix elasticity regulates the secretory profile of human bone marrow-derived multipotent mesenchymal stromal cells (MSCs). Biochemical and Biophysical Research Communications. 2009;389:663-7.
[62] Kasper G, Dankert N, Tuischer J, Hoeft M, Gaber T, Glaeser JD, et al. Mesenchymal Stem Cells Regulate Angiogenesis According to Their Mechanical Environment. STEM CELLS. 2007;25:903-10.
[63] Wilson CJ, Kasper G, Schütz MA, Duda GN. Cyclic strain disrupts endothelial network formation on Matrigel. Microvascular Research. 2009;78:358-63.
[64] Chun TH, Sabeh F, Ota I, Murphy H, McDonagh KT, Holmbeck K, et al. MT1-MMP-dependent neovessel formation within the confines of the three-dimensional extracellular matrix. The Journal of cell biology. 2004;167:757-67.
[65] Stratman AN, Saunders WB, Sacharidou A, Koh W, Fisher KE, Zawieja DC, et al. Endothelial cell lumen and vascular guidance tunnel formation requires MT1-MMP-dependent proteolysis in 3-dimensional collagen matrices. Blood. 2009;114:237-47.

[66] Collen A, Hanemaaijer R, Lupu F, Quax PH, van Lent N, Grimbergen J, et al. Membrane-type matrix metalloproteinase-mediated angiogenesis in a fibrin-collagen matrix. Blood. 2003;101:1810-7.
[67] Kroon ME, Koolwijk P, van Goor H, Weidle UH, Collen A, van der Pluijm G, et al. Role and localization of urokinase receptor in the formation of new microvascular structures in fibrin matrices. Am J Pathol. 1999;154:1731-42.
[68] Hiraoka N, Allen E, Apel IJ, Gyetko MR, Weiss SJ. Matrix metalloproteinases regulate neovascularization by acting as pericellular fibrinolysins. Cell. 1998;95:365-77.
[69] Ghajar CM, Blevins KS, Hughes CCW, George SC, Putnam AJ. Mesenchymal stem cells enhance angiogenesis in mechanically viable prevascularized tissues via early matrix metalloproteinase upregulation. Tissue engineering. 2006;12:2875-88.
[70] Ghajar CM, Kachgal S, Kniazeva E, Mori H, Costes SV, George SC, et al. Mesenchymal cells stimulate capillary morphogenesis via distinct proteolytic mechanisms. Experimental Cell Research. 2010;316:813-25.
[71] Kachgal S, Putnam A. Mesenchymal stem cells from adipose and bone marrow promote angiogenesis via distinct cytokine and protease expression mechanisms. Angiogenesis. 2011;14:47-59.
[72] Kachgal S, Carrion B, Janson IA, Putnam AJ. Bone marrow stromal cells stimulate an angiogenic program that requires endothelial MT1-MMP. J Cell Physiol. 2012;227:3546-55.
[73] Lafleur MA, Forsyth PA, Atkinson SJ, Murphy G, Edwards DR. Perivascular cells regulate endothelial membrane type-1 matrix metalloproteinase activity. Biochemical and biophysical research communications. 2001;282:463-73.
[74] Saunders WB, Bohnsack BL, Faske JB, Anthis NJ, Bayless KJ, Hirschi KK, et al. Coregulation of vascular tube stabilization by endothelial cell TIMP-2 and pericyte TIMP-3. J Cell Biol. 2006;175:179-91.
[75] Yana I, Sagara H, Takaki S, Takatsu K, Nakamura K, Nakao K, et al. Crosstalk between neovessels and mural cells directs the site-specific expression of MT1-MMP to endothelial tip cells. J Cell Sci. 2007;120:1607-14.
[76] Kurpinski K, Lam H, Chu J, Wang A, Kim A, Tsay E, et al. Transforming Growth Factor-β and Notch Signaling Mediate Stem Cell Differentiation into Smooth Muscle Cells. STEM CELLS. 2010;28:734-42.
[77] Taylor KL, Henderson AM, Hughes CCW. Notch Activation during Endothelial Cell Network Formation in Vitro Targets the Basic HLH Transcription Factor HESR-1 and Downregulates VEGFR-2/KDR Expression. Microvascular Research. 2002;64:372-83.
[78] Hirschi KK, Rohovsky SA, D'Amore PA. PDGF, TGF-β, and Heterotypic Cell–Cell Interactions Mediate Endothelial Cell–induced Recruitment of 10T1/2 Cells and Their Differentiation to a Smooth Muscle Fate. The Journal of Cell Biology. 1998;141:805-14.
[79] Hirschi KK, Rohovsky SA, Beck LH, Smith SR, D'Amore PA. Endothelial Cells Modulate the Proliferation of Mural Cell Precursors via Platelet-Derived Growth Factor-BB and Heterotypic Cell Contact. Circulation Research. 1999;84:298-305.
[80] Ding R, Darland DC, Parmacek MS, D'amore PA. Endothelial-mesenchymal interactions in vitro reveal molecular mechanisms of smooth muscle/pericyte differentiation. Stem cells and development. 2004;13:509-20.

[81] Au P, Tam J, Fukumura D, Jain RK. Bone marrow–derived mesenchymal stem cells facilitate engineering of long-lasting functional vasculature. Blood. 2008;111:4551-8.
[82] Ghajar CM, Kachgal S, Kniazeva E, Mori H, Costes SV, George SC, et al. Mesenchymal cells stimulate capillary morphogenesis via distinct proteolytic mechanisms. Experimental cell research. 2010;316:813-25.
[83] Ceccarelli J, Cheng A, Putnam A. Mechanical Strain Controls Endothelial Patterning During Angiogenic Sprouting. Cel Mol Bioeng. 2012;5:463-73.
[84] Montesano R, Pepper MS, Orci L. Paracrine induction of angiogenesis in vitro by Swiss 3T3 fibroblasts. J Cell Sci. 1993;105 (Pt 4):1013-24.
[85] Nehls V, Drenckhahn D. A microcarrier-based cocultivation system for the investigation of factors and cells involved in angiogenesis in three-dimensional fibrin matrices in vitro. Histochem Cell Biol. 1995;104:459-66.
[86] Nakatsu MN, Sainson RC, Aoto JN, Taylor KL, Aitkenhead M, Perez-del-Pulgar S, et al. Angiogenic sprouting and capillary lumen formation modeled by human umbilical vein endothelial cells (HUVEC) in fibrin gels: the role of fibroblasts and Angiopoietin-1. Microvasc Res. 2003;66:102-12.
[87] Nakatsu MN, Sainson RC, Perez-del-Pulgar S, Aoto JN, Aitkenhead M, Taylor KL, et al. VEGF(121) and VEGF(165) regulate blood vessel diameter through vascular endothelial growth factor receptor 2 in an in vitro angiogenesis model. Laboratory investigation; a journal of technical methods and pathology. 2003;83:1873-85.
[88] Sainson RC, Aoto J, Nakatsu MN, Holderfield M, Conn E, Koller E, et al. Cell-autonomous notch signaling regulates endothelial cell branching and proliferation during vascular tubulogenesis. FASEB journal : official publication of the Federation of American Societies for Experimental Biology. 2005;19:1027-9.
[89] Sainson RC, Johnston DA, Chu HC, Holderfield MT, Nakatsu MN, Crampton SP, et al. TNF primes endothelial cells for angiogenic sprouting by inducing a tip cell phenotype. Blood. 2008;111:4997-5007.
[90] Newman AC, Chou W, Welch-Reardon KM, Fong AH, Popson SA, Phan DT, et al. Analysis of Stromal Cell Secretomes Reveals a Critical Role for Stromal Cell–Derived Hepatocyte Growth Factor and Fibronectin in Angiogenesis. Arteriosclerosis, Thrombosis, and Vascular Biology. 2013.
[91] Newman AC, Nakatsu MN, Chou W, Gershon PD, Hughes CCW. The requirement for fibroblasts in angiogenesis: fibroblast-derived matrix proteins are essential for endothelial cell lumen formation. Molecular Biology of the Cell. 2011;22:3791-800.
[92] Berthod F, Germain L, Tremblay N, Auger FA. Extracellular matrix deposition by fibroblasts is necessary to promote capillary-like tube formation in vitro. J Cell Physiol. 2006;207:491-8.
[93] Chen X, Aledia AS, Ghajar CM, Griffith CK, Putnam AJ, Hughes CC, et al. Prevascularization of a Fibrin-Based Tissue Construct Accelerates the Formation of Functional Anastomosis with Host Vasculature. Tissue engineering Part A. 2009;15:1363-71.
[94] Chen X, Aledia AS, Popson SA, Him L, Hughes CC, George SC. Rapid Anastomosis of Endothelial Progenitor Cell-Derived Vessels with Host Vasculature Is Promoted by a High Density of Cotransplanted Fibroblasts. Tissue Eng Part A. 2010;16:585-94.

[95] Melero-Martin JM, Khan ZA, Picard A, Wu X, Paruchuri S, Bischoff J. In vivo vasculogenic potential of human blood-derived endothelial progenitor cells. Blood. 2007;109:4761-8.
[96] Au P, Daheron LM, Duda DG, Cohen KS, Tyrrell JA, Lanning RM, et al. Differential in vivo potential of endothelial progenitor cells from human umbilical cord blood and adult peripheral blood to form functional long-lasting vessels. Blood. 2008;111:1302-5.
[97] Shepherd BR, Jay SM, Saltzman WM, Tellides G, Pober JS. Human aortic smooth muscle cells promote arteriole formation by coengrafted endothelial cells. Tissue engineering Part A. 2009;15:165-73.
[98] Hegen A, Blois A, Tiron CE, Hellesoy M, Micklem DR, Nor JE, et al. Efficient in vivo vascularization of tissue-engineering scaffolds. Journal of tissue engineering and regenerative medicine. 2011;5:e52-62.
[99] Traktuev DO, Merfeld-Clauss S, Li J, Kolonin M, Arap W, Pasqualini R, et al. A population of multipotent CD34-positive adipose stromal cells share pericyte and mesenchymal surface markers, reside in a periendothelial location, and stabilize endothelial networks. Circ Res. 2008;102:77-85.
[100] Melero-Martin JM, De Obaldia ME, Kang SY, Khan ZA, Yuan L, Oettgen P, et al. Engineering robust and functional vascular networks in vivo with human adult and cord blood-derived progenitor cells. Circ Res. 2008;103:194-202.
[101] Au P, Tam J, Fukumura D, Jain RK. Bone marrow-derived mesenchymal stem cells facilitate engineering of long-lasting functional vasculature. Blood. 2008;111:4551-8.
[102] Koike N, Fukumura D, Gralla O, Au P, Schechner JS, Jain RK. Creation of long-lasting blood vessels. Nature. 2004;428:138-9.
[103] Oswald J, Boxberger S, Jorgensen B, Feldmann S, Ehninger G, Bornhauser M, et al. Mesenchymal stem cells can be differentiated into endothelial cells in vitro. Stem cells. 2004;22:377-84.
[104] Ferreira LS, Gerecht S, Shieh HF, Watson N, Rupnick MA, Dallabrida SM, et al. Vascular progenitor cells isolated from human embryonic stem cells give rise to endothelial and smooth muscle like cells and form vascular networks in vivo. Circ Res. 2007;101:286-94.
[105] Traktuev DO, Prater DN, Merfeld-Clauss S, Sanjeevaiah AR, Saadatzadeh MR, Murphy M, et al. Robust functional vascular network formation in vivo by cooperation of adipose progenitor and endothelial cells. Circ Res. 2009;104:1410-20.
[106] Levenberg S, Rouwkema J, Macdonald M, Garfein ES, Kohane DS, Darland DC, et al. Engineering vascularized skeletal muscle tissue. Nat Biotechnol. 2005;23:879-84.
[107] Stevens KR, Kreutziger KL, Dupras SK, Korte FS, Regnier M, Muskheli V, et al. Physiological function and transplantation of scaffold-free and vascularized human cardiac muscle tissue. Proceedings of the National Academy of Sciences of the United States of America. 2009;106:16568-73.

Chapter 3

Protease-Sensitive PEG Hydrogels Regulate Vascularization *In Vitro* and *In Vivo*

3.1 Introduction

Recapitulating angiogenesis *in vitro* and *in vivo* is of critical interest to the fields of tissue engineering and therapeutic angiogenesis. Current successes in tissue engineering are significantly limited by the inability to generate functional vasculature, which is necessary because diffusion is insufficient to meet the metabolic demands of larger tissues. Engineering vasculature is also of interest for the treatment of ischemic diseases, such as peripheral artery disease (PAD), a cause of significant morbidity in the United States in the form of critical limb ischemia (CLI) and other related conditions [1].

To address the need for vascularization, several cell-based approaches have been pursued. One promising approach to therapeutic vascularization involves the co-delivery of endothelial cells (ECs) with supportive stromal cells in a biomaterial system that supports neovascularization *in vivo* [2-4]. Natural hydrogel materials, such as fibrin,

collagen, and Matrigel, have been widely used in this approach by our laboratory [2, 5-8] and others [4, 9-13] as they are well known to support angiogenesis and vasculogenesis. However, such natural materials have inherent limitations, including variability associated with the original source and processing approaches, the potential for immunogenicity, and undefined biological functionalities [14]. Consequently, many investigators have alternatively pursued the use of synthetic materials as cell delivery substrates [14-17]. Such materials have their own advantages and disadvantages, but it is the general consensus that a blank slate material upon which key biological functionalities can be conferred (i.e. via peptide conjugation) offers the potential for enhanced control over cell function. Furthermore, this level of control is essential to better define the multiple roles of the extracellular matrix (ECM) on vascularization.

Peptide-functionalized poly(ethylene glycol) (PEG) hydrogel systems have been widely exploited to investigate the role of distinct biological signals in modulating cell invasion and in complex processes, such as vascularization, *in vitro* [18-29]. In these systems, PEG is typically functionalized with peptide sequences susceptible to cleavage by cell-derived matrix metalloproteases (MMPs) and with RGD, a minimal integrin-binding domain isolated from fibronectin that has been ubiquitously tethered to a variety of biomaterials to render them adhesive [14]. Ideally, these systems should undergo degradation at a rate that promotes the rapid formation of stable vasculature. To this end, tuning of the material platform is required to achieve sufficiently rapid cell migration, proliferation, and organization into tubular structures without compromising the patency or functionality of the resulting vasculature. The majority of early studies in this area utilized a MMP-cleavable peptide composed of a collagen-derived cleavage

sequence, GPQG↓IWGQ (cleavage site indicated by↓), with flanking regions on either side to facilitate crosslinking via thiol or amine chemistries. Cell invasion and vascularization were improved in these gels when compared to non-degradable controls [22, 26, 29]. More recent studies have used MMP-cleavable peptides that are cleaved with faster kinetics for studies of cell migration and vascularization *in vitro* with promising results [21, 25, 30, 31]. Others have tuned the mechanical properties of the construct to indirectly alter the extent of proteolysis needed to support robust vascularization [25, 26]. This technique has experienced some success, but, perhaps due to microstructural differences in materials with similar bulk properties, the optimal mechanical regime has been found to differ substantially among constructs with differing PEG chemistries. As a whole, these prior studies suggest functionalized PEG gels are a viable option to support vascularization, thereby warranting further study.

Despite this focus on elucidating the role of matrix mechanics and degradation *in vitro*, few studies have focused on translating these findings *in vivo* to further motivate the design of pro-angiogenic materials. Additionally, many of the materials utilized for investigations *in vitro* are less suitable for use *in vivo*, due to the requirement for light (UV or visible) to initiate polymerization. To date, *in vivo* studies of vascularization in PEG-peptide constructs have focused on controlled delivery of VEGF to facilitate the ingrowth of host vessels into gels incorporating the slowly degradable GPQG↓IWGQ peptide [26, 28, 32, 33]. While PEG-based materials have shown significant potential in the context of this cell-mediated release paradigm [34], comparatively few studies have demonstrated the utility of PEG hydrogels as suitable matrices to direct the vascularization of transplanted cells *in vivo*.

The goal of this work was to investigate the roles of gel mechanical properties and susceptibility to proteolysis in vascular morphogenesis *in vitro* and *in vivo*, thereby bridging the gap between *in vitro* mechanistic studies and translation-focused *in vivo* applications. We fabricated PEG hydrogels via Michael-type addition of PEG macromers and cysteine-containing MMP-sensitive and adhesive peptides, and then characterized their ability to support vascularization from endothelial cells and stromal fibroblasts. Two MMP-sensitive peptides were used for crosslinking, GPQG↓IWGQ (slow degradation) and VPMS↓MRGG (more rapid degradation [21]). RGD was used as an adhesive moiety to facilitate cell attachment to the PEG gels. Materials were characterized and subsequently investigated for their capacity to support vascular morphogenesis over a period of two weeks *in vitro* and in subcutaneous pockets on the dorsal flank of SCID mice *in vivo*.

3.2 Methods

3.2.1 Cell Isolation and Culture

Human umbilical vein endothelial cells (HUVECs, henceforth referred to as ECs) were harvested from fresh umbilical cords according to a previously established protocol [35]. ECs were cultured in supplemented Endothelial Growth Medium (EGM-2, Lonza, Walkersville, MD) at 37^{o}C and 5% CO_2 and used at passage 3. Normal human lung fibroblasts (NHLFs, Lonza) were cultured in M199 (Invitrogen Corporation, Carlsbad, CA) with 10% fetal bovine serum (FBS), 1% penicillin/streptomycin (Mediatech, Manassas, VA), and 0.5% gentamicin (Invitrogen) at 37^{o}C and 5% CO_2 and

used prior to passage 15. Cells were cultured in monolayers until reaching 80% confluency and passaged with 0.05% trypsin-EDTA (Invitrogen).

3.2.2 PEG Hydrogel Formation

Hydrogels were formed via a Michael-type addition reaction of 4-arm PEG vinyl sulfone (henceforth termed PEG-VS) (20 kDa, JenKem USA, Allen, TX) with a combination of thiol-containing adhesive and protease-sensitive peptides by modifying a published protocol [36]. To prepare the gels, PEG-VS was dissolved in HEPES (50 mM, pH 8.4, supplemented with growth factors from endothelial medium bullet kit) at the appropriate concentration to produce gels of 3.5% or 5% (w/v) total solids content. The adhesive peptide (CGRGDS, Genscript, Piscataway, NJ) was added to the PEG solution at 10 μg/ml in HEPES to yield a final adhesive site density upon gelation of 500 μM and the solution was reacted 30 minutes at room temperature. Following conjugation of RGD, bis-cysteine-containing crosslinking peptides were added in HEPES such that -SH and -VS groups were present at a 1:1 molar ratio. Gels were polymerized with 1 of 2 peptides, Ac-GCRD-GPQG↓IWGQ-DRCG-NH_2 or Ac-GCRD-VPMS↓MRGG-DRCG-NH_2 (cleavage site indicated by↓). After mixing, precursor solutions (3.5% PEG-G, 5% PEG-G, 3,5% PEG-V, and 5% PEG-V) were polymerized for 1 hour at 37^{o}C in Teflon molds for rheology experiments or in sterile 1-ml syringes with the needle end cut off for all other experiments [37]. After polymerization gels were transferred to medium or PBS, as appropriate. All gels were formed under aseptic conditions from precursors that were filtered through a 0.22 um syringe filter.

3.2.2 Mechanical Characterization of PEG Gels

Bulk mechanical properties were characterized via parallel plate rheology on pre-swollen gels. Following polymerization in Teflon molds, 100 µl gels were swollen overnight in PBS at 37^{o}C. Measurements were obtained on an AR G2 rheometer (TA Instruments, New Castle, DE) equipped with a Peltier stage and an 8 mm geometry. Both surfaces were coated with P800 sandpaper (3M, St. Paul, MN) and the gap was adjusted to apply a constant 0.1 N force to prevent slip during measurement. For each gel, a 5 minute time sweep was followed by a frequency sweep from 0.1 to 10 Hz at 5% strain and then a strain sweep from 0.1 to 50% at 1 Hz. Reported shear storage modulus (G') values are the average over the linear viscoelastic region of the frequency sweep.

The equilibrium volumetric swelling ratio was also obtained for each gel type. Cell-free gels 50 µl in volume were polymerized in cut off syringes, as described above, and swollen at 37^{o}C in PBS for 48 hours. At this point, each gel was weighed, frozen, and lyophilized, to give values for the wet and dry weight of each gel. The volumetric swelling ratio was calculated from the mass swelling ratio according to a previously described method [38]:

$$Q = 1 + \frac{\rho_{polymer}}{\rho_{solvent}}(q - 1)$$

where q is the mass swelling ratio (wet weight/final dry weight), $\rho_{polymer}$ is the polymer density (1.07 g/ml for PEG), and $\rho_{solvent}$ is the density of the buffer (~1 g/ml).

Cell-mediated bulk hydrogel degradation was assessed by monitoring the swelling ratio of 50 µl gels containing 10^6 ECs/ml and 10^6 NHLFs/ml. Gels were

cultured at 37^{o}C and 5% CO_2 up to 14 days. The swelling ratio was determined as for gels without cells.

3.2.3 Dextran Release from PEG Gels

The bulk transport of dextran through the hydrogels was quantified as described previously [39] to probe the relative ease of diffusion of macromolecular species through different hydrogel formulations. Acellular hydrogels were prepared under aseptic conditions with 5 µg of 70 kDa Texas red-conjugated dextran (Life Technologies) incorporated in each 50 µl gel. Hydrogels were incubated in sterile PBS at 37^{o}C and the supernatant was aseptically collected and replaced with fresh PBS at 1, 3, 6, 12, 24, and 72 hours after polymerization. After 72 hours, gels were digested with 40 IU collagenase (Worthington Biochemical, Lakewood, NJ) in PBS to release any remaining dextran. The supernatants from each time point and the degraded gels were measured with a Fluoroskan Ascent FL (Thermo Scientific) plate reader at Ex:560/Em:620. The mass of dextran in each sample was determined by comparison to a standard curve of dextran in PBS.

3.2.4 Vasculogenesis Assay in PEG Hydrogels

ECs were fluorescently labeled via retroviral transduction with a gene encoding mCherry (Clonteck, Mountain View, CA) as previously described [5]. Lipofectamine 2000 (Life Technologies) was used to transfect Phoenix Ampho cells (Orbigen, San Diego, CA) with a plasmid encoding for mCherry. Viral supernatant was collected after 48 hours, passed through a 0.45 µm syringe filter and supplemented with 5 µg/ml

Polybrene (EMD Millipore, Billerica, MA) prior to incubation with EC for 6 hours. The medium was changed to EGM-2 and cells were cultured overnight. Transduction was repeated via another round of viral infection the following day, and the ECs were then grown to confluence and used directly in the vasculogenesis assay. Constructs were polymerized in 50 µl aliquots using cut off syringes. Cell mixtures in a 1:1 ratio of ECs and NHLFs were added for a total of 10^5 cells/gel. Following polymerization, cell-seeded constructs were cultured in fully supplemented EGM-2 in a 12-well plate with the media changed every other day. At 7 and 14 days post-fabrication, gels from each condition were washed several times with PBS and then fixed with formalin prior to imaging. Low magnification fluorescent images were obtained of vessel network formation in each gel. Each gel was imaged at 5 locations in the interior of the gel using an Olympus IX81 spinning disk confocal microscope (Olympus, Center Valley, PA) with a Hammamatsu (Bridgewater, NJ) camera. Average total network length was determined as described previously [40] for each condition using the automated Angiogenesis Module in Metamorph Premier Software (Molecular Devices Inc., Sunnyvale, CA).

To monitor the effect of inhibition of MMP or plasmin-mediated degradation on organization into vascular networks, a subset of experiments was conducted with a broad-spectrum MMP inhibitor, GM6001, in DMSO or the serine protease inhibitor aprotinin, added to both the gel precursor solution and the culture medium. As a control, additional constructs were treated with the vehicle alone (DMSO). GM6001 (EMD Chemicals, San Diego, CA) was added at 10 µM and aprotinin (Sigma) was added at 2.2 µM, as used in previous work from our lab[6]. Inhibitors were replenished

with each media change. At 7 days post-fabrication, gels were fixed then imaged at low magnification.

3.2.5 PEG Hydrogel Implantation in SCID Mice and Laser Doppler Perfusion Imaging

All animal procedures were performed following a protocol approved by the University of Michigan Committee on Use and Care of Animals in accordance with NIH guidelines for the use of laboratory animals. Male 6-8-week old C.B.-17/SCID mice (Taconic Labs, Hudson, NY) were used for all experiments. Anesthetic/analgesic cocktail of 95 mg/kg ketamine (MWI Vet, Boise, ID), 9.5 mg/kg xylazine (MWI Vet, Boise, ID), and 0.059 mg/kg buprenorphine (Bedford Laboratories, Bedford, OH) was delivered to each mouse via intraperitoneal injection. The dorsal flank of each mouse was cleared of fur by shaving followed by the application of a depilatory agent (Nair, Fisher Scientific, Pittsburgh, PA). The region was then sterilized with betadine (Thermo Fisher Scientific, Fremont, CA) and wiped down with an alcohol pad. Implants were prepared as described above; PEG was mixed with RGD before administering the drug cocktail to mice to ensure a 30 minute incubation time elapsed before polymerization of the gels. Prior to initiation of the procedure, cell mixtures in a 1:1 ratio of ECs:NHLFs were prepared and aliquoted to yield a total of 3 million cells per injection sample (300 µl total volume, or 10 million total cells/ml). As prior studies from our lab using fibrin [41] and from others using PEG-VS gels without VEGF [32] have illustrated that minimal vascularization is seen in acellular controls, all implants contained cells and gel conditions alone were varied. Just prior to implantation, the bis-cysteine peptide in HEPES was combined with the PEG+RGD solution, the medium was aspirated from the

top of the cell pellet, and the cells were resuspended in the gel precursor. Solutions were immediately injected subcutaneously on the dorsal flank of the mouse, with two implants placed per animal. Animals were kept stationary for 5 minutes to allow for implant gelation and then subjected to laser Doppler perfusion imaging (LDPI, Perimed AB, Sweden). Each mouse was imaged in triplicate. Mice were then placed in fresh cages for recovery. At days 4, 7, and 14, mice were anesthetized with the cocktail described above and then subjected again to LDPI. Surgeons were not blinded to the experimental conditions.

3.2.6 Dextran Tracer Injection and Implant Removal

Implants were retrieved after 7 or 14 days following systemic administration of a functionality-defining tracer, as described in previous work from our laboratory [41]. Briefly, a 70 kDa Texas Red-conjugated dextran (λex/em of 595/615 nm, Invitrogen) was used to assess inosculation of the transplanted cells within the implant with host vessels. Following LDPI at each retrieval time point, each mouse was placed in a restraint device and 200 µl of a 5 mg/ml dextran solution in PBS was injected via the tail vein. After injection, mice were moved to fresh cages and the tracer was allowed to circulate systemically for 10 minutes. Animals were then euthanized and the implants were surgically excised.

3.2.7 Implant Processing and Histology

All explants were fixed 1 hour in 4% PFA and then moved to 0.4% PFA overnight. Following fixation, samples were rinsed several times in cold PBS and then

transferred to a sterile solution of 30% sucrose in PBS for 48 hours at 4^{o}C. At this time, explants were transferred to a mixture containing 2 parts 30% sucrose in PBS and 1 part OCT embedding compound (Andwin Scientific, Schaumburg, IL) for another 24 hours at 4^{o}C. Explants were then transferred to 100% OCT and kept another 24 hours at 4^{o}C. Each sample was then finally embedded in 100% OCT in a disposable plastic mold (Fisher Scientific, Pittsburgh, PA) and flash frozen on the surface of liquid nitrogen. Frozen sections were generated from each sample by the histology core at the University of Michigan School of Dentistry.

Sections were stained for human CD31 using both immunohistochemistry (IHC) and immunofluorescence (IF). After staining, sections were imaged using an Olympus IX81 spinning disk confocal microscope with a DP2-Twain (Olympus) color camera for visualizing IHC stained slides and a Hammamatsu camera for visualizing fluorescent-stained sections.

For IHC staining, tissues were warmed at room temperature and rinsed with PBS. Sections were incubated with 0.05% trypsin-EDTA for 10 minutes at 37^{o}C for antigen retrieval and washed with DI water then TBS-T. Sections were blocked 5 minutes using a peroxidase blocking solution (Dako EnVision System-HRP (DAB) kit, Dako, Carpinteria, CA). Primary antibody (human anti-mouse CD31, Dako) was diluted 1:50 in TBS-T and applied to slides. Following incubation overnight at 4^{o}C, slides were treated for 30 minutes with the HRP-conjugated anti-mouse secondary antibody provided in the kit. Prior to imaging, slides were mounted with xylene mounting medium (Fisher Scientific) and a #1 coverslip. One set of sections was imaged without any

counterstain; the remaining sections were counterstained with hematoxylin and eosin and then imaged.

For IF staining, slides were warmed for 20 minutes then rinsed three times with PBS. Sections were blocked with 5% goat serum in PBS to eliminate non-specific protein binding. The primary antibody (human CD31, Santa Cruz Biotechnology, Inc., Santa Cruz, CA) was diluted 1:50 in 5% goat serum and added to samples for an overnight incubation at 4^{o}C. The unbound antibody was removed at the end of the incubation with three washes with PBS. The secondary antibody (Alexa Fluor 488 goat anti-rabbit, Invitrogen) was added to tissues at a 1:100 dilution and tissues were incubated 30 minutes at room temperature. The unbound antibody was removed by three additional washes with PBS. Slides were then mounted with VectaShield (Vector Labs, Burlingame, CA) and covered with a #1 glass coverslip prior to imaging. Representative images were chosen for each condition.

Using sections stained with hCD31 via IHC, the number of blood vessels derived from transplanted human cells were quantified manually. Structures were considered blood vessels if they exhibited a rim of positive hCD31 stain and a hollow lumen. The average number of vessels per field of view in each section was determined by averaging the values obtained by two independent evaluators for at least 5 images per animal taken at 40x.

3.2.8 Statistics

All statistical analyses were performed using GraphPad Prism (GraphPad Software, La Jolla, CA). Data are from $n \geq 3$ and are reported as mean ± SEM.

Analyses were performed with one or two-way ANOVA followed by Bonferroni ‘s multiple comparison post-tests. Statistical significance was assumed when $p < 0.05$.

3.3 Results

3.3.1 Gelation and Mechanical Characterization

PEG-based hydrogels were prepared by reacting PEG-VS with cysteine-containing adhesive peptides and bis-cysteine containing cross-linking peptides (see schematic in Figure 3-1A). One of two different cross-linking peptides were used: GPQG↓IWGQ (henceforth abbreviated as PEG-G) or VPMS↓MRGG (PEG-V). Gelation occurred within 5 minutes and crosslinking was complete within 1 hour, as assessed with shear rheology (data not shown). Mechanical characterization of pre-swollen gels composed of 3.5 and 5% w/v and each degradable peptide via shear rheology revealed that the storage modulus (G’) did not vary as a function of the crosslinking peptide used, but increased significantly with increasing gel solids content (Figure 3-1B). Measurement of the volumetric swelling ratio for each gel type indicated that the 3.5% gels swelled significantly more than 5% gels (Figure 3-1C). Extent of swelling did not significantly differ between PEG-G and PEG-V gels.

In addition, because gels that undergo bulk degradation exhibit increases in swelling ratio over the course of degradation [19], the swelling ratio with cells was also obtained to assess the role of cell-mediated degradation in remodeling of the gel networks crosslinked with each peptide (Figure 3-1D). At day 1, swelling ratio values for each condition matched those obtained for gels without cells. Over the course of 2 weeks, statistically significant changes in swelling ratio were observed for PEG-V, but

not PEG-G gels. Constructs without cells did not undergo significant changes in swelling over the course of 14 days (data not shown), suggesting that proteolysis, and not hydrolysis, mediates the observed effects.

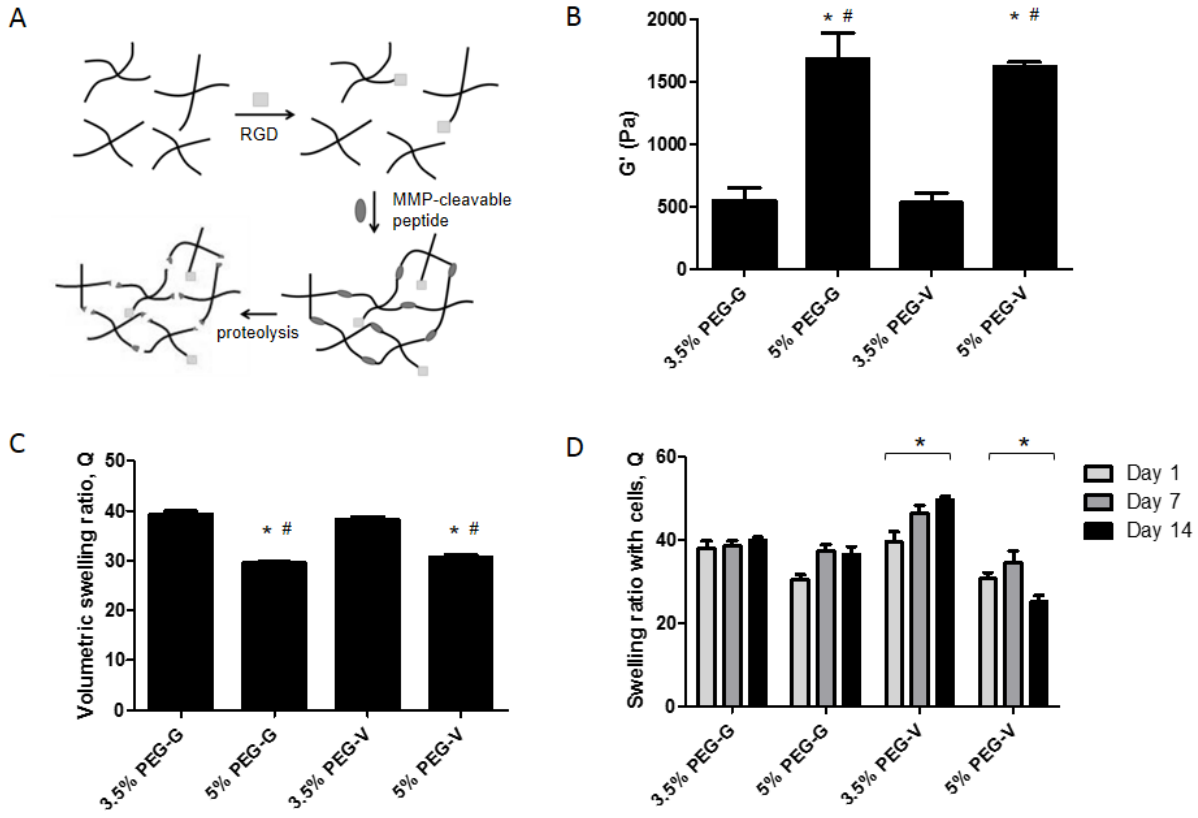

Figure 3-1 Formation and mechanical characterization of PEG hydrogels.. A. Hydrogels were formed via Michael-type addition of cysteine-containing RGD and MMP-degradable peptides (GCRD-GPQG↓IWGQ-DRCG and GCRD-VPMS↓MRGG-DRCG, cleavage at ↓) with 4-arm PEG vinyl sulfone. Gels are susceptible to MMP-mediated degradation but not hydrolysis. B. Hydrogels were polymerized, swollen, and their mechanical properties tested via shear rheology. All gels tested contained 500 μM RGD. *Significantly different from 3.5%G. #Significantly different from 3.5%V. $p < 0.05$, one-way ANOVA followed by Bonferroni post-tests. C. Volumetric swelling ratios of equilibrated acellular gels. *Significantly different from 3.5%G. #Significantly different from 3.5%V. $p < 0.05$, one-way ANOVA followed by Bonferroni post-tests. D. Swelling ratio of hydrogels containing cells changed significantly (indicated with *) from Day 1 to 14 in 3.5% and 5% V gels. $p < 0.05$, two-way ANOVA followed by Bonferroni post-tests.

3.3.2 Dextran Release from PEG Hydrogels

Cumulative release profiles of fluorescent dextran were generated for each hydrogel, and the data were normalized to the total mass of dextran entrapped (Figure 3-2A). Experimental data were fit to the following equation, corresponding to a first-order exponential approximation[39] of Fickian diffusion through a planar slab[42], using non-linear least squares regression:

$$M = M_o + (M_f - M_o)[1 - e^{-Kt}] \quad (2)$$

The equation modeled the release data for 3.5% PEG-G, 5% PEG-G, 3.5% PEG-V, and 5% PEG-V gels (R^2: 0.91, 0.89, 0.80, 0.85, respectively). From these data, the rate constant, K, was calculated for all hydrogel formulations, and a sum-of-squares F-test

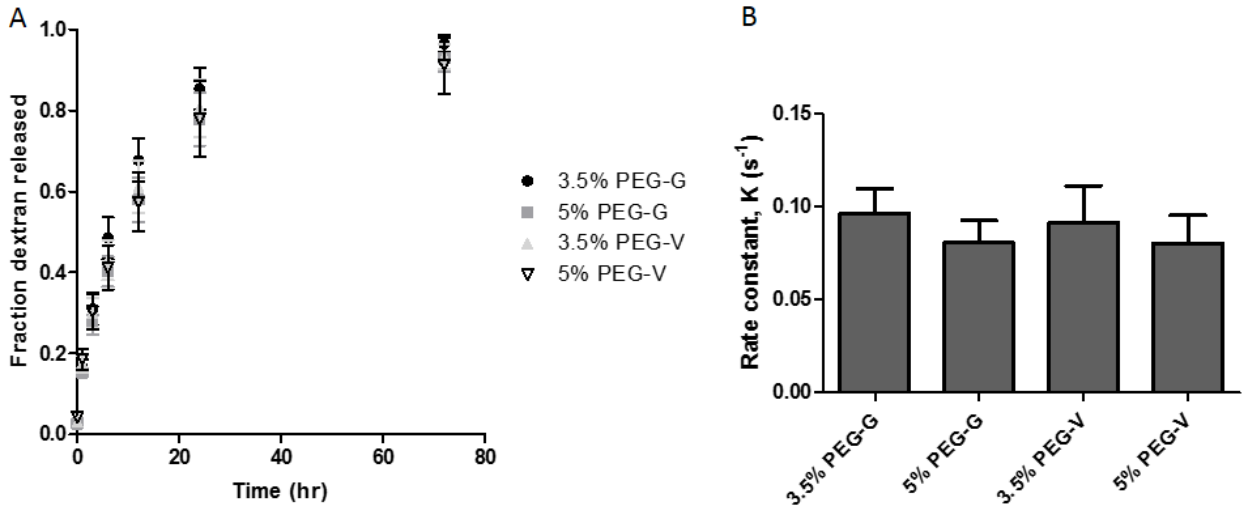

Figure 3-2 Dextran release from PEG gels. A. To assess bulk transport within the hydrogels, the release of 70 kDa Texas red-conjugated dextran entrapped within polymerized gels was measured over 72 hours. B. Rate constants, K, were determined by fitting release profiles to a first-order exponential approximation. No significant differences were found across gel formulations. $p > 0.05$, sum-of-squares F-test.

demonstrated no significant differences between release rates across gel formulation (Figure 3-2B).

3.3.3 Vascularization of PEG Gels In Vitro

Co-encapsulation of ECs and NHLFs in PEG-peptide hydrogels resulted in the formation of primitive capillary-like networks in all conditions over a period of 2 weeks

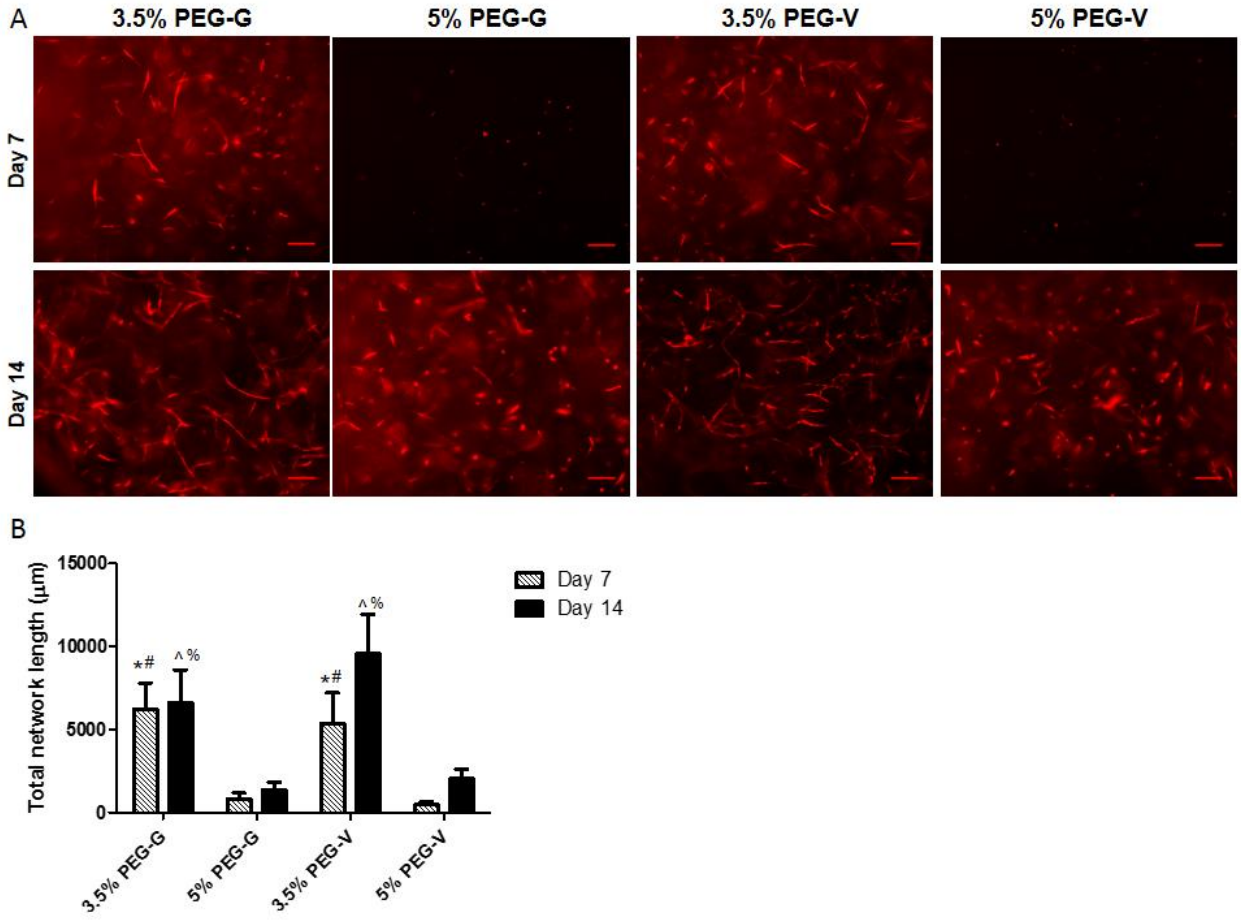

Figure 3-3. Vasculogenesis in vitro was monitored in PEG hydrogels of different w/v% and cross-linked with either of two degradable peptides.. A. mCherry tagged ECs co-encapsulated with unlabeled fibroblasts organized into vascular networks in gels, and were imaged after 7 or 14 days (scale bars = 200 μm). B. Quantification of the total lengths of the vessel networks showed that the extent of vascularization was significantly higher in lower w/v% gels and slightly increased at later time points in PEG-V gels. Significant differences were found via 1-way ANOVA followed by Bonferroni post-tests and are indicated according to the following symbols: * compared to 5% PEG-G at 7 days, # compared to 5% PEG-V at 7 days, ^ compared to 5% PEG-G at 14 days, and % compared to 5% PEG-V at 14 days, $p < 0.05$.

(Figure 3-3A). Labeling ECs with the mCherry gene facilitated visualization of network formation and quantification using the Angiogenesis Module in Metamorph. The extent of vascularization, as measured by total network length, differed significantly based on gel identity (Figure 3-3B). Lower w/v% gels supported more robust vascularization in PEG-G and PEG-V gels. Network length at day 7 was comparable between PEG-G and PEG-V gels at matching w/v%. By day 14, PEG-V gels appeared to support

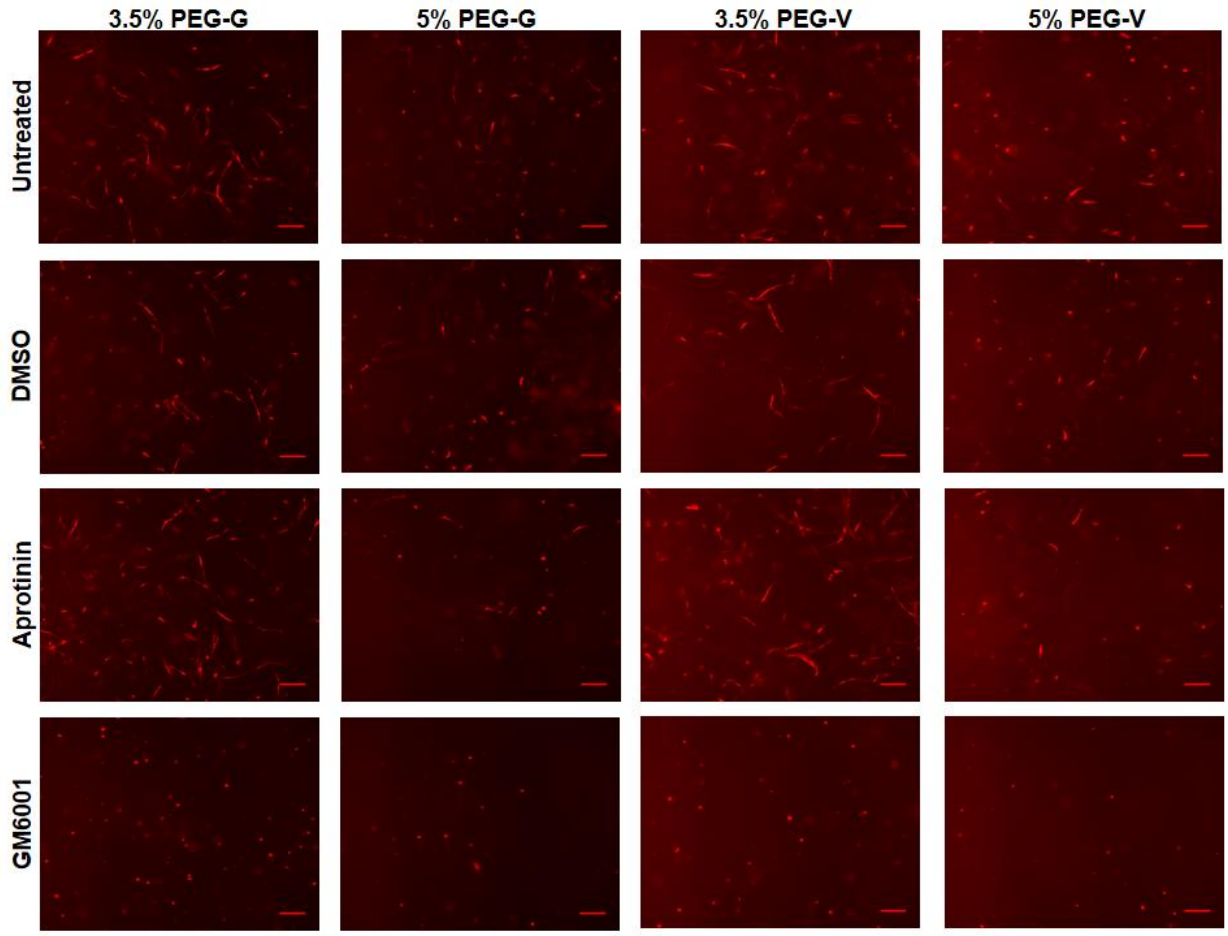

Figure 3-4. Vasculogenesis with protease inhibitors.. . Vasculogenesis was monitored *in vitro* in gels of different w/v% and crosslinking peptides in untreated control gels and in the presence of 10 μM GM6001, DMSO, or 2.2 μM aprotinin in gels and culture media. mCherry tagged-ECs co-encapsulated with unlabeled fibroblasts organized into vascular networks in control gels and in gels containing DMSO or aprotinin, but not in gels containing GM6001. Constructs were fixed and imaged after 7 days (scale bars = 200 μm)

increased vascularization compared to day 7 values and to PEG-G gels. Upon statistical analysis, however, differences between days 7 and 14 and between matched PEG-G and PEG-V gels were not significant.

EC tubule formation was attenuated in the presence of the broad-spectrum MMP inhibitor, GM6001 (Figure 3-4). ECs remained round and did not organize into tubules in the presence of GM6001 in all gel formulations tested, regardless of peptide identity or hydrogel w/v%. By contrast, the addition of either a DMSO vehicle or the serine protease inhibitor aprotinin had no significant effects.

3.3.4 Non-Invasive Perfusion Measurement of PEG Hydrogels Implanted In Vivo

PEG hydrogels containing ECs and NHLFs were injected subcutaneously on the dorsal flank of SCID mice and the vascularization by the implanted cells and subsequent inosculation with the host were monitored over 14 days. LDPI was used to monitor perfusion through the implant non-invasively. Measurements were performed immediately after implant placement and then again at 4, 7, and 14 days after implantation (Figure 3-5). For all conditions, perfusion qualitatively increased over the course of the experiment. LDPI data suggest the rate of implant perfusion differs as a function of peptide identity, with significant increases in perfusion seen between 0 and 4 days for PEG-V gels only. In contrast, PEG-G gels appear to undergo less pronounced and slower changes in perfusion, particularly between 0 and 4 days, as assessed by LDPI.

3.3.5 Histological Analysis of Harvested Tissues

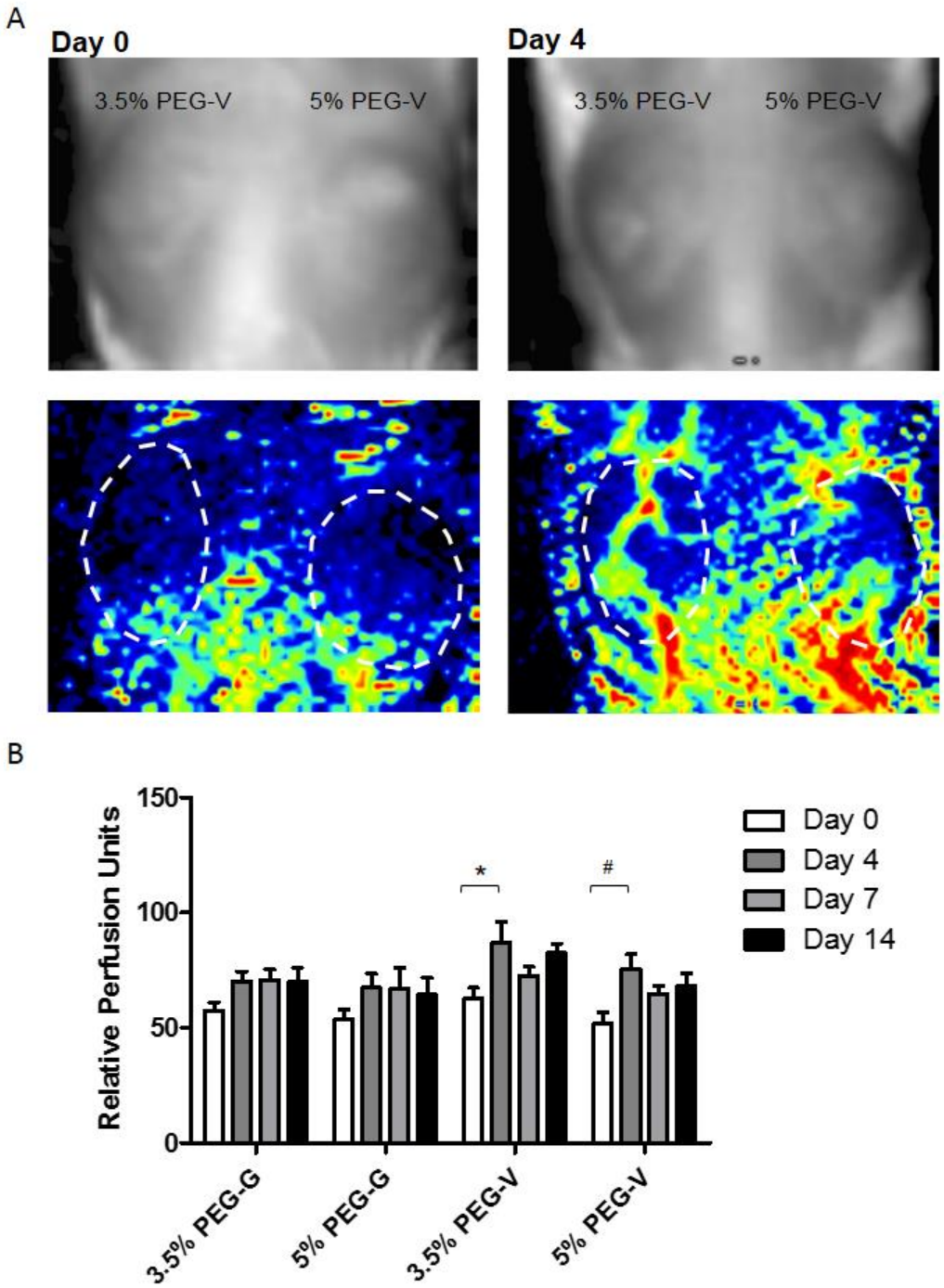

Figure 3-5. Laser Doppler perfusion imaging was used to non-invasively quantify blood flow after subcutaneous injection of gel constructs.. .(A) Upper images show implant location on mouse. Lower images are LDPI heat maps indicating degree of perfusion. (B) Quantification of relative perfusion shows differences between gel constructs. Statistically significant effects for both day and gel composition were found by 2-way ANOVA. Statistically significant increases in perfusion were observed from days 0 to 4 for 3.5% PEG-V (*) and 5% PEG-V (#). $p < 0.05$ 2-way ANOVA followed by Bonferroni post-tests.

Upon retrieval from the subcutaneous space, the implanted PEG-based constructs exhibited visible redness, suggesting that implants anastomosed with to the host vasculature within 7 days *in vivo* (Figure 3-6).

Cryosections stained for human CD31 demonstrated that all four of the hydrogel compositions tested supported the transplanted human ECs (Figure 3-7A). These human CD31-stained sections showed the presence of lumen-containing networks (arrows) containing host erythrocytes (inset), indicating the formation of a perfused vascular network from the transplanted human ECs for all gel formulations tested (Figure 3-7A). All implants contained a clearly delineated border between mouse tissue and the PEG gel, suggesting that the ingrowth of host connective tissue into these PEG gels is relatively slow. However, local gel degradation and cell-mediated matrix deposition in the periphery of vessels, illustrated by the presence of eosinophilic matrix around hCD31-stained vasculature, was observed, particularly at day 14; the remainder of the gel persisted intact.

Qualitatively, differences in vasculature were observed across conditions. However, quantification of vessel density showed the extent of vascularization differed significantly only between 3.5% and 5% PEG-V implants harvested at 7 days (Figure 3-7B). Systemic administration of a fluorescent dextran tracer further confirmed inosculation of host vessels with those that form within the PEG gel implants. Imaging of cryosectioned implants stained with hCD31 from tracer-injected animals revealed dextran-perfused vessels (red) lined with human CD31+ cells (green) in all gel types (Figure 3-8).

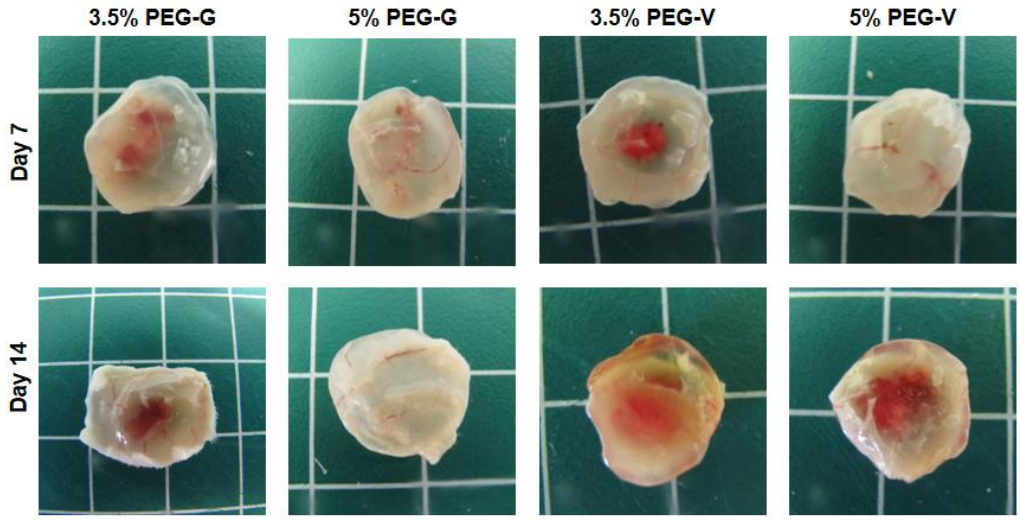

Figure 3-6. .Macroscopic images of implants harvested at days 7 and 14. Visible redness within implants suggested implant vasculature inosculated with host vessels in all gel constructs after implantation.

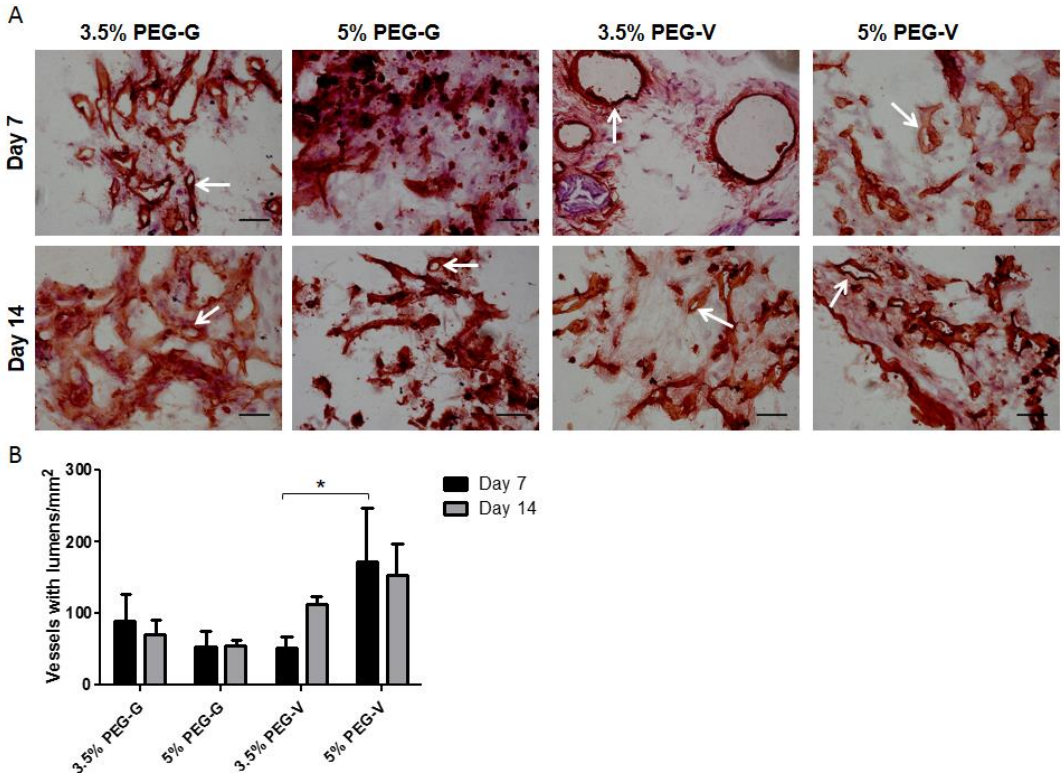

Figure 3-7. Staining for human vessels.. A. IHC and H&E staining of cryosections from implants retrieved after 7 or 14 days *in vivo*. Sections were stained for human CD31, counterstained with H&E, and then imaged at 40x (scale bars = 50 μm). Arrows point to representative hCD31-positive vessels. B. Vessel density was quantified from stained sections and compared with a 2-way ANOVA followed by Bonferroni post-tests. There was a significantly higher density of vessels in the 5% PEG-V gels compared to the 3.5% PEG-V gels at 7 days.

3.4 Discussion

In this study, we demonstrated PEG hydrogels functionalized with adhesive and MMP-degradable peptides support the formation of vascular networks from encapsulated cells both *in vitro* and *in vivo*. By varying the solids content of the hydrogels and the identity of the protease-sensitive cross-linking peptides, we investigated the respective roles of gel mechanical properties and the kinetics of proteolysis in vasculogenesis. Our investigation of dextran transport demonstrated no significant differences between gel formulations, suggesting limitations in the transport of nutrients or growth factors are not responsible for differences in vascular network formation in the *in vitro* model. Our *in vitro* results showed that increasing solids content to increase gel mechanical properties significantly attenuated vascular morphogenesis in 3D. Nevertheless, the formation of vessel networks was quantitatively similar for the two different cross-linking peptides studied. Our *in vivo* results showed that all gel formulations supported the formation of perfused vasculature from transplanted cells and vessel density was not attenuated in more highly crosslinked or in less degradable gels. Collectively, these findings demonstrate that engineered biosynthetic hydrogels have translational potential to deliver cells that promote vascularization in engineered or ischemic tissues.

Prior studies have demonstrated the utility of PEG-based hydrogels for 3D cell cultures [16, 43-45] and as materials to direct tissue regeneration *in vivo* [19, 46]. However, the number of reports in which this family of materials has been applied to fundamental studies of neovascularization remains relatively small. Among these, most

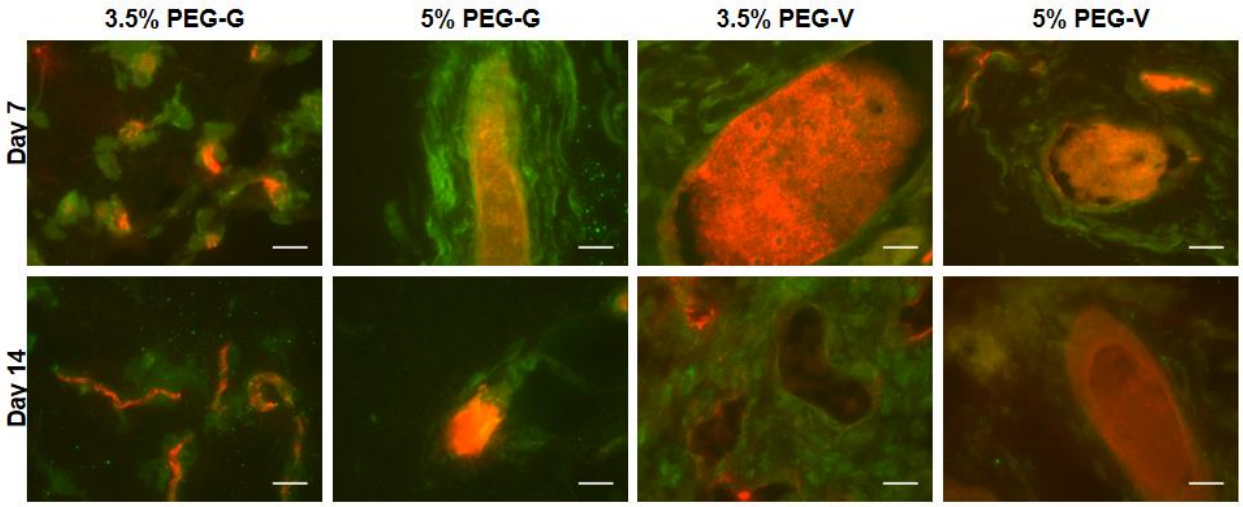

Figure 3-8.. Red fluorescent 70-kDa dextran was administered systemically to mice prior to implant retrieval on day 7. Following fixation and cryosectioning, tissues were stained for human CD31 (green) and imaged. Red present within hCD31+ structures indicated inosculation of host and implant vasculature (scale bars = 25 μm).

have focused on photopolymerizable PEG-diacrylate hydrogels, showing that proteolytically degradable variants support the assembly of microvascular networks *in vitro* [25, 26, 29, 47] and *in vivo* [26, 28], and support ingrowth of host vessels following release of VEGF [33]. Another recent study exploited PEG-norbornene as the base material, and encapsulated ECs in hydrogel arrays formed via photopolymerization [48]. By contrast, gels formed via Michael-type addition reactions of cysteine-containing cross-linking peptides with PEG-vinyl sulfone have shown potential as delivery agents for VEGF that promote vascular in growth *in vivo* [32]. However, our study is the first, to our knowledge, demonstrating their ability to support vascular morphogenesis from encapsulated cells *in vitro*. As a tool, this biomaterial platform is critical as a means to better define the instructive role of the microenvironment on the formation of vascular networks, and provides a system for defining additional cues to an initially bioinert

material in a way that should complement existing efforts to deconstruct natural materials (e.g., fibrin, collagen). By varying the identity of the cross-linking peptides to alter the rates of proteolysis and tuning the solids content of the gels to alter the mechanical properties, we have investigated the impact of two key matrix cues on vascular morphogenesis both *in vitro* and *in vivo*.

To alter gel degradation rates, we selected two peptides that are cleaved at different rates by several MMPs, although others recently reported on gels crosslinked by peptides with more specific susceptibilities [49]. GPQG↓IWGQ is based on a motif derived from type I collagen, and is cleaved by several MMPs that have been implicated in vascularization [36, 50]. VPMS↓MRGG was identified from a peptide library screening [51] and is degraded more quickly than GPQG↓IWGQ by MMPs 1 and 2 in solution and in gels [21]. Quantification of hydrogel swelling in the presence of cells revealed that PEG-V gels underwent significant changes in swelling behavior over 14 days, which were not observed in PEG-G gels. These data suggest the encapsulated ECs and fibroblasts more rapidly degrade PEG-V than PEG-G gels, in agreement with the published comparative rates of degradation of the two peptides by MMPs 1 and 2 [21, 51]. Despite the measured differences in gel swelling in the presence of ECs and NHLFs, vascularization in PEG-V gels *in vitro* was not statistically higher than in PEG-G gels. This may result from a delay between the onset of degradation and matrix vascularization, an idea corroborated by the qualitative increase in vascularization of PEG-V gels at later time points *in vitro*. Nonetheless, vascular network formation within these hydrogels was also verified to be MMP-dependent based on the observation that morphogenesis was attenuated in the presence of the broad-spectrum MMP inhibitor,

GM6001. Fibroblast migration in similar gels has also been shown to depend on MMPs [22, 52], but our data demonstrate that MMPs are also required for vascularization.

In addition to proteolytic susceptibility, we altered gel solids content to investigate the roles of initial crosslink density and mechanical properties on vascularization. The swelling ratio and shear modulus of PEG-G and PEG-V gels at matched solids content did not differ. This indicates that peptide identity did not modulate bulk network structure substantively, in agreement with another recent study [49]. Changing solids content, however, did significantly alter both shear modulus and swelling ratio, as expected, and influenced vessel formation *in vitro*. Hydrogels with an initially high crosslink density (5 w/v% gels) supported vascular network formation to a significantly lower degree over 2 weeks in culture than those gels with a lower initial crosslink density (3.5 w/v% gels). This observed decrease is consistent with previous studies from our laboratory using PEG-collagen hydrogels [39], and from another study that showed crosslinking density attenuated radial sprouting from endothelial and smooth muscle cell spheroids encapsulated in PEGDA-derived hydrogels [25]. As a whole, these studies suggest initial crosslinking density is an important modulator of vascular morphogenesis, even in matrices that cells can remodel.

The results of our animal studies underscore the importance of characterizing angiogenic response both *in vitro* and *in vivo*, as constructs which minimally supported vascularization *in vitro* (e.g. 5 w/v% gels) underwent robust vascularization when implanted into subcutaneous locations. In all PEG constructs, vessels formed from the transplanted human cells and inosculated with the host vasculature within a week of implantation. From LDPI, relative perfusion through the subcutaneous implants

increased rapidly in PEG-V gels in the 4 days following implantation, but was not sustained through the 14 day study. In contrast, no significant increases in relative perfusion were observed for PEG-G gels. However, the histological evidence suggested that vascularization occurs at quantitatively similar levels in both PEG-G and PEG-V gels over the 2 week observation period. Furthermore, 5% PEG-V gels supported quantitatively higher levels of vascularization than 3.5% PEG-V gels at day 7, in contrast to the result from the *in vitro* studies. This difference may be due to the proteolytic milieu in the two scenarios. *In vivo*, proteases are secreted by a variety of cell types, including interstitial and inflammatory cells in addition to endothelial cells [53], while our *in vitro* model only accounts for the contribution of endothelial and stromal support cells. These data demonstrate that the set of matrix cues determined to be optimal for vascular morphogenesis *in vitro* may be distinct from those necessary to maximize vascularization *in vivo*.

3.5 Conclusion

The co-delivery of endothelial cells and NHLFs in PEG hydrogel constructs of varying degradability and mechanical properties resulted in the formation of vasculature *in vitro* and *in vivo*. Overall, fewer differences were evident between gel conditions *in vivo* compared to *in vitro*, suggesting that the *in vivo* environment may be more permissive to vascularization. This finding is of particular interest in designing therapies for clinical use, and underscores the limitations of *in vitro* systems to fully recapitulate the more clinically relevant *in vivo* environment. Overall, we have demonstrated that an injectable, PEG-based synthetic material that polymerizes *in situ* is well-suited as a

vehicle for cell-based vascularization therapies and may represent a viable alternative to more invasive treatment options for ischemic diseases.

3.6 References

[1] Facts about Peripheral Artery Disease (P.A.D.). In: Services USDoHaH, editor.2006.
[2] Chen X, Aledia AS, Ghajar CM, Griffith CK, Putnam AJ, Hughes CC, et al. Prevascularization of a Fibrin-Based Tissue Construct Accelerates the Formation of Functional Anastomosis with Host Vasculature. Tissue engineering Part A. 2009;15:1363-71.
[3] Chen X, Aledia AS, Popson SA, Him L, Hughes CC, George SC. Rapid Anastomosis of Endothelial Progenitor Cell-Derived Vessels with Host Vasculature Is Promoted by a High Density of Cotransplanted Fibroblasts. Tissue engineering Part A. 2010;16:585-94.
[4] Au P, Tam J, Fukumura D, Jain RK. Bone marrow-derived mesenchymal stem cells facilitate engineering of long-lasting functional vasculature. Blood. 2008;111:4551-8.
[5] Ghajar CM, Chen X, Harris JW, Suresh V, Hughes CC, Jeon NL, et al. The effect of matrix density on the regulation of 3-D capillary morphogenesis. Biophysical journal. 2008;94:1930-41.
[6] Ghajar CM, Kachgal S, Kniazeva E, Mori H, Costes SV, George SC, et al. Mesenchymal cells stimulate capillary morphogenesis via distinct proteolytic mechanisms. Experimental cell research. 2010;316:813-25.
[7] Kachgal S, Putnam AJ. Mesenchymal stem cells from adipose and bone marrow promote angiogenesis via distinct cytokine and protease expression mechanisms. Angiogenesis. 2011;14:47-59.
[8] Kachgal S, Carrion B, Janson IA, Putnam AJ. Bone marrow stromal cells stimulate an angiogenic program that requires endothelial MT1-MMP. Journal of cellular physiology. 2012.
[9] Melero-Martin JM, Khan ZA, Picard A, Wu X, Paruchuri S, Bischoff J. In vivo vasculogenic potential of human blood-derived endothelial progenitor cells. Blood. 2007;109:4761-8.
[10] Melero-Martin JM, De Obaldia ME, Kang SY, Khan ZA, Yuan L, Oettgen P, et al. Engineering robust and functional vascular networks in vivo with human adult and cord blood-derived progenitor cells. Circ Res. 2008;103:194-202.
[11] Morin KT, Tranquillo RT. In vitro models of angiogenesis and vasculogenesis in fibrin gel. Experimental cell research. 2013;319:2409-17.
[12] Au P, Daheron LM, Duda DG, Cohen KS, Tyrrell JA, Lanning RM, et al. Differential in vivo potential of endothelial progenitor cells from human umbilical cord blood and adult peripheral blood to form functional long-lasting vessels. Blood. 2008;111:1302-5.
[13] Koike N, Fukumura D, Gralla O, Au P, Schechner JS, Jain RK. Creation of long-lasting blood vessels. Nature. 2004;428:138-9.
[14] Collier JH, Segura T. Evolving the use of peptides as components of biomaterials. Biomaterials. 2011;32:4198-204.

[15] Adelow C, Segura T, Hubbell JA, Frey P. The effect of enzymatically degradable poly(ethylene glycol) hydrogels on smooth muscle cell phenotype. Biomaterials. 2008;29:314-26.
[16] Anderson SB, Lin CC, Kuntzler DV, Anseth KS. The performance of human mesenchymal stem cells encapsulated in cell-degradable polymer-peptide hydrogels. Biomaterials. 2011;32:3564-74.
[17] Bahney CS, Hsu CW, Yoo JU, West JL, Johnstone B. A bioresponsive hydrogel tuned to chondrogenesis of human mesenchymal stem cells. FASEB journal : official publication of the Federation of American Societies for Experimental Biology. 2011;25:1486-96.
[18] Kraehenbuehl TP, Ferreira LS, Zammaretti P, Hubbell JA, Langer R. Cell-responsive hydrogel for encapsulation of vascular cells. Biomaterials. 2009;30:4318-24.
[19] Lutolf MP, Lauer-Fields JL, Schmoekel HG, Metters AT, Weber FE, Fields GB, et al. Synthetic matrix metalloproteinase-sensitive hydrogels for the conduction of tissue regeneration: engineering cell-invasion characteristics. Proceedings of the National Academy of Sciences of the United States of America. 2003;100:5413-8.
[20] Lutolf MP, Raeber GP, Zisch AH, Tirelli N, Hubbell JA. Cell-Responsive Synthetic Hydrogels. Advanced materials. 2003;15:888-92.
[21] Patterson J, Hubbell JA. Enhanced proteolytic degradation of molecularly engineered PEG hydrogels in response to MMP-1 and MMP-2. Biomaterials. 2010;31:7836-45.
[22] Raeber GP, Lutolf MP, Hubbell JA. Mechanisms of 3-D migration and matrix remodeling of fibroblasts within artificial ECMs. Acta biomaterialia. 2007;3:615-29.
[23] Raeber GP, Lutolf MP, Hubbell JA. Part II: Fibroblasts preferentially migrate in the direction of principal strain. Biomechanics and modeling in mechanobiology. 2008;7:215-25.
[24] Seliktar D, Zisch AH, Lutolf MP, Wrana JL, Hubbell JA. MMP-2 sensitive, VEGF-bearing bioactive hydrogels for promotion of vascular healing. 2003.
[25] Sokic S, Papavasiliou G. Controlled Proteolytic Cleavage Site Presentation in Biomimetic PEGDA Hydrogels Enhances Neovascularization In Vitro. Tissue engineering Part A. 2012.
[26] Moon JJ, Saik JE, Poche RA, Leslie-Barbick JE, Lee SH, Smith AA, et al. Biomimetic hydrogels with pro-angiogenic properties. Biomaterials. 2010;31:3840-7.
[27] Leslie-Barbick JE, Shen C, Chen C, West JL. Micron-scale spatially patterned, covalently immobilized vascular endothelial growth factor on hydrogels accelerates endothelial tubulogenesis and increases cellular angiogenic responses. Tissue engineering Part A. 2011;17:221-9.
[28] Leslie-Barbick JE, Saik JE, Gould DJ, Dickinson ME, West JL. The promotion of microvasculature formation in poly(ethylene glycol) diacrylate hydrogels by an immobilized VEGF-mimetic peptide. Biomaterials. 2011;32:5782-9.
[29] Miller JS, Shen CJ, Legant WR, Baranski JD, Blakely BL, Chen CS. Bioactive hydrogels made from step-growth derived PEG-peptide macromers. Biomaterials. 2010;31:3736-43.
[30] Sokic S, Papavasiliou G. FGF-1 and proteolytically mediated cleavage site presentation influence three-dimensional fibroblast invasion in biomimetic PEGDA hydrogels. Acta biomaterialia. 2012;8:2213-22.

[31] Phelps EA, Headen DM, Taylor WR, Thule PM, Garcia AJ. Vasculogenic bio-synthetic hydrogel for enhancement of pancreatic islet engraftment and function in type 1 diabetes. Biomaterials. 2013;34:4602-11.
[32] Zisch AH, Lutolf MP, Ehrbar M, Raeber GP, Rizzi SC, Davies N, et al. Cell-demanded release of VEGF from synthetic, biointeractive cell-ingrowth matrices for vascularized tissue growth. FASEB journal : official publication of the Federation of American Societies for Experimental Biology. 2003.
[33] Phelps EA, Landazuri N, Thule PM, Taylor WR, Garcia AJ. Bioartificial matrices for therapeutic vascularization. Proceedings of the National Academy of Sciences of the United States of America. 2010;107:3323-8.
[34] Lutolf MP, Hubbell JA. Synthetic biomaterials as instructive extracellular microenvironments for morphogenesis in tissue engineering. Nature biotechnology. 2005;23:47-55.
[35] Ghajar CM, Blevins KS, Hughes CC, George SC, Putnam AJ. Mesenchymal Stem Cells Enhance Angiogenesis in Mechanically Viable Prevascularized Tissues via Early Matrix Metalloproteinase Upregulation. Tissue engineering. 2006;12:2875-88.
[36] Lutolf MP, Hubbell JA. Synthesis and Physicochemical Characterization of End-Linked Poly(ethylene glycol)-co-peptide Hydrogels Formed by Michael-Type Addition. Biomacromolecules. 2003;4:713-22.
[37] Khetan S, Burdick J. Cellular encapsulation in 3D hydrogels for tissue engineering. Journal of visualized experiments : JoVE. 2009.
[38] Martens PJ, Bryant SH, Anseth KS. Tailoring the Degradation of Hydrogels Formed from Multivinyl Poly(ethylene glycol) and Poly(vinyl alcohol) Macromers for Cartilage Tissue Engineering. Biomacromolecules. 2003;4:283-92.
[39] Singh RK, Seliktar D, Putnam AJ. Capillary morphogenesis in PEG-collagen hydrogels. Biomaterials. 2013;34:9331-40.
[40] Grainger SJ, Putnam AJ. Assessing the Permeability of Engineered Capillary Networks in a 3D Culture. PloS one. 2011;6:1-9.
[41] Grainger SJ, Carrion B, Ceccarelli J, Putnam AJ. Stromal Cell Identity Influences the In Vivo Functionality of Engineered Capillary Networks Formed by Co-delivery of Endothelial Cells and Stromal Cells. Tissue engineering Part A. 2013.
[42] Watkins AW, Anseth KS. Investigation of Molecular Transport and Distributions in Poly(ethylene glycol) Hydrogels with Confocal Laser Scanning Microscopy. Macromolecules. 2005;38:1326-34.
[43] Bott K, Upton Z, Schrobback K, Ehrbar M, Hubbell JA, Lutolf MP, et al. The effect of matrix characteristics on fibroblast proliferation in 3D gels. Biomaterials. 2010;31:8454-64.
[44] Kyburz KA, Anseth KS. Three-dimensional hMSC motility within peptide-functionalized PEG-based hydrogels of varying adhesivity and crosslinking density. Acta biomaterialia. 2013;9:6381-92.
[45] Patterson J, Martino MM, Hubbell JA. Biomimetic materials in tissue engineering. Materials today. 2010;13:14-22.
[46] Saik JE, Gould DJ, Watkins EM, Dickinson ME, West JL. Covalently immobilized platelet-derived growth factor-BB promotes angiogenesis in biomimetic poly(ethylene glycol) hydrogels. Acta biomaterialia. 2011;7:133-43.

[47] Turturro MV, Christenson MC, Larson JC, Young DA, Brey EM, Papavasiliou G. MMP-sensitive PEG diacrylate hydrogels with spatial variations in matrix properties stimulate directional vascular sprout formation. PloS one. 2013;8:e58897.
[48] Nguyen EH, Zanotelli MR, Schwartz MP, Murphy WL. Differential effects of cell adhesion, modulus and VEGFR-2 inhibition on capillary network formation in synthetic hydrogel arrays. Biomaterials. 2013.
[49] Bracher M, Bezuidenhout D, Lutolf MP, Franz T, Sun M, Zilla P, et al. Cell specific ingrowth hydrogels. Biomaterials. 2013;34:6797-803.
[50] Nagase H, Fields GB. Human Matrix Metalloproteinase Specificity Studies Using Collagen Sequence-Based Synthetic Peptides. Biopolymers. 1996;40:399-416.
[51] Turk BE, Huang LL, Piro ET, Cantley LC. Determination of protease cleavage site motifs using mixture-based oriented peptide libraries. Nature biotechnology. 2001;19:661-7.
[52] Raeber GP, Lutolf MP, Hubbell JA. Molecularly engineered PEG hydrogels: a novel model system for proteolytically mediated cell migration. Biophysical journal. 2005;89:1374-88.
[53] Ghajar CM, George SC, Putnam AJ. Matrix Metalloproteinase Control of Capillary Morphogenesis. Crit Rev Eukaryot Gene Expr. 2008;18:251-78.

Chapter 4

Biosynthetic PEG Hydrogels Support Revascularization of Ischemic Tissue

4.1 Introduction

Cardiovascular disease (CVD) is the leading cause of mortality in the United States and globally [1, 2]. The clinical manifestations of CVD vary, but several conditions, notably coronary heart disease (CHD) and peripheral artery disease (PAD), are characterized by poor tissue perfusion, resulting primarily from the deposition of atherosclerotic plaques on the interior of blood vessel walls [3, 4]. Currently, approximately 15.4 and 10-12 million Americans suffer from CHD and PAD, respectively [3, 5]. In these patients, chronic vascular insufficiency results in tissue ischemia and, in advanced stage disease, tissue loss and death.

Despite ongoing improvements in therapeutic interventions for these patients, there is a persistent need for novel cardiovascular therapies and approaches to minimize costly interventions and improve efficacy for a broad patient population. Current therapies include lifestyle modification, pharmaceuticals, and surgical

approaches [3]. In late stage disease, the two former approaches are insufficient to address ischemia and co-morbidities restrict surgical options for many patients [6-9]. Thus, substantial research has focused on the development of non-invasive vascular therapies to ameliorate the underlying ischemia [9-12]. The approaches utilized can be broken down into a few overarching categories: the delivery of genes or trophic factors, the delivery of cells, and/or the delivery of materials.

Gene or trophic factor delivery aids in re-perfusion to ischemic tissue in animal models, and was vetted in early clinical trials [10]. Nonetheless, to date no therapy utilizing this approach has been approved by FDA, and randomized, controlled double-blind trials have delivered mixed results regarding efficacy for these therapies [9, 13]. Typically, growth factor therapies deliver one of several growth factors using recombinant proteins or viral vectors [9, 10]. Among the most commonly utilized factors are bFGF, FGF-1, HGF, and VEGF. The complex spatial and temporal presentation of soluble effectors mediated by cells is not fully recreated in these approaches because they primarily rely on the action of a single growth factor [14, 15]. *In vivo*, angiogenesis depends on a complex interplay between various angiogenic mediators [6, 16-18], which cannot be effectively re-created with a single factor. Additionally, the efficacy of growth factor delivery approaches often is stymied by poor retention and stability of the protein or vector upon delivery. Thus, recent research has focused on alternate approaches, including the delivery of multiple growth factors [19], or simply the utilization of cells or a scaffold to the same end.

Cell delivery is of particular interest, in part because *in vitro* studies [20] demonstrate the ability of cells to function as growth factor producers, effectively

rendering unnecessary the delivery of exogenous growth factors. The delivery of vascular progenitor cells, in addition to other supportive cells, to revascularize tissue is of substantial research interest, but has not yet been vetted clinically [12]. Nonetheless, a wealth of pre-clinical data suggests cell delivery approaches- particularly those delivering cells directly to the site of ischemia- are effective at enhancing tissue perfusion recovery following ischemic insult [21-31]. Substantial variation exists regarding the cells used. Some cell-based approaches rely on the delivery of co-cultures of endothelial and support cells to facilitate vascularization [21], while others deliver single cell types or even minimally characterized, autologous mixed cell populations. Several studies have demonstrated the delivery of endothelial cells can potentiate re-vascularization following ischemic insult [22-28]. In other studies, the delivery of adipose- or bone marrow-derived stem cells alone [29-32] improved function following induction of limb ischemia in a murine model. Alternately, the infusion of minimally purified hematopoietic stem cell populations into ischemic tissue can enhance neovascularization [33, 34], despite poor characterization of the cells present within the infusion. Nonetheless, several studies suggest individual cell types alone are not as effective in supporting vascularization as mixtures of cells containing both supportive cell types and endothelial cells [20, 21, 35-39]. These data motivate the co-culture approach utilized in this study.

Materials development is likewise employed to potentiate revascularization in combination with either of the above strategies (i.e. growth factor delivery and/or cell delivery). The delivery of cells in a scaffold enhances cell engraftment [40]. Scaffolds may additionally be utilized to deliver relevant factors for vascularization in a controlled

manner [40-44]. Results from clinical trials of cell-based therapies suggest simple infusions have significant limitations, including massive cell death- approaching 90%- upon transplantation [28]. Poor cell engraftment is characteristic of cell therapies targeting a variety of tissues, and the delivery of cells within a scaffold improved graft survival across several tissues and applications, including transplantation of cells for regeneration of cardiac tissue [40, 41], the liver [42], or bone marrow [43]. These approaches enhanced both survival and function of the transplant, and highlight the potential of scaffolds to enhance response to cell-based therapies. In the context of peripheral ischemia, studies have demonstrated recovery is enhanced when endothelial progenitor cells are delivered in conjunction with a variety of scaffolds, including collagen [45], modified-alginate [28], and polylactic-co-glycolic acid [46].

Our approach to re-vascularize ischemic tissue was built on an extensive literature that led us to pursue a hybrid strategy involving the delivery of cells within a hydrogel. Though natural materials support robust vascularization in several *in vitro* and *in vivo* models [36, 39, 47-53], they are highly variable, due to source and processing issues and raise concerns from the perspective of potential immunogenicity. Synthetic materials, instead present a different set of concerns; namely, they must be carefully tailored to present the appropriate biological signals to support cell processes such as adhesion, migration, proliferation, and, in the context of our work, vessel morphogenesis. This study utilizes poly(ethylene glycol)-based hydrogels as a supportive matrix for therapeutic vascularization. PEG hydrogels allow presentation of well-defined biological signals that can be tuned to match the translational application, are reproducible, and are generally considered to be biocompatible.

In the preceding chapter, we optimized a biosynthetic PEG hydrogel system for the encapsulation of endothelial and stromal cell co-cultures. PEG hydrogels supported the formation of endothelial cell (EC) tubules upon encapsulation with support cells *in vitro* and perfused blood vessels from encapsulated cells delivered in a subcutaneous implant *in vivo* [54]. Despite the variety of matrices used for cell delivery in therapeutic vascularization, few researchers have used PEG-based scaffolds for this application. Studies have investigated the formation of vasculature from implanted cells in PEG gels [55, 56], and the recruitment of host vasculature [57]. While PEG hydrogels have been used to deliver VEGF to an ischemic limb [58], this class of scaffold has not been used as a cell delivery vehicle to ischemic tissue. Thus, we chose to deliver endothelial and stromal cells within a biosynthetic PEG hydrogel to tissue rendered ischemic by femoral artery ligation (FAL). FAL is a well-established model of hindlimb ischemia that is considered to approximate the clinical manifestations of PAD and CLI. Further, to better assess the ability of the PEG hydrogels to support revascularization of the ischemic limb, we compared the response following FAL to that stimulated by a well-studied natural material: fibrin. Fibrin is a naturally-occurring biopolymer that is found in the provisional matrix of healing wounds and is widely demonstrated to support vascularization [59]. Assessments of flow to the limb as a whole, as well as histological assessment of the implants were utilized to investigate the differential ability of the materials to support vascularization.

4.2 Methods

4.2.1 Cell Isolation and Culture

Human umbilical vein endothelial cells (HUVECs, or henceforth ECs) were isolated according to a previously described protocol [54]. ECs were cultured in supplemented endothelial growth medium (EGM-2, Lonza, Walkersville, MD) at 37C and 5% CO_2 and were used at passage 3. Normal human lung fibroblasts (NHLFs, Lonza) were cultured in M199 (Invitrogen Corporation, Carlsbad, CA) with 10% fetal bovine serum (FBS), 1% penicillin/streptomycin (Mediatech, Manassas, VA), and 0.5% gentamicin (Invitrogen) at 37C and 5% and used prior to passage 15. Cells were cultured in monolayers until 80% confluent and then passaged with 0.05% trypsin-EDTA (Invitrogen).

4.2.2 PEG and Fibrin Gel Preparation

PEG and fibrin gels were formed according to previously established protocols [39, 54]. PEG hydrogels were polymerized via Michael-type addition reaction of 4-arm PEG vinyl sulfone (PEG-VS; 20 kDa, JenKem USA, Allen, TX) with a combination of thiol-containing adhesive and protease-sensitive peptides. Briefly, PEG-VS in HEPES (50mM, pH 8.4, supplemented with growth factors from endothelial medium bullet kit) was combined with the adhesive peptide solution (10 μg μl^{-1} CGRGDS in HEPES, Genscript, Piscataway, NJ) to yield a final adhesive site density upon gelation of 500 μM and the solution was reacted 30 minutes at room temperature prior to addition of the crosslinking peptide. Bis-cysteine-containing crosslinking peptides were added in HEPES to form gels with 3.5% (w/v) total solids content and a 1:1 molar ratio of –SH and –VS groups. Gels were polymerized with one of two peptides, Ac-GCRD-GPQG↓IWGQ-DRCG-NH_2 (3.5% G gels) or Ac-GCRD-VPMS↓MRGG-DRCG-NH_2 (3.5%

V gels) (Genscript, cleavage site indicated by↓). The two crosslinking peptides used -GPQG↓IWGQ and VPMS↓MRGG- are degraded at different rates by proteases relevant to vascularization (Supplemental Figure 4) [54, 60]. Fibrin gels were prepared at 2.5 mg/ml in serum-free EGM-2 with 5% FBS and 1 U/ml thrombin (Sigma). The bulk mechanical properties of the PEG and fibrin gels were not matched. Instead, the concentrations for each were chosen based on previous studies investigating vascularization in the materials. PEG gels with 3.5% solids have been demonstrated to support vascularization [54] and the fibrinogen concentration used approximately matches that present in circulating blood and has been used in previous studies in our lab [61].

4.2.3 Assessment of Hydrogel Degradation Kinetics

Hydrogel degradation kinetics were evaluated via incubation of gels with recombinant MMP2, as described in a previously published protocol [55]. Gel degradation was assessed by monitoring the change in wet weight upon incubation with recombinant MMP2 (enzyme purchased from EMD Millipore). Hydrogels were prepared as described above and swollen overnight prior to incubation with the enzyme solution. The enzyme was prepared at 1 nM in degradation buffer (100 mM tricine, 200 mM NaCl, 10 mM $CaCl_2$, 0.05% Brij 35 at pH 7.5) and 100 µl gels were incubated in 250 µl enzyme solution at 37C and 5% CO_2, with fresh solution added daily.

4.2.4 Induction of Ischemia and Implant Delivery

All animal procedures were performed according to a protocol approved by the University of Michigan Committee on the Use and Care of Animals in accordance with

NIH guidelines for the use of laboratory animals. Male six- to eight-week-old C.B.-17/SCID mice (Taconic Labs, Hudson, NY) were used for all experiments. Before the surgical procedures, animals were administered an anesthetic/analgesic cocktail of 95 mg kg^{-1} ketamine (Fort Dodge Animal Health, Fort Dodge, IA), 9.5 mg kg^{-1} xylazine (Lloyd Laboratories, Shenandoah, IA), and 0.059 mg kg^{-1} buprenorphine (Reckitt Benckiser, Richmond, VA) via intraperitoneal injection. Both hindlimbs of each mouse were cleared of fur by shaving and the use of a depilatory agent (Nair, Fisher Scientific, Pittsburgh, PA). The region was then sterilized with betadine (Thermo Fisher Scientific, Fremont, CA) and wiped down with an alcohol pad. After hair removal and disinfection, a skin incision was made over the femoral artery moving caudally from the inguinal ligament to the popliteal bifurcation and the connective tissue was dissected from the femoral artery. The femoral artery and vein were then ligated with triple surgical knots using Ethicon 5-0 sutures (Ethicon, Somerville, NJ) immediately distal to the level of the profunda femoral artery and again just proximal to the bifurcation of the saphenous and popliteal arteries. The superficial femoral was transected from the tissue between these ligation points. Implants (n = 5) per condition were prepared as described above. Prior to initiation of the procedure, mixtures of ECs and NHLFs in a 1:1 ratio were prepared and aliquoted to yield 10 million total cells/ml gel precursor solution. Implants with a total volume of 300 µl were prepared with and without cells for 3 gel compositions-fibrin, 3.5% PEG-G, and 3.5% PEG-V- and delivered via intramuscular injection to 3 locations spaced equally between the proximal and distal ligation sites. Following injection, animals were kept stationary for 5 min to allow for implant gelation. Surgeons were not blinded to the experimental conditions.

4.2.5 Laser Doppler Perfusion Imaging and Magnetic Resonance Angiography

Animals were subjected to laser Doppler perfusion imaging (LDPI, Perimed AB, Sweden) immediately following induction of ischemia and again at days 4, 7, and 14. Each mouse was imaged in triplicate. Mice were placed in fresh cages for recovery. For days 4, 7, and 14, mice were anesthetized with the cocktail described above prior to imaging via LDPI. Although the penetration depth of LDPI into tissue is minimal (1-2 mm), others have demonstrated it is an effective proxy for more invasive methods of assessing tissue vascularity and LDPI data correlates to capillary density in several murine models of ischemic hindlimb [62, 63]. In the results, perfusion is reported as the ratio of the relative perfusion to the ischemic limb compared to the contralateral. ROIs were selected to match anatomically from the ischemic to contralateral limb and to encompass the region distal to the site of ligation.

All magnetic resonance imaging was performed at 7T using a 4-cm-inner diameter volume coil (Direct Drive console and Milipede radiofrequency coil, Agilent, Santa Clara, CA). Animals were anesthetized and maintained on isoflurane in oxygen for the duration of imaging. Body temperature was maintained at $37^{o}C \pm 0.2$. Imaging was performed 24 hours after femoral artery ligation to demonstrate the attenuation of flow to the femoral artery of the ipsilateral limb. After a pilot scan to confirm positioning, mice underwent a 3D spoiled gradient echo sequence (flip angle = 30^{o}, FOV = $(3\ cm)^3$, TR = 20 msec, TE = 3 msec, spectral width = 50 kHz, isotropic matrix of 128, NEX = 2). Total acquisition time was eleven minutes. Data sets were zero-filled to 256^3 and visualized by maximum intensity projection (MIP) in the coronal plane.

4.2.6 Dextran Tracer Injection and Implant Removal

Implants were retrieved either 7 or 14 days after inducing ischemia following systemic administration of a labeled dextran. Selectively permeable mature capillaries are impermeable to dextrans of molecular weight exceeding 65 kDa [59]. Thus, a 70 kDa Texas Red-conjugated dextran ($\lambda_{ex/em}$ of 595/615 nm, Invitrogen) was chosen to administer to better assess the inosculation and permeability of engineered vessels within the implants. The dextran molecule contains free lysines, which can be fixed in formalin, thus allowing the localization of the tracer to be visualized in histological sections. Following LDPI at the retrieval time point, each mouse was placed in a restraint device and 200 µl of a 5 mg/ml dextran solution in PBS was injected via the tail vein. After injection, mice were moved to fresh cages and the tracer was allowed to circulate systemically for 10 min prior to euthanasia. Hindlimb muscle tissue between the ligation sites was dissected from the limb.

4.2.7 Implant Processing and Histology

All tissues were fixed overnight at 4^{o}C in Z-fix (Anatech, Battle Creek, MI). Following fixation, samples were rinsed thrice with cold PBS and then transferred to 70% ethanol until histological processing. Samples were processed according to a standard procedure and embedded in paraffin. Tissues were oriented to generate sections with the limb in cross section. Sections (5 µm thick) were generated at regular intervals along the limb, to ensure sampling of implant volume was consistent across

the tissue harvested. For all staining procedures, paraffin sections were rehydrated according to a standard protocol [38].

Sections were stained for human CD31, alpha-smooth muscle actin (α-SMA), and calponin using a standard immunohistochemical stain. Briefly, following rehydration and antigen unmasking, sections were washed with TBS-T and then blocked 5 minutes with a peroxidase blocking solution (Dako EnVision System-HRP (DAB) kit, Dako, Carpinteria, CA). Primary antibodies were diluted 1:50 in TBS-T and applied to slides. Following incubation overnight at 4^{o}C, slides were incubated for 30 minutes at room temperature with the HRP-conjugated anti-mouse secondary antibody provided in the Dako kit. Slides were dehydrated and mounted with xylene-based mounted medium (Fisher Scientific) prior to imaging.

For lectin staining, samples were first rehydrated and steamed in an antigen unmasking solution (Dako, Carpinteria, CA). Sections were then rinsed several times with PBS and then incubated for 45 minutes with either fluorescein-labeled Bandeiraea Simplicifolia I (BS-1) or Ulex Europaeus Agglutinin I (UEA-1) lectin (Vector Labs, Burlingame, CA). BS-1 lectin is specific for mouse ECs and UEA-1 is specific for human ECs. Slides were then rinsed in PBS, dehydrated, and mounted as described above.

Using sections stained with hCD31 via IHC with no H&E counterstain, the number of blood vessels derived from human cells within the implant was quantified manually. Images were taken at 20x in the interior of the implant and vessels were quantified for 10 images per animal by a blinded observer. Blood vessels were included

in the quantification if they exhibited a border of hCD31+ cells and an unstained, hollow lumen.

4.2.8 Statistics

All statistical analyses were performed using GraphPad Prism (GraphPad Software, La Jolla, CA). Data are from n = 5 and are reported as mean ± SEM. Statistical analyses consisted of a one or two-way ANOVA followed by post-tests implementing Bonferroni's multiple comparison correction. Statistical significance was assumed when $p < 0.05$.

4.3 Results

4.3.1 Hindlimb Ischemia Induced by Femoral Artery Ligation (FAL)

Ischemia was induced by excising the segment of the femoral artery and vein bounded proximally by the deep femoral artery and distally by the bifurcation of the popliteal and saphenous arteries (Figure 4-1). Mice were treated immediately after ischemic induction with the hydrogel constructs outlined above. Gels composed of fibrin or PEG, 3.5% G or 3.5% V, were injected intramuscularly, with or without cells, after ligation. Prior to recovery, mice underwent LDPI to non-invasively assess perfusion to the ischemic limb. Following FAL, perfusion to the ischemic (ipsilateral) limb was 25% of perfusion to the unoperated, contralateral limb (Figure 4-2). The extent of ischemia induced by FAL did not significantly vary across experimental conditions (Figure 4-2). Mice with a perfusion ratio of less than 0.075, or 7.5%, were excluded from the study to remain compliant with the endpoints regarding autoamputation stipulated in our UCUCA

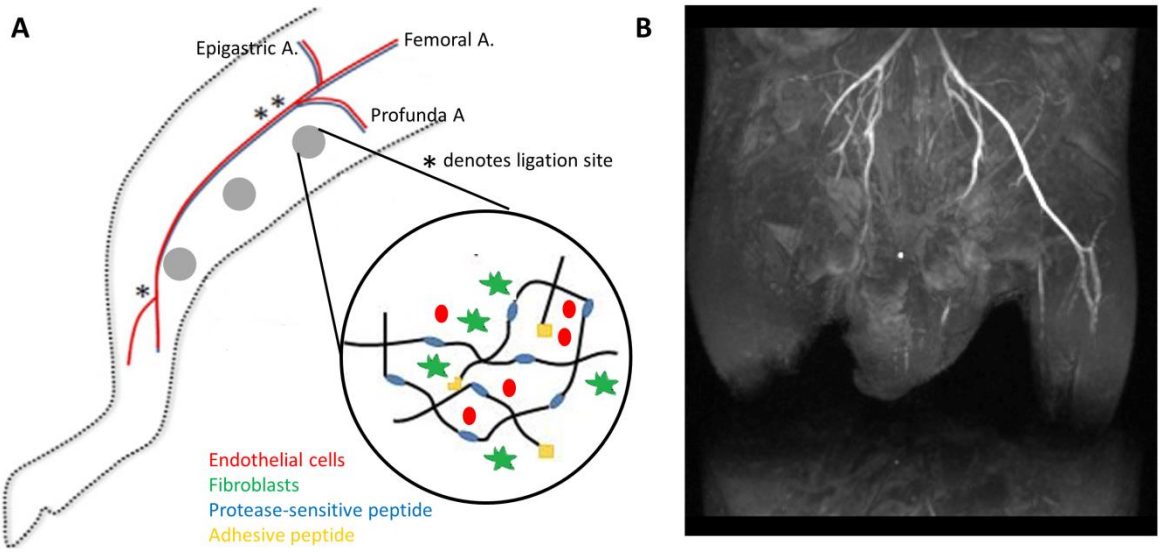

Figure 4-1. A. Model of hindlimb ischemia.FAL schematic adapted with permission[7]. Hydrogel precursor was delivered intramuscularly with ECs and NHLFs or no cells to the ischemic limb of SCID mice following femoral artery ligation. Gels were delivered at 3 sites (gray circles). Ligation sites are indicated by *. EC, endothelial cells; NHLF, normal human lung fibroblast. Fibrin controls (not depicted) were delivered in the same manner as PEG hydrogels. B. Magnetic resonance angiography confirms the ligation and excision of the femoral artery to render the ipsilateral limb ischemic.

protocol.

The attenuation of flow to the ischemic limb was corroborated by magnetic resonance angiography (MRA). Mice were imaged 24 hours after surgery and flow to the superficial femoral artery in the ipsilateral limb was not evident (Figure 4-1).

4.3.2 Delivery of Hydrogel Constructs Restores Perfusion to the Ischemic Limb

Perfusion to the ischemic limb increased significantly in the two weeks following FAL and implant delivery across all experimental conditions (Figure 4-2). Within four days of FAL, the LDPI ratio significantly increased in all animals except those containing acellular fibrin implants. In these mice, significant reperfusion was evident by day 7. Fibrin implants with cells were notable for supporting increased perfusion one week after FAL compared to other gel constructs and compared to other time points.

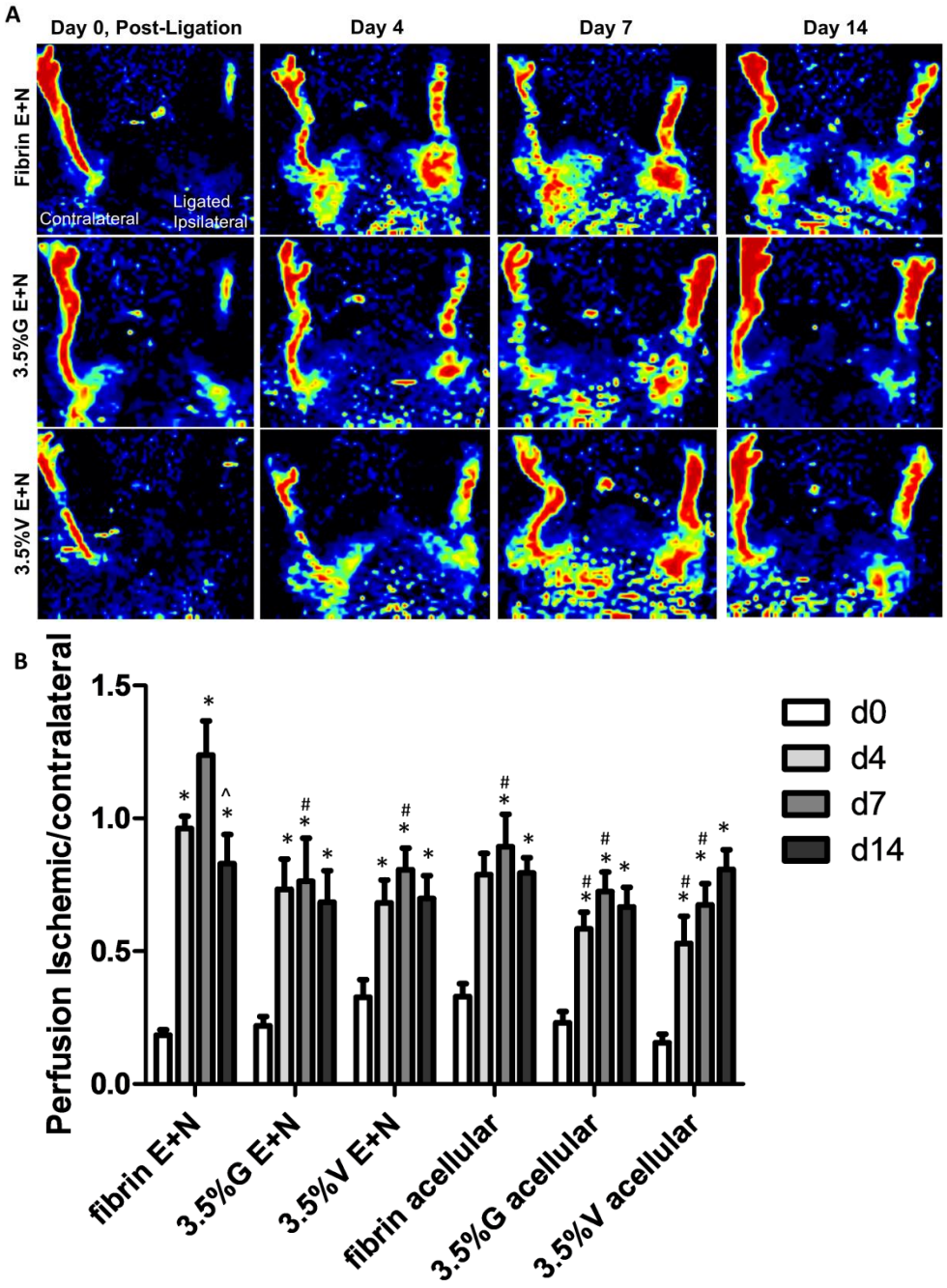

Figure 4-2. Laser Doppler Perfusion imaging (LDPI) was used to non-invasively quantify blood perfusion after intramuscular delivery of gel constructs to ischemic limb. (A) Images represent LDPI heat maps demonstrating degree of perfusion to ischemic and contralateral limbs. Images of acellular constructs not shown. B. Quantification of relative perfusion demonstrates differences between gel constructs. Statistically significant effects for both day and gel composition were found by 2-way ANOVA. Perfusion increased significantly over 14 days in all constructs, and perfusion of limbs containing fibrin implants with cells was significantly increased compared to other implants at matched time points. * denotes significance compared to day 0 within experimental groups and ^ denotes significance compared to day 7 within experimental groups. # indicates significance versus fibrin implants with cells at matched time points. $p < 0.05$ 2-way ANOVA followed by Bonferroni post-tests.

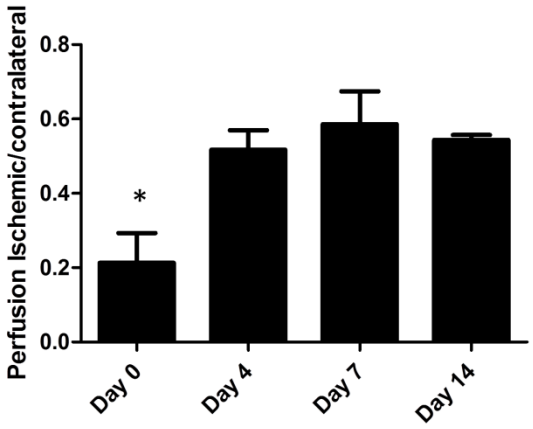

Figure 4-3. Laser Doppler Perfusion imaging (LDPI) was used to non-invasively quantify blood perfusion after femoral artery ligation in animals not treated with gel constructs. Perfusion increased significantly over 14 days. $p < 0.05$ 1-way ANOVA followed by Bonferroni post-tests.

Perfusion through limbs treated with fibrin gels reached 120% one week after ligation, but this effect did not persist to the two week time point. In contrast, other gel constructs did not support complete restoration of perfusion to the ischemic limb (values ranged from 60 and 80% compared to the contralateral limb), but perfusion did not drop at later time points in these gels. By day 14, there were no statistical differences in reperfusion to the ischemic tissue in mice treated with fibrin gels and cells in comparison to other gel conditions. No statistical differences in reperfusion were found based on crosslinking peptide identity in PEG hydrogels. Acellular PEG gels supported reperfusion to a similar extent as PEG gels with cells. Mice that underwent FAL without delivery of an implant or cells demonstrated some reperfusion, but values plateaued at approximately 50% (Figure 4-3).

4.3.3 Implants are Remodeled and Support Capillary Formation

Transplanted HUVECs organized into perfused vessels following delivery to the ischemic limb via injectable hydrogel constructs. Paraffin sections stained for human

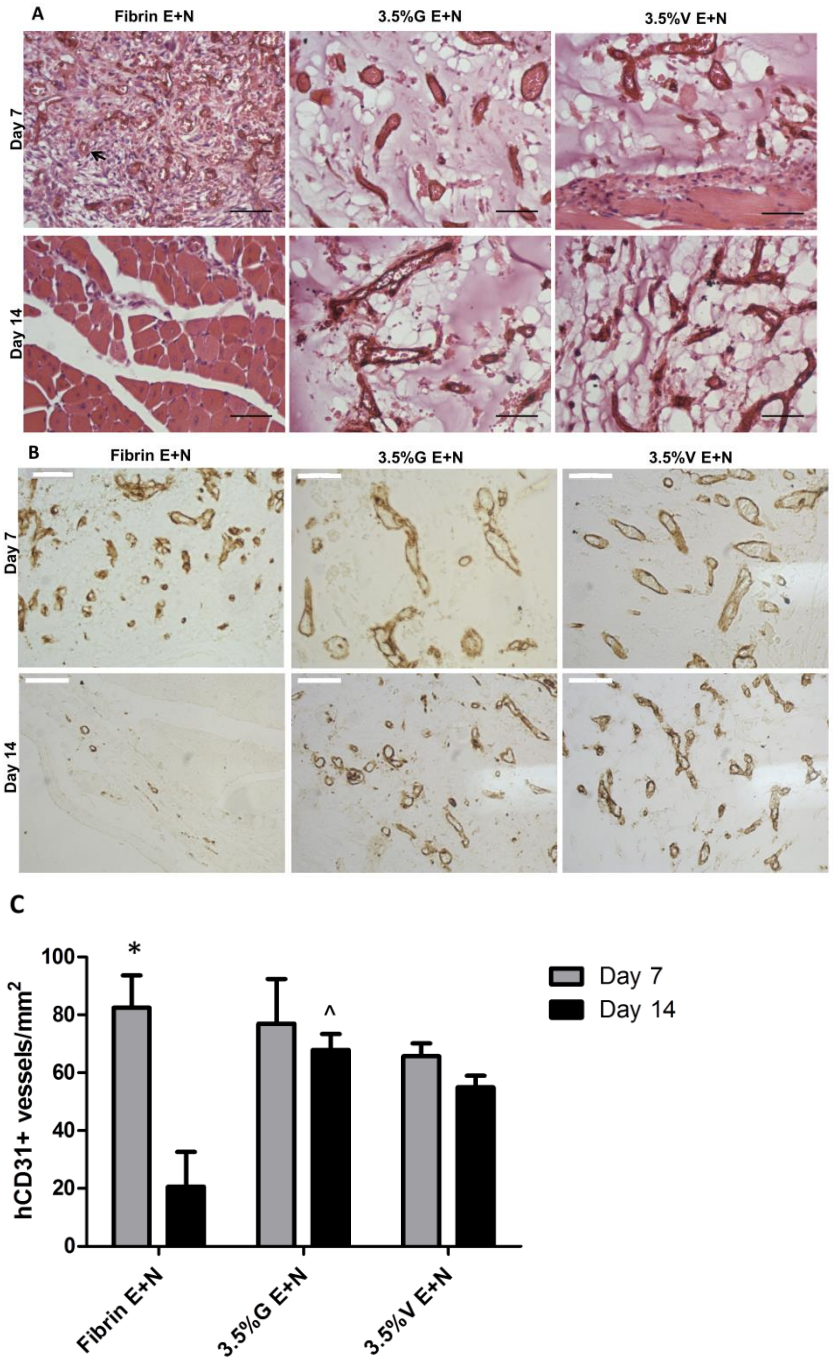

Figure 4-4. Section harvested from mice 1 and 2 weeks after FAL. A. hCD31 IHC and H&E staining of paraffin sections from implants retrieved after 7 or 14 days *in vivo*. All implants contain ECs and NHLFs. Acellular implants (not shown) were not hCD31+. B. Slides stained with hCD31 but not counterstained to facilitate vessel quantification (all images 40x, scale bars= 50 μm). C. Quantification of hCD31+ vessels perfused with RBCs demonstrates differences between gel constructs. Statistically significant effects for both day and gel composition were found by 2-way ANOVA. Vessel density was not statistically different for PEG and fibrin gels at day 7, however, vessel density decreased significantly in fibrin gels at day 14. * denotes significance compared to day 14 within experimental groups and ^ denotes significance versus fibrin implants with cells at matched time points. $p < 0.05$ 2-way ANOVA followed by Bonferroni post-tests.

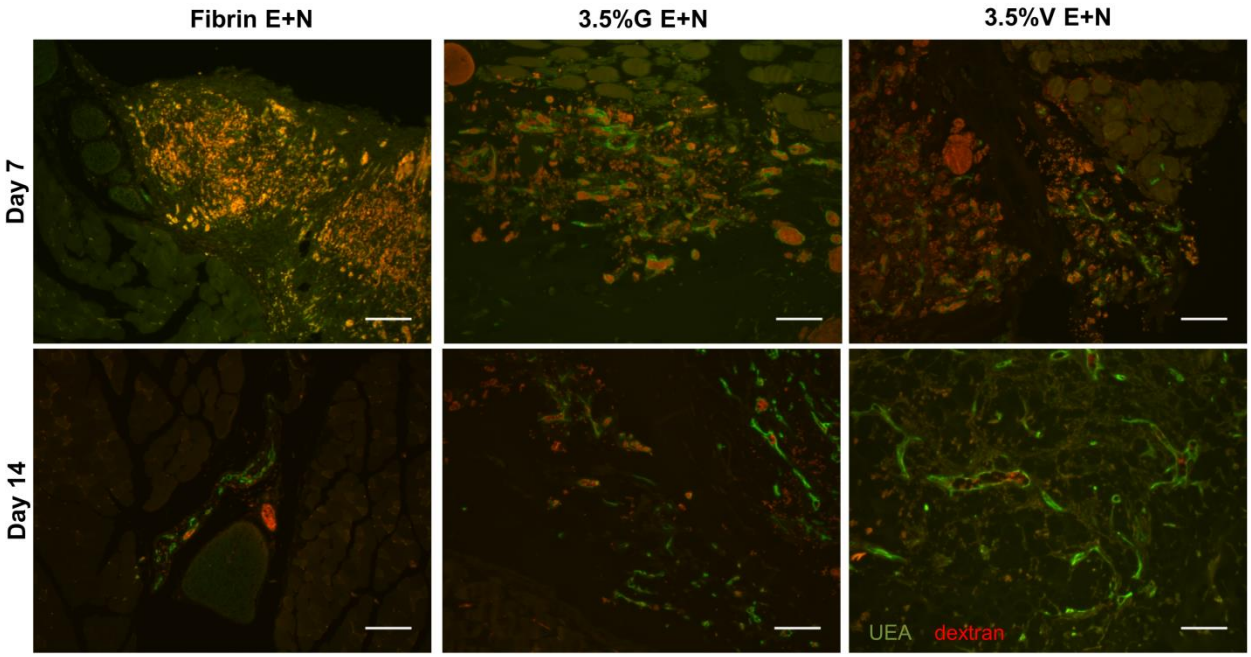

Figure 4-5. Red fluorescent 70 kDa dextran was administered systemically to mice prior to implant removal on day 7 or 14. Paraffin embedded slides were stained for UEA-1 lectin (green) and imaged. Red present within UEA-1+ structures indicates inosculation of host and implant vasculature (scale bars = 100 μm)

CD31 and H&E demonstrate that vessels formed from human ECs and inosculated with host vasculature within one week of implantation in both fibrin and PEG constructs (Figure 4-4). Not all vessels stained positive for human CD31 in fibrin implants (Figure 4-4A, black arrow), indicating mouse vessels were present within the construct. All vessels in the PEG implants stained positive for human CD31. Host erythrocytes were evident in the lumens of vessels formed in the three hydrogel materials. The insoculation of host vessels with implant vasculature was further confirmed by the presence of a systemically administered fluorescent dextran tracer in the lumens of neovessels formed in the implant (Figure 4-5). Sections from tracer-injected animals were stained with fluorescein-tagged UEA-1 to identify human ECs. Dextran-perfused vessels (red) in the implant region were circumscribed by human UEA-1+ cells (green). Qualitatively, differences in the vasculature between conditions were observed from

UEA-1 stained sections. The presence of red signal in the interstitial space indicates extravascular leakage occurred in all implants with cells, particularly at the day 7 time point.

As expected, histological sections from acellular implants demonstrated no positive staining for human CD31. Additionally, PEG implants without cells remained almost entirely intact after 2 weeks *in vivo* and were not extensively remodeled via host ingrowth. This histologic finding was corroborated by macroscopic images of acellular PEG implants (Figure 4-6), which remained nearly transparent with no evident vessels even after two weeks *in vivo*. In contrast, implants delivered with cells had a pink hue and individual vessels were easily identified in the gels.

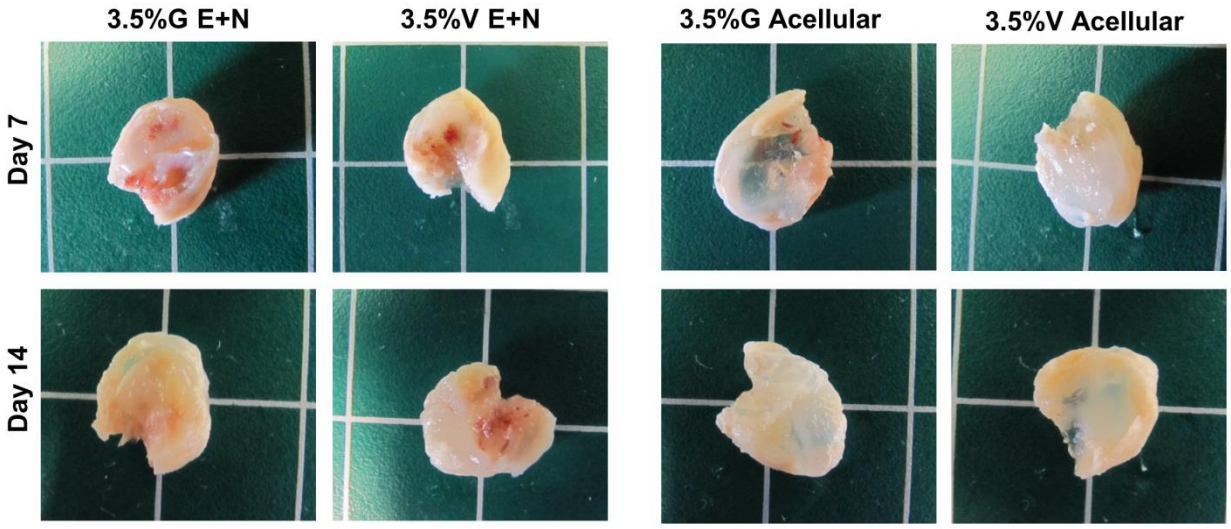

Figure 4-6. Macroscopic images of selected implants demonstrates distinct differences in extent of remodeling of acellular PEG gels compared to those which delivered cells.

The density of human-derived vessels in the ischemic limb was quantified manually from human CD31-stained sections without H&E counterstaining (Figure 4-4B). One week after FAL and implant delivery vessel density was comparable for the

three gel formulations (Figure 4-4C). By the following week, vessel density had dropped significantly in animals treated with fibrin constructs and cells. Vessel density did not drop from days 7 to 14 in PEG implants. No significant differences were observed between the 3.5%G and 3.5%V hydrogels.

4.3.4 Investment of Engineered Capillaries with Pericytes

Pericytes associated with human-derived vessels within PEG and fibrin implants. Tissues were stained for α-SMA and calponin to probe the association of supportive pericytes with engineered vessels. α-SMA is used extensively as a pericyte marker, while calponin is regarded to be more specific for mature smooth muscle[59]. IHC staining for α-SMA revealed some positive staining within implants harvested at days 7 and 14 for all three gel types used to deliver human cells (Figure 4-7). In the PEG gels α-SMA+ vessels were more evident at day 14. For fibrin gels, substantial α-SMA staining was observed at day 7. At day 14, despite significant regression of vessels in fibrin tissues (Figure 4-4C), those that persist stain positive for α- SMA. No positive staining for human calponin was evident in any of the gel constructs (Figure 4-8).

4.3.5 Perfused Vasculature Evident in Muscle Surrounding Implant

Sections from dextran tracer-injected animals were stained with BS-1 lectin to identify mouse ECs and assess revascularization in the region around the implants. Perfused mouse EC-lined vessels were interspersed between muscle fibers in the region surrounding constructs with and without cells (Figure 4-9). The regularity and distribution of vessels varied by implant condition. BS-1+ structures were less uniformly

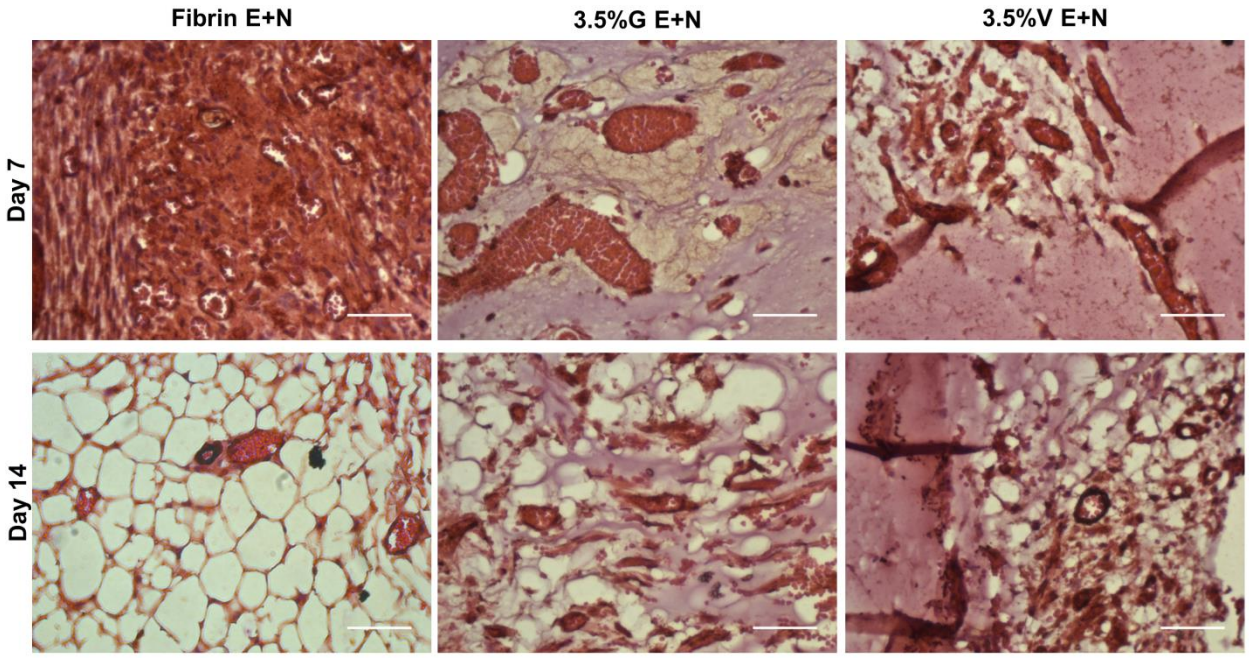

Figure 4-7. IHC and H&E staining of paraffin sections from implants retrieved after 7 or 14 days in vivo. Sections were stained for α-SMA, counterstained with H&E, and then imaged at 40x (scale bars= 50 μm). All implants contain ECs and NHLFs. Positive staining for α-SMA increases from day 7 to day 14, which suggests vessels undergo stabilization by pericytes during this period.

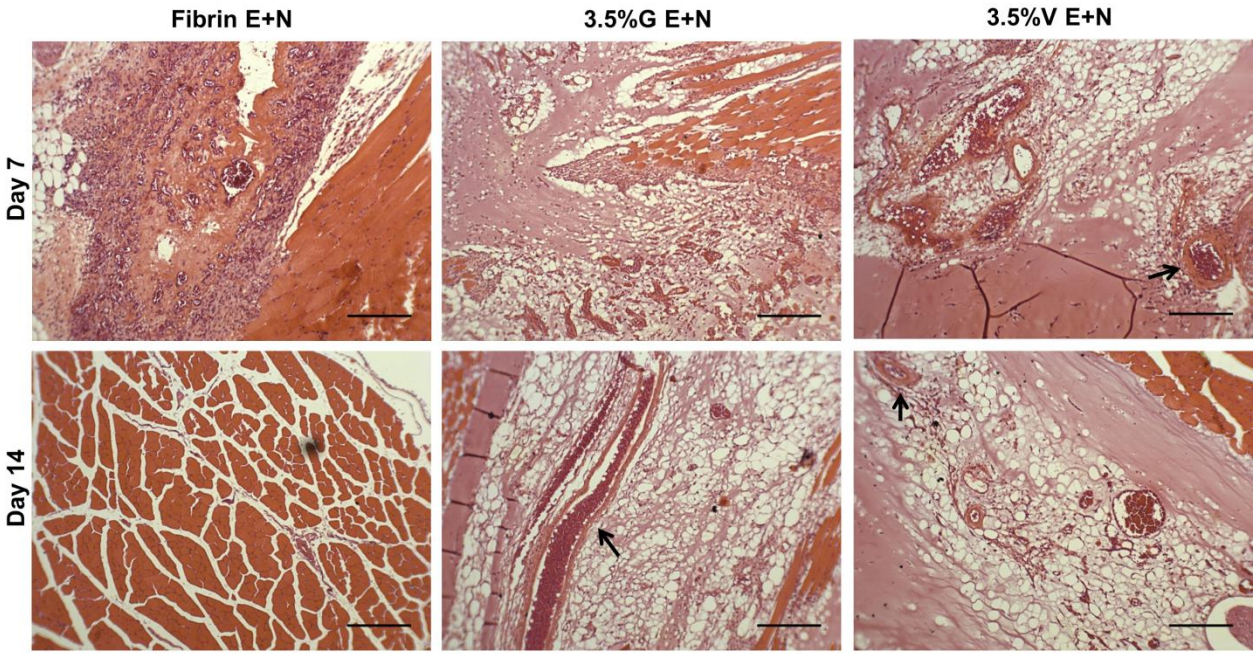

Figure 4-8. IHC for human calponin and H&E staining of paraffin sections from implants with ECs and NHLFs retrieved after 7 or 14 days in vivo. All images are 10x (scale bars= 200 μm). Positive staining for human calponin is not evident in any gel constructs, suggesting implanted NHLFs do not function as mature smooth muscle. By day 14, some vessels in PEG implants appear to have associated smooth muscle (black arrows). The lack of positive staining for human calponin suggests these are host-derived.

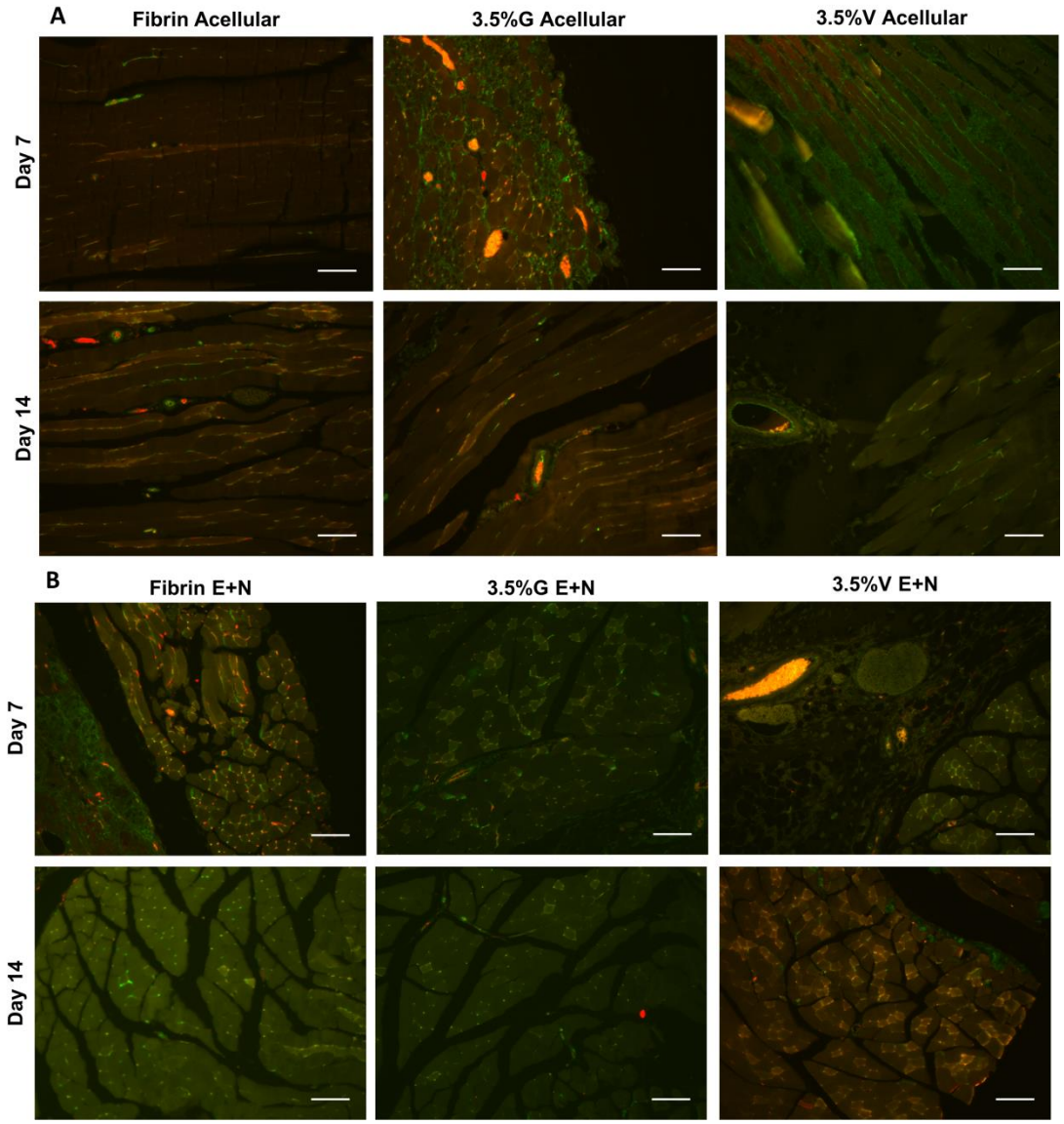

Figure 4-9. Red fluorescent 70 kDa dextran was administered systemically to mice prior to implant removal on day 7 or 14. Paraffin embedded slides were stained for BS-1 lectin (green) and imaged (A, acellular gels; B, gels with ECs and NHLFs). BS-1 lectin stains mouse endothelial cells, and allowed us to assess host vascularization in response to implant delivery and induction of ischemia. A. Mouse vasculature is evident within the muscle. Irregular spacing of muscle and gaps between fibers suggest differential revascularization compared to muscle adjacent to gels delivering cells (see B). B. Most vessels within the muscle are BS-1+, while the majority of vessels in the implant are lined with human, not mouse endothelial cells (see Figure 5 as well) (scale bars = 100 μm).

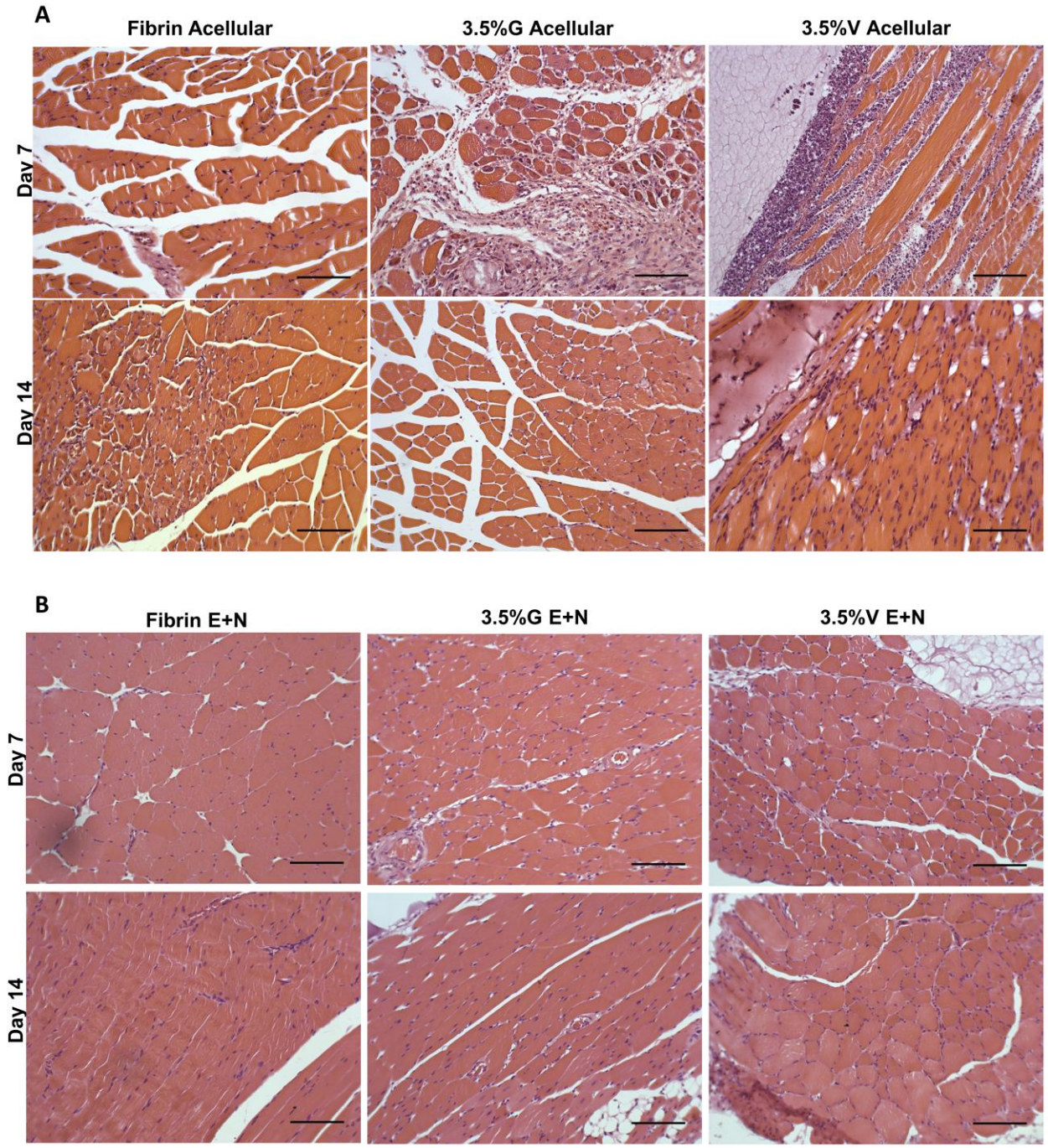

Figure 4-10. H&E staining of paraffin sections from acellular (A) or cellular (B) implants retrieved after 7 or 14 days in vivo. Sections were stained and then imaged at 20x (scale bars= 100 μm). Acellular gels evidence increased inflammatory infiltrate in muscle around implant than gels with ECs and NHLFs, particularly at day 7.

distributed in acellular gels. Host inflammatory and endothelial cells infiltrated the endomysium surrounding muscle fibers in tissues with acellular PEG gels. This effect is strongly evident from BS-1 staining at day 7, and somewhat diminished by day 14. The infiltration of muscle endomysium around acellular implants was further corroborated by H&E-stained sections (Figure 4-10). Moreover, H&E staining demonstrates muscle fibers have centrally located, and not peripheral, nuclei at day 14. The presence of central nuclei suggests the muscle is in the process of regeneration at this time, but has not yet normalized. In muscle near implants with cells some infiltrate is evident, but the enlargement of the endomysium is not as pronounced (Figure 4-10). Muscle adjacent to implants delivering cells was nearly uniformly perfused with host vessels in tissues harvested 7 and 14 days after implantation. Muscle fibers were not separated by a thick layer of connective tissue in these tissues.

4.4 Discussion

In this work, a well-established murine model of hindlimb ischemia was utilized to investigate the ability of PEG-based hydrogels and fibrin to potentiate re-vascularization. Following induction of ischemia, injectable gels were used to deliver endothelial and stromal support cells intramuscularly with angiogenesis monitored in the ischemic limb for 2 weeks.

Surgical ligation of the femoral artery is a well-established technique which mimics the chronic ischemia experienced in human patients with peripheral artery disease (PAD) and critical limb ischemia (CLI) [63]. With regards to the extent of ischemia induced by ligation, substantial variability is described in the literature. This

variability likely results from both intrinsic mouse strain-dependent differences in endogenous re-vascularization upon induction of ischemia [64-67], as well as the use of different ligation sites by researchers [7, 8, 63]. We chose to utilize a ligation model wherein the femoral artery and vein are ligated immediately distal to the origin of the deep femoral and superior epigastric arteries and again proximal to the saphenous and popliteal bifurcation. The artery and vein are then excised in this region. This model results in minimal autoamputation compared to more severe models in which the deep femoral is ligated and is permissive to collateralization as the arteriole bed remains intact [7, 8]. With this model, perfusion drops to approximately 25% of the control limb immediately following ligation [63] and normalizes to between one and two thirds of baseline within 7 days of ligation [7, 8], even in the absence of therapeutic intervention. Our results corroborate previously published studies, with perfusion returning to 50% of the contralateral limb within 2 weeks of ligation. This restoration of perfusion presumably results from a combination of angiogenesis in the ischemic tissues and arteriogenesis in the area upstream to the ligation. Arteriogenesis, the remodeling of pre-existing arterioles into larger diameter arteries, occurs in response to changes in hemodynamic forces [15, 19, 68, 69] and may be particularly important to reperfuse tissues not treated with implants or cells. Our study primarily aims to augment angiogenesis within the ischemic region, but the contribution of arteriogenesis, particularly in response to implant delivery is an area of interest that warrants further study.

We utilized a hybrid strategy to restore perfusion to tissue following FAL, wherein endothelial and stromal cells were delivered within a biosynthetic PEG hydrogel or

fibrin. Two variants of the PEG hydrogel were utilized, with differences in the relative susceptibility of the peptide crosslinker to MMP-mediated degradation [54]. The response following FAL in animals implanted with PEG was compared to that stimulated by fibrin. Differences in the density and distribution of vessels, as well as reperfusion to the ischemic tissue, were evident between conditions. However, all gels delivering cells resulted in the formation of human CD31+ vessels with distinct lumens and, by day 14 post-FAL, pericytic association with the nascent vessels. An abnormal pericyte coat is associated with several pathologies, and association of pericytes with nascent vessels is considered to be critical for vessel stabilization as well as control of vascular permeability [59, 70]. PEG and fibrin gels evidenced vessels with well-circumscribed lumens staining positive for α-SMA. Unfortunately, due to nonspecificity of the antibody used, no conclusions may be drawn regarding the origin of the pericytes. Despite ubiquitous positive staining for α-SMA, no conditions stained positive for human calponin. This corroborates results previously published in our lab[59], wherein subcutaneous fibrin implants containing ECs and fibroblasts did not express calponin. These data suggest that the fibroblasts cannot function as mature smooth muscle despite their association with capillaries and further remodeling of the nascent vessels by host smooth muscle may be necessary for maturation of these structures. Indeed, some vessels in implants harvested at day 14 appear to be circumscribed by smooth muscle, suggesting host tissue may facilitate maturation of tubules formed from transplanted ECs. The investment with pericytes of capillaries formed in the PEG gels suggests the material not only supports the formation of EC tubules, but also facilitates

stabilization of these vessels. Further investigation is needed to assess the permeability and longer-term stability these vessels.

As described above, fibrin and PEG constructs supplemented with cells supported vascularization to differing extents. Fibrin supported enhanced vascularization at early time points, as assessed by both LDPI and histology, but did not outperform PEG constructs at later time points. PEG hydrogels were structurally stable and showed minimal vessel regression. Interestingly, this response was not modulated by tuning degradability of the crosslinking peptide (i.e. no significant differences were found between 3.5%G and 3.5%V constructs). This result corroborates our prior work as well as other studies [54, 55]. Previously, we demonstrated endothelial cell tubulogenesis *in vitro* was highly dependent on PEG hydrogel mechanical properties, but not degradability [54]. Others have demonstrated that vascularization is not significantly enhanced in hydrogels containing MT1-MMP-sensitive peptides as compared to gels containing MMP2-sensitive peptides[55]. Overall, these data suggest PEG gels facilitate vascularization, but are sufficiently robust to persist *in vivo* for weeks.

Intrinsic differences in peptide degradability may not be sufficiently pronounced to result in different functional response. In fact, degradation by recombinant MMP2 did not significantly differ for 3.5%G and 3.5%V hydrogels (Figure 4-11). Fibrin gels were degraded significantly more rapidly in this assay. Fibrin gels support extensive vascularization early after implantation, but cannot sustain the vessels formed, perhaps due to rapid degradation. A recent study suggested decelerating fibrin degradation can enhance vessel density in fibrin implants[71] which corroborates our hypothesis relating

vessel density to extent of material degradation. Implications of this result are highly relevant to ongoing strategies to revascularize ischemic tissues, as these data hint at the value of a structurally stable material that can sustain neovessels beyond the first weeks following ischemic insult.

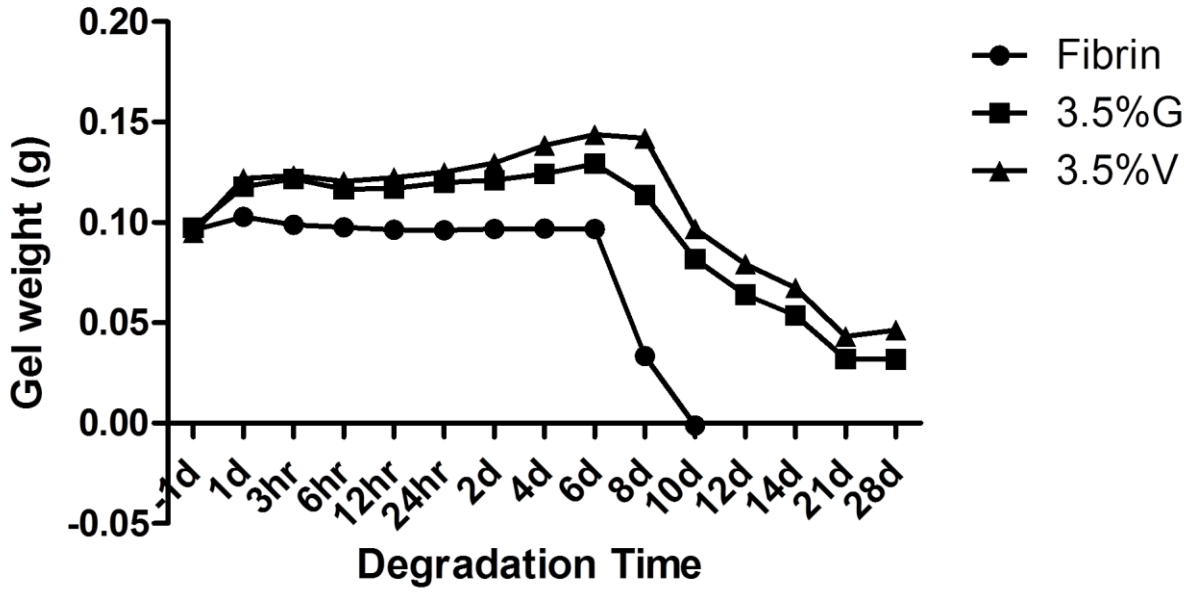

Figure 4-11. Fibrin gels are more rapidly degraded than 3.5%G or 3.5%V gels in the presence of 1 nM recombinant MMP2.

Heretofore, we have primarily discussed implant vasculature in hydrogels delivering cells. In the context of perfusion recovery, however, the acellular gels and the host response in tissues surrounding the implant merit discussion. Surprisingly, perfusion of acellular gels, as measured by LDPI, was not attenuated compared to cell-impregnated gels by 14 days after implantation. These data suggest that, despite the lack of vasculature within the implant, compensatory mechanisms allow for reperfusion in response to the material alone. In this regard, the muscle surrounding the acellular gels remains more heavily infiltrated at day 7 with immune cells and host stromal and endothelial cells. Reperfusion may be partially explained by the immune stimulus

presented by the gels and growth factors contained in the medium that we encapsulated within the gels. Additionally, the process of arteriogenesis upstream of the implant site may be modulated by the gel construct, but this remains to be determined. Indeed, it is worth noting that a previous study demonstrated that delivery of VEGF formulated for sustained release to a site distal in the ischemic limb modulated collateralization upstream [72]. The acellular implants appear to support revascularization to the ischemic tissue, yet we did not assess the muscle function or longer-term recovery in these animals, which could yield differences when compared to cellular implants.

Taken together, our data suggest that PEG hydrogels hold potential as a cell delivery vehicle for therapeutic vascularization, but further studies are necessary to investigate the ability of these materials to support the regeneration of ischemic tissue. Additional work will also be needed to investigate the long-term functional recovery of the ischemic tissue, along with restoration of blood flow. Additionally, young, healthy animals were used in this study and further investigation regarding the response in animals that better model patients with PAD and CLI is warranted. Nonetheless, this study demonstrates PEG hydrogels support revascularization of ischemic tissue and merit further investigation for applications in therapeutic vascularization.

4.5 References

[1] CDC/NCHS, National Vital Statistics System.
[2] Cardiovascular diseases (CVDs). In: Organization WH, editor. Media centre. Geneva: World Health Organization; 2013.
[3] Facts about Peripheral Artery Disease (P.A.D.). In: Services USDoHaH, editor.2006.
[4] US National Library of Medicine NIoH. Coronary Heart Disease. 2010.
[5] Go AS, Mozaffarian D, Roger VL, Benjamin EJ, Berry JD, Blaha MJ, et al. Heart disease and stroke statistics--2014 update: a report from the American Heart Association. Circulation. 2014;129:e28-e292.

[6] Deveza L, Choi J, Yang F. Therapeutic angiogenesis for treating cardiovascular diseases. Theranostics. 2012;2:801-14.
[7] Brenes RA, Jadlowiec CC, Bear M, Hashim P, Protack CD, Li X, et al. Toward a mouse model of hind limb ischemia to test therapeutic angiogenesis. Journal of vascular surgery. 2012;56:1669-79; discussion 79.
[8] Lotfi S, Patel AS, Mattock K, Egginton S, Smith A, Modarai B. Towards a more relevant hind limb model of muscle ischaemia. Atherosclerosis. 2013;227:1-8.
[9] Simons M, Ware JA. Therapeutic angiogenesis in cardiovascular disease. Nature reviews Drug discovery. 2003;2:863-71.
[10] Tongers J, Roncalli JG, Losordo DW. Therapeutic angiogenesis for critical limb ischemia: microvascular therapies coming of age. Circulation. 2008;118:9-16.
[11] Yang Z, von Ballmoos MW, Diehm N, Baumgartner I, Kalka C, Di Santo S. Call for a reference model of chronic hind limb ischemia to investigate therapeutic angiogenesis. Vascular pharmacology. 2009;51:268-74.
[12] Losordo DW, Dimmeler S. Therapeutic angiogenesis and vasculogenesis for ischemic disease: part II: cell-based therapies. Circulation. 2004;109:2692-7.
[13] Kito T, Shibata R, Ishii M, Suzuki H, Himeno T, Kataoka Y, et al. iPS cell sheets created by a novel magnetite tissue engineering method for reparative angiogenesis. Scientific reports. 2013;3:1418.
[14] Chen RR, Silva EA, Yuen WW, Mooney DJ. Spatio-temporal VEGF and PDGF delivery patterns blood vessel formation and maturation. Pharmaceutical research. 2007;24:258-64.
[15] Semenza GL. Vasculogenesis, angiogenesis, and arteriogenesis: mechanisms of blood vessel formation and remodeling. Journal of cellular biochemistry. 2007;102:840-7.
[16] Carmeliet P, Jain RK. Molecular mechanisms and clinical applications of angiogenesis. Nature. 2011;473:298-307.
[17] Potente M, Gerhardt H, Carmeliet P. Basic and therapeutic aspects of angiogenesis. Cell. 2011;146:873-87.
[18] Davis GE, Kim DJ, Meng CX, Norden PR, Speichinger KR, Davis MT, et al. Control of vascular tube morphogenesis and maturation in 3D extracellular matrices by endothelial cells and pericytes. Methods in molecular biology. 2013;1066:17-28.
[19] Cao Y, Hong A, Schulten H, Post MJ. Update on therapeutic neovascularization. Cardiovasc Res. 2005;65:639-48.
[20] Newman AC, Nakatsu MN, Chou W, Gershon PD, Hughes CC. The requirement for fibroblasts in angiogenesis: fibroblast-derived matrix proteins are essential for endothelial cell lumen formation. Molecular biology of the cell. 2011;22:3791-800.
[21] Lovett M, Lee K, Edwards A, Kaplan DL. Vascularization Strategies for Tissue Engineering. Tissue Eng Part B. 2009;15:353-70.
[22] Asai J, Takenaka H, Ii M, Asahi M, Kishimoto S, Katoh N, et al. Topical application of ex vivo expanded endothelial progenitor cells promotes vascularisation and wound healing in diabetic mice. International wound journal. 2013;10:527-33.
[23] Cho SW, Moon SH, Lee SH, Kang SW, Kim J, Lim JM, et al. Improvement of postnatal neovascularization by human embryonic stem cell derived endothelial-like cell transplantation in a mouse model of hindlimb ischemia. Circulation. 2007;116:2409-19.

[24] Margariti A, Winkler B, Karamariti E, Zampetaki A, Tsai TN, Baban D, et al. Direct reprogramming of fibroblasts into endothelial cells capable of angiogenesis and reendothelialization in tissue-engineered vessels. Proceedings of the National Academy of Sciences of the United States of America. 2012;109:13793-8.
[25] Miranville A, Heeschen C, Sengenes C, Curat CA, Busse R, Bouloumie A. Improvement of postnatal neovascularization by human adipose tissue-derived stem cells. Circulation. 2004;110:349-55.
[26] O E, Lee BH, Ahn HY, Shin JC, Kim HK, Kim M, et al. Efficient nonadhesive ex vivo expansion of early endothelial progenitor cells derived from CD34+ human cord blood fraction for effective therapeutic vascularization. FASEB journal : official publication of the Federation of American Societies for Experimental Biology. 2011;25:159-69.
[27] Rufaihah AJ, Huang NF, Jame S, Lee JC, Nguyen HN, Byers B, et al. Endothelial cells derived from human iPSCS increase capillary density and improve perfusion in a mouse model of peripheral arterial disease. Arterioscler Thromb Vasc Biol. 2011;31:e72-9.
[28] Silva EA, Kim ES, Kong HJ, Mooney DJ. Material-based deployment enhances efficacy of endothelial progenitor cells. Proceedings of the National Academy of Sciences of the United States of America. 2008;105:14347-52.
[29] Kang Y, Park C, Kim D, Seong CM, Kwon K, Choi C. Unsorted human adipose tissue-derived stem cells promote angiogenesis and myogenesis in murine ischemic hindlimb model. Microvascular research. 2010;80:310-6.
[30] Kinnaird T, Stabile E, Burnett MS, Shou M, Lee CW, Barr S, et al. Local delivery of marrow-derived stromal cells augments collateral perfusion through paracrine mechanisms. Circulation. 2004;109:1543-9.
[31] Moon MH, Kim SY, Kim YJ, Kim SJ, Lee JB, Bae YC, et al. Human Adipose Tissue-Derived Mesenchymal Stem Cells Improve Postnatal Neovascularization in a Mouse Model of Hindlimb Ischemia. Cell Physiol Biochem. 2006;17:279-90.
[32] Rehman J, Traktuev D, Li J, Merfeld-Clauss S, Temm-Grove CJ, Bovenkerk JE, et al. Secretion of angiogenic and antiapoptotic factors by human adipose stromal cells. Circulation. 2004;109:1292-8.
[33] Kamihata H, Matsubara H, Nishiue T, Fujiyama S, Tsutsumi Y, Ozono R, et al. Implantation of Bone Marrow Mononuclear Cells Into Ischemic Myocardium Enhances Collateral Perfusion and Regional Function via Side Supply of Angioblasts, Angiogenic Ligands, and Cytokines. Circulation. 2001;104:1046-52.
[34] Urbich C, Dimmeler S. Endothelial progenitor cells: characterization and role in vascular biology. Circ Res. 2004;95:343-53.
[35] Foubert P, Matrone G, Souttou B, Lere-Dean C, Barateau V, Plouet J, et al. Coadministration of endothelial and smooth muscle progenitor cells enhances the efficiency of proangiogenic cell-based therapy. Circ Res. 2008;103:751-60.
[36] Chen X, Aledia AS, Ghajar CM, Griffith CK, Putnam AJ, Hughes CC, et al. Prevascularization of a Fibrin-Based Tissue Construct Accelerates the Formation of Functional Anastomosis with Host Vasculature. Tissue engineering Part A. 2009;15:1363-71.
[37] Chen X, Aledia AS, Popson SA, Him L, Hughes CC, George SC. Rapid Anastomosis of Endothelial Progenitor Cell-Derived Vessels with Host Vasculature Is

Promoted by a High Density of Cotransplanted Fibroblasts. Tissue engineering Part A. 2010;16:585-94.
[38] Kniazeva E, Kachgal S, Putnam AJ. Effects of extracellular matrix density and mesenchymal stem cells on neovascularization in vivo. Tissue engineering Part A. 2011;17:905-14.
[39] Ghajar CM, Chen X, Harris JW, Suresh V, Hughes CC, Jeon NL, et al. The effect of matrix density on the regulation of 3-D capillary morphogenesis. Biophysical journal. 2008;94:1930-41.
[40] Suuronen EJ, Kuraitis D, Ruel M. Improving cell engraftment with tissue engineering. Seminars in thoracic and cardiovascular surgery. 2008;20:110-4.
[41] Simpson D, Liu H, Fan TH, Nerem R, Dudley SC, Jr. A tissue engineering approach to progenitor cell delivery results in significant cell engraftment and improved myocardial remodeling. Stem cells. 2007;25:2350-7.
[42] Kedem A, Perets A, Gamlieli-Bonshtein I, Dvir-Ginzberg M, Mizrahi S, Cohen S. Vascular Endothelial Growth Factor-Releasing Scaffolds Enhance Vascularization and Engraftment of Hepatocytes Transplanted on Liver Lobes. Tissue engineering. 2005;11:715-22.
[43] Daga A, Muraglia A, Quarto R, Cancedda R, Corte G. Enhanced engraftment of EPO-transduced human bone marrow stromal cells transplanted in a 3D matrix in non-conditioned NOD/SCID mice. Gene therapy. 2002;9:915-21.
[44] Rustad KC, Wong VW, Sorkin M, Glotzbach JP, Major MR, Rajadas J, et al. Enhancement of mesenchymal stem cell angiogenic capacity and stemness by a biomimetic hydrogel scaffold. Biomaterials. 2012;33:80-90.
[45] Suuronen EJ, Veinot JP, Wong S, Kapila V, Price J, Griffith M, et al. Tissue-engineered injectable collagen-based matrices for improved cell delivery and vascularization of ischemic tissue using CD133+ progenitors expanded from the peripheral blood. Circulation. 2006;114:I138-44.
[46] Saif J, Schwarz TM, Chau DY, Henstock J, Sami P, Leicht SF, et al. Combination of injectable multiple growth factor-releasing scaffolds and cell therapy as an advanced modality to enhance tissue neovascularization. Arterioscler Thromb Vasc Biol. 2010;30:1897-904.
[47] Ghajar CM, Kachgal S, Kniazeva E, Mori H, Costes SV, George SC, et al. Mesenchymal cells stimulate capillary morphogenesis via distinct proteolytic mechanisms. Experimental cell research. 2010;316:813-25.
[48] Kachgal S, Putnam AJ. Mesenchymal stem cells from adipose and bone marrow promote angiogenesis via distinct cytokine and protease expression mechanisms. Angiogenesis. 2011;14:47-59.
[49] Melero-Martin JM, Khan ZA, Picard A, Wu X, Paruchuri S, Bischoff J. In vivo vasculogenic potential of human blood-derived endothelial progenitor cells. Blood. 2007;109:4761-8.
[50] Melero-Martin JM, De Obaldia ME, Kang SY, Khan ZA, Yuan L, Oettgen P, et al. Engineering robust and functional vascular networks in vivo with human adult and cord blood-derived progenitor cells. Circ Res. 2008;103:194-202.
[51] Morin KT, Tranquillo RT. In vitro models of angiogenesis and vasculogenesis in fibrin gel. Experimental cell research. 2013;319:2409-17.

[52] Au P, Daheron LM, Duda DG, Cohen KS, Tyrrell JA, Lanning RM, et al. Differential in vivo potential of endothelial progenitor cells from human umbilical cord blood and adult peripheral blood to form functional long-lasting vessels. Blood. 2008;111:1302-5.
[53] Koike N, Fukumura D, Gralla O, Au P, Schechner JS, Jain RK. Creation of long-lasting blood vessels. Nature. 2004;428:138-9.
[54] Vigen M, Ceccarelli J, Putnam AJ. Protease-Sensitive PEG Hydrogels Regulate Vascularization In Vitro and In Vivo. Macromol Biosci. 2014.
[55] Sokic S, Christenson MC, Larson JC, Appel AA, Brey EM, Papavasiliou G. Evaluation of MMP substrate concentration and specificity for neovascularization of hydrogel scaffolds. Biomaterials Science. 2014;2:1343.
[56] Moon JJ, Saik JE, Poche RA, Leslie-Barbick JE, Lee SH, Smith AA, et al. Biomimetic hydrogels with pro-angiogenic properties. Biomaterials. 2010;31:3840-7.
[57] Zisch AH, Lutolf MP, Ehrbar M, Raeber GP, Rizzi SC, Davies N, et al. Cell-demanded release of VEGF from synthetic, biointeractive cell-ingrowth matrices for vascularized tissue growth. FASEB journal : official publication of the Federation of American Societies for Experimental Biology. 2003.
[58] Phelps EA, Landazuri N, Thule PM, Taylor WR, Garcia AJ. Bioartificial matrices for therapeutic vascularization. Proceedings of the National Academy of Sciences of the United States of America. 2010;107:3323-8.
[59] Grainger SJ, Carrion B, Ceccarelli J, Putnam AJ. Stromal Cell Identity Influences the In Vivo Functionality of Engineered Capillary Networks Formed by Co-delivery of Endothelial Cells and Stromal Cells. Tissue engineering Part A. 2013.
[60] Patterson J, Hubbell JA. Enhanced proteolytic degradation of molecularly engineered PEG hydrogels in response to MMP-1 and MMP-2. Biomaterials. 2010;31:7836-45.
[61] Ghajar CM, Blevins KS, Hughes CCW, George SC, Putnam AJ. Mesenchymal stem cells enhance angiogenesis in mechanically viable prevascularized tissues via early matrix metalloproteinase upregulation. Tissue engineering. 2006;12:2875-88.
[62] Couffinhal T, Silver M, P. ZL, Kearney M, Witzenbichler B, Isner JM. Mouse Model of Angiogenesis. Am J Pathol. 1998;152:1667-79.
[63] Limbourg A, Korff T, Napp LC, Schaper W, Drexler H, Limbourg FP. Evaluation of postnatal arteriogenesis and angiogenesis in a mouse model of hind-limb ischemia. Nature protocols. 2009;4:1737-46.
[64] Chalothorn D, Faber JE. Strain-dependent variation in collateral circulatory function in mouse hindlimb. Physiol Genomics. 2010;42:469-79.
[65] Scholz D, Ziegelhoeffer T, Helisch A, Wagner S, Friedrich C, Podzuweit T, et al. Contribution of Arteriogenesis and Angiogenesis to Postocclusive Hindlimb Perfusion in Mice. J Mol Cell Cardiol. 2002;34:775-87.
[66] Helisch A, Wagner S, Khan N, Drinane M, Wolfram S, Heil M, et al. Impact of mouse strain differences in innate hindlimb collateral vasculature. Arterioscler Thromb Vasc Biol. 2006;26:520-6.
[67] Greenberg JI, Suliman A, Barillas S, Angle N. Mouse Models of Ischemic Angiogenesis and Ischemia-Reperfusion Injury. Methods in Enzymology. 2008;444:159-74.
[68] Scholz D, Cai W, Schaper W. Arteriogenesis, a new concept of vascular adaptation in occlusive disease. 4. 2001.

[69] Schaper W, Scholz D. Factors regulating arteriogenesis. Arterioscler Thromb Vasc Biol. 2003;23:1143-51.
[70] Armulik A, Abramsson A, Betsholtz C. Endothelial/pericyte interactions. Circ Res. 2005;97:512-23.
[71] Thomson KS, Dupras SK, Murry CE, Scatena M, Regnier M. Proangiogenic microtemplated fibrin scaffolds containing aprotinin promote improved wound healing responses. Angiogenesis. 2014;17:195-205.
[72] Greve JM, Chico TJ, Goldman H, Bunting S, Peale FV, Jr., Daugherty A, et al. Magnetic resonance angiography reveals therapeutic enlargement of collateral vessels induced by VEGF in a murine model of peripheral arterial disease. Journal of magnetic resonance imaging : JMRI. 2006;24:1124-32.

Chapter 5

Conclusions and Future Directions

5.1 Contributions of this Thesis

In this work, we have developed a biosynthetic, PEG-based hydrogel system which supports the formation of vasculature from encapsulated cells both *in vitro* and *in vivo*. In comparison to fibrin, an extensively-studied natural material, PEG gels supported the formation of vasculature that persisted for weeks *in vivo*. Three specific aims were formulated and executed to investigate the ability of the gel system to support vascularization.

Aim 1: Construct and characterize PEG-based hydrogels with tailored proteolytic susceptibility and adhesive ligand density, and demonstrate their ability to support the adhesion, viability, and spreading of both endothelial cells (ECs) and normal human lung fibroblasts (NHLFs) in 3D.

We developed a robust PEG hydrogel platform that allowed tuning of construct mechanical properties via alterations in solids content and tuning of proteolytic degradability via alteration of the gel crosslinking peptide. Gels were crosslinked with 2 peptides that are cleaved with distinct kinetics by several MMPs: GPQG↓IWGQ (slow degradation) and VPMS↓MRGG (more rapid degradation). The hydrogels supported adhesion, viability, and spreading of ECs and NHLFs.

Aim 2: Using an established 3D *in vitro* model system, assess the ability of the PEG-based gels synthesized in aim 1 to support vasculogenesis from ECs and NHLFs.

PEG hydrogels supported the formation of endothelial cell networks *in vitro* in co-culture with NHLFs. Network formation was significantly attenuated in more highly crosslinked hydrogels (i.e., those containing higher weight fractions), but was not significantly altered by changing the degradability of the crosslinking peptide. Nonetheless, MMP-mediated degradation was required for vascularization in this system as inhibition with a broad-spectrum MMP inhibitor, but not the serine-protease inhibitor aprotinin, abrogated vessel formation.

Aim 3: Compare the neovascular response of PEG-based constructs containing ECs and NHLFs to that obtained with fibrin-based constructs following implantation in a dorsal, subcutaneous location as well as intramuscularly in an ischemic hindlimb.

Vessels formed from ECs transplanted with fibroblasts in all PEG implants in both *in vivo* models. In the subcutaneous model, we determined high initial mechanical properties did not attenuate vascularization to the same extent as occurred *in vitro*. All PEG gels supported neovascularization to some extent, and implant vessels inosculated with host circulation. In the ischemic limb model, we demonstrated PEG hydrogels supported maintenance of vessel networks for more prolonged periods of time compared to fibrin gels, indicating that PEG hydrogels facilitate degradation to the extent required for vascularization, but have sufficient mechanical integrity after 2 weeks *in vivo* to maintain implant vasculature.

5.2 Discussion

In aim 1, we developed and optimized the PEG hydrogel platform used in aims 2 and 3. To this end, PEG hydrogels were formed by Michael-type addition of multi-arm PEG vinyl sulfone and cysteine-containing MMP-degradable peptides. Network mechanical properties and proteolytic sensitivity have been demonstrated to modulate EC morphogenesis in several material systems. Thus, we tuned gel solids content and proteolyzable peptide identity to allow investigation of these parameters in our system. Gel shear modulus increased three fold in constructs with 5%, instead of 3.5% solids. Correspondingly, volumetric swelling ratio dropped in the more crosslinked hydrogels. After initial studies with PEG gels crosslinked with the more slowly degraded peptide, GPQG↓IWGQ, we fabricated hydrogels with the more rapidly degraded VPMS↓MRGG. Mechanical characterization demonstrated that the bulk mechanical properties of these gels at matched solids content do not differ. However, peptide identity did significantly

modulate the rate at which these materials were remodeled by cells and by recombinant MMPs. Early studies with our hydrogel system yielded low endothelial cell viability. After changing to a more supportive buffer system and pH we were able to increase viability of ECs. NHLF viability was robust in all gel formulations tested. The completion of these studies completed the first aim, and led us to concurrent investigation of the PEG gel platform in studies *in vitro* and *in vivo*.

The second aim focused on assessing the ability of ECs to organize into vessel networks within PEG hydrogels *in vitro*. Initial studies suggested that the addition of exogenous fibronectin may enhance network formation in an *in vitro* model of angiogenesis, but further investigation demonstrated this result was not statistically meaningful. Thus, aim 2 focused primarily on demonstrating PEG gels support vasculogenesis of ECs encapsulated with NHLFs. Tubule density was demonstrated to drop precipitously in more highly crosslinked gels. Crosslinking peptide identity did not statistically modulate the extent of network formation. Potentially, differences between the more and less degradable gels may be evident at longer time points. Alternately, the differences in degradability may not be relevant in the context of the proteases used in vascularization within these materials. Vascularization was demonstrated to be MMP-dependent. Inhibition of MMPs, but not the plasminogen activators/plasmin proteolytic axis, diminished vascularization.

Finally, in aim 3 we investigated the formation of vasculature from ECs implanted with NHLFs in the PEG hydrogels in dorsal subcutaneous implants and in an ischemic hindlimb. For the subcutaneous model, PEG hydrogel precursor was prepared and then injected into a pocket created on the dorsal flank of immune-compromised mice.

Implant vascularization was monitored over time via non-invasive LDPI. Histological assessments were used to further assess the extent of vascularization and vessel morphology across PEG gel conditions. PEG hydrogels consistently supported the formation of vessels within the implant region, and the inosculation of these structures with the host circulation. In the subcutaneous implants, increased gel solids content did not attenuate vessel density. This contrasts the *in vitro* results, and hints at the differences in proteolytic milieu in the *in vivo* environment.

Based on the minimal differences observed *in vivo* between constructs of different solids content, we investigated only 3.5% PEG gels in the ischemic hindlimb model of vascularization. These studies were aimed at demonstrating the ability of PEG gels to support vascularization in a more physiologically relevant context. The murine model of hindlimb ischemia mimics the attenuation in blood flow to the limb seen in patients with advanced PAD and CLI. The hypoxic microenvironment and presence of necrotic muscle more closely recapitulates the clinically relevant scenario. To execute these studies, we ligated and excised the femoral artery and vein in the region between the branching of the deep femoral artery and popliteal and saphenous arteries. Following femoral artery ligation, PEG constructs were delivered intramuscularly, with or without cells, and reperfusion of the limb was monitored. All constructs supported reperfusion to some extent. Notably, upon comparison with control fibrin implants, PEG implants supported more sustained revascularization. Regression of vasculature was evident by 14 days post-FAL in fibrin, but not PEG constructs. These data suggest the PEG gels hold promise for therapeutic vascularization, as they both support the formation of perfused vessels and remain mechanically intact for longer periods of time

upon implantation *in vivo*, which may be important to support long-lasting, mature vasculature.

In all, the data presented in this thesis demonstrate that biosynthetic, MMP-degradable PEG hydrogels are a promising material platform for the delivery of cells for therapeutic vascularization. Additionally, the materials hold promise for tissue engineering, as they potentially can be modified to support the addition of parenchymal, as well as vascular, elements.

5.2 Future Directions

The results of this thesis suggest PEG gels hold potential for therapeutic angiogenesis and tissue engineering. Our data open up several additional avenues of research. Generally, future areas of interest can be split into two categories: those focused on mechanistic elucidation of how the PEG gels support vascularization and how they can be engineered to better support this process, and those focused on further characterizing the ability of the material to facilitate revascularization in a clinical context. To a degree, these approaches will go hand-in-hand, as results from one area may motivate the second.

There are several relevant future studies that would facilitate a better mechanistic understanding of the process of vascularization in these PEG gels. In this work, we used PEG gels tethered with the minimally-required adhesive peptide for viability, RGD, and then crosslinked the constructs with MMP-sensitive crosslinking peptides. Despite the success of these constructs at inducing vascularization *in vitro* and *in vivo*, we suggest this process may be enhanced by further optimization of the material platform,

and more thorough investigation of the role of proteolysis in mediating vascularization in the PEG gels.

First, the adhesive motif utilized in the thesis has been ubiquitously used in PEG literature to facilitate cells adhesion, but may not be most relevant for re-creating a microenvironment similar to that encountered by ECs *in vivo*. Our studies with fibronectin (see appendices) were aimed at assessing the importance of integrin-mediated adhesion and signaling on the process of vascularization in the PEG constructs. However, the results of these investigations are incomplete. Fibronectin was incorporated non-covalently into the constructs. This non-covalent method of incorporation may attenuate the ability of cells to generate traction and respond to binding motifs on the molecule may be attenuated. Studies have demonstrated a role for fibronectin fibrillogenesis and the exposure of cryptic binding motifs on EC response in 3D, which may not be re-created in the soluble environment [1, 2]. In lieu of covalently linking fibronectin to the hydrogel, more simple strategies could be utilized to alter the adhesive milieu of the PEG gels. PEG hydrogels with both the prototypical RGD motif, and the synergy domain from fibronectin, PHSRN, support increased proliferation in PEG gels[3]. Modulating our PEG scaffold to additionally include PHSRN would be experimentally facile, and be advantageous from a translational perspective, as peptides can be easily synthesized and do not suffer the same clinical concerns as naturally-derived proteins. Another fibronectin-derived peptide motif, REDV, could be incorporated into the PEG scaffolds [4, 5]. Alternately, others have demonstrated the laminin-derived peptide YIGSR can be used in conjunction with RGD to enhance spreading on PEG gels [6-8]. The relative abundance of laminin in the

basement membrane underlying vessels *in vivo* gives this approach relevance from a physiological perspective.

Moving away from the adhesive properties of the hydrogel construct, proteolytic susceptibility could be more carefully tailored and investigated. The two peptides we used, GPQG↓IWGQ and VPMS↓MRGG, are degraded at different rates by several MMPs, but are not highly specific to particular members of the MMP family. Thus, it may be of value to incorporate peptides more specific to the MMPs relevant in vascularization. Others have published sequences that may facilitate this investigation [9]. As our studies suggest modifying peptide identity is minimally complex (as long as few hydrophobic residues are present) and that bulk mechanical properties do not change with alterations in the crosslinking peptide, this is a promising area of research. In these proposed hydrogel constructs, and in those described above, investigation of EC morphogenesis *in vitro* and *in vivo* are critical areas that need to be addressed.

In the context of clinical applications, our results suggest PEG hydrogels hold promise for therapeutic vascularization. However, our work to date suffers some limitations that merit additional investigation. First, our animal model does not perfectly recapitulate the clinical condition it aims to model. Young, healthy animals have been demonstrated to recover from ischemic insult more easily than animals that more closely match the patient demographic with PAD [10, 11]. Allowing mice to age may be prohibitively expensive, but using non-obese diabetic (NOD)-SCID mice merits consideration. As these mice are immunodeficient, their use would facilitate analyses of human-derived cells in implants. This strain has been extensively vetted as a model animal for diabetes and CVD research.

Additionally, though we have investigated revascularization of the ischemic tissue, we have not assessed the functional recovery of the muscle thoroughly, nor have we introduced any vascular challenges to the recovering mice. Challenges to the new vasculature could include response to exercise, MRA after administration of the β1-adrenergic agonist dobutamine, and measurement of muscle fiber contractile properties following ischemic induction and delivery of various PEG gels with cells [12]. Permeability of the neovasculature also merits further investigation- this could be probed via additional MRA to look both at edema and tracer leakage into the ischemic tissue. Alternately, vessel permeability could be assessed by monitoring the movement of a dye, for example Evans blue, into the extravascular space.

The question of cell choice remains a concern in our studies. Others have demonstrated fibroblasts may not be ideal to support the formation of functional, stable vessels. Additionally, lung fibroblasts and umbilical vein endothelial cells are not a viable source of cells for clinical applications. For further study, EPCs and AdSCs or MSCs could be delivered in PEG gels to the ischemic tissue instead of HUVECs and fibroblasts. Moreover, studies could be conducted with immune-competent animals, either of a standard genetic background or ApoE knockouts, to deliver autologous AdSCs within PEG matrices.

Finally, for clinical applications and tissue engineering, the introduction of more sophisticated biological signals into the PEG gels may be warranted. Recombinant growth factors could be tethered into PEG construct- this has been demonstrated with VEGF [13, 14]. Potentially, factors could be introduced to not only facilitate vascularization, but also promote development of additional parenchymal tissue

elements in the PEG gels. Lastly, covalent tethering may not be required to enhance cell response within PEG constructs. For instance, others have shown soluble Tβ4 entrapped in PEG gels improves EC adhesion and survival [15]. TGF-β encapsulation was demonstrated to have a similar effect in another study [13]. PEG gels could be loaded with GM-CSF for implantation *in vivo*, with or without cells, to enhance recruitment of host progenitors.

Overall, PEG hydrogels show promise for application in tissue engineering and therapeutic vascularization. Further studies will allow these approaches to be vetted more thoroughly, and aid in the clinical translation of the technology.

5.4 References

[1] Zhou X, Rowe RG, Hiraoka N, George JP, Wirtz D, Mosher DF, et al. Fibronectin fibrillogenesis regulates three-dimensional neovessel formation. Genes & development. 2008;22:1231-43.

[2] Barker TH. The role of ECM proteins and protein fragments in guiding cell behavior in regenerative medicine. Biomaterials. 2011;32:4211-4.

[3] Benoit DS, Anseth KS. The effect on osteoblast function of colocalized RGD and PHSRN epitopes on PEG surfaces. Biomaterials. 2005;26:5209-20.

[4] Hubbell JA, Massia SP, Desai NP, Drumheller PD. Endothelial Cell-Selective Materials for Tissue Engineering in the Vascular Graft via a New Receptor. Nature biotechnology. 1991;9:568-72.

[5] Massia SP, Hubbell JA. Vascular Endothelial Cell Adhesion and Spreading Promoted by the Peptide REDV of the IIICS Region of Plasma Fibronectin is Mediated by Integrin Alpha4 Beta1. The Journal of biological chemistry. 1992;267:14019-26.

[6] Boateng SY, Lateef SS, Mosley W, Hartman TJ, Hanley L, Russell B. RGD and YIGSR synthetic peptides facilitate cellular adhesion identical to that of laminin and fibronectin but alter the physiology of neonatal cardiac myocytes. Am J Physiol Cell Physiol. 2005;288:C31-C8.

[7] Choi WS, Bae JW, Joung YK, Park KD, Lee MH, Park JC, et al. Fabrication of Endothelial Cell-Specific Polyurethane Surfaces co-Immobilized with GRGDS and YIGSR Peptides. Macromolecular Research. 2009;17:458-63.

[8] Fittkau MH, Zilla P, Bezuidenhout D, Lutolf MP, Human P, Hubbell JA, et al. The selective modulation of endothelial cell mobility on RGD peptide containing surfaces by YIGSR peptides. Biomaterials. 2005;26:167-74.

[9] Turk BE, Huang LL, Piro ET, Cantley LC. Determination of protease cleavage site motifs using mixture-based oriented peptide libraries. Nature biotechnology. 2001;19:661-7.
[10] Madeddu P, Emanueli C, Spillmann F, Meloni M, Bouby N, Richer C, et al. Murine models of myocardial and limb ischemia: diagnostic end-points and relevance to clinical problems. Vascular pharmacology. 2006;45:281-301.
[11] Lotfi S, Patel AS, Mattock K, Egginton S, Smith A, Modarai B. Towards a more relevant hind limb model of muscle ischaemia. Atherosclerosis. 2013;227:1-8.
[12] Faulkner JA, Brooks SV. Contractile Properties of Skeletal Muscles from Young, Adult, and Aged Mice. J Physiol. 1988;404:71-82.
[13] Seliktar D, Zisch AH, Lutolf MP, Wrana JL, Hubbell JA. MMP-2 sensitive, VEGF-bearing bioactive hydrogels for promotion of vascular healing. 2003.
[14] Zisch AH, Lutolf MP, Ehrbar M, Raeber GP, Rizzi SC, Davies N, et al. Cell-demanded release of VEGF from synthetic, biointeractive cell-ingrowth matrices for vascularized tissue growth. FASEB journal : official publication of the Federation of American Societies for Experimental Biology. 2003.
[15] Kraehenbuehl TP, Ferreira LS, Zammaretti P, Hubbell JA, Langer R. Cell-responsive hydrogel for encapsulation of vascular cells. Biomaterials. 2009;30:4318-24.

Appendix 1 : Synthesis of Multiarm PEG Vinyl Sulfone

A1.1 Materials

Glassware (see diagram for setup)

Nomex lab coat

Splash goggles

Face mask

Tubing

2 rubber septa

3 way valve with stopcock

Stir plate

Stir bar

Buchner funnel

Filter paper

Desiccator with drierite

Class D Fire Extinguisher (optional)

Aluminum foil

Ice bath

4-1L flasks (or clean 1 repeatedly…)

Vacuum flask

Vacuum Dessicator

Lyophilizer

Toluene

Dichloromethane, anhydrous, dried over molecular sieves

Diethyl ether

Acetone

Powdered Lime

Argon

PEG

Divinyl sulfone

Sodium Hydride

A1.2 Notes

Sodium hydride (NaH) is flammable, toxic, and corrosive. It is water reactive and incompatible with acids, alcohols, and strong oxidizing agents. During this reaction, always wear chemical splash goggles and a face shield. Wear leather or Kevlar gloves beneath nitrile gloves and a fire-resistant (Nomex) lab coat. Do not wear synthetic clothing. Call 911 in case of emergency or OSEH HazMat (3-4568) if spill small. Refer to SOP before performing experiment to go over procedures in case of spills or fires. Use class D fire extinguisher, not ABC. See SOP for storage directions as well.

A1.3 Protocol

1. Purchase powdered form of NaH. Store in a dessicator filled with drierite. After placing the NaH container in the dessicator evacuate the air and flush with argon. Check drierite regularly to see if still dry (changes color to purple when spent).
2. Dry DCM in molecular sieves for 1 day prior to reaction. Prepare 2 waste containers for pyrophoric material (the first containing dry waste, the second for liquid).
3. When ready to start the experiment, clear the hood of all superfluous equipment and setup inert gas line: tubing goes from argon cylinder to 3-way stopcock. From there, plastic tubing goes to the gas inlet arm of the reaction vessel (not attached yet) and the gas bubbler. Keep the 3-way stopcock 8-12 inches above the reaction vessel. Set the stopcock with the middle arrow pointing downwards so flow goes to all 3 lines when gas is turned on (but don't turn on gas yet!). Add 15 mm DCM to the bubbler.
4. Clean glassware with soap and water, and rinse with ddH_2O. Rinse all glassware with acetone and dry using inert gas line.
5. Make sure there is a stir bar in the dry 3-arm RB reaction flask, then weigh out PEG (4-arm PEG-OH 20kDa, 5g.) into the flask, making sure to get no PEG on the neck of the vessel. Add 200 mL toluene to reaction vessel and start stirring. Set up distillation apparatus and perform gas/vac cycle on reaction flask/distillation setup 2x (2 min each) then cap reaction vessel (both arms, don't turn caps down though).
6. Turn on argon inlet (set pressure at 10.5 psi) and allow gas to flow through vessel. Leave cap slightly ajar to flush for ~2 min, then close and allow gas to flow through bubbler. Adjust the bubbler rate to 1 bubble/sec. Turn Si bath heat up to 100^oC (try with thermometer in Si bath not reaction vessel). Once toluene starts to boil

vigorously turn on the water jacket. Keep an eye on the bubbler (want ~1 bubble/sec), the Si oil (want not to overflow), and the glass joints (want no vapor escaping). Allow toluene to completely evaporate, remove Si bath, and allow reaction vessel and hot plate to cool (keep reaction vessel closed so under inert atmosphere).

7. Once cool, lower reaction flask to just above stir plate, add 300 mL dry DCM (dried overnight over molecular sieves) to dissolve the PEG, and resume stirring. After adding solvent recap the open arm and attach 1 side arm to the argon line.
8. Again, establish inert atmosphere by doing the following: open regulator slowly and set argon pressure to 10.5 PSI. The bubbler should start to bubble slowly as the argon slowly fills the entire tubing setup. Remove the cap of the reaction vessel to displace any air. After displacing all of the air, replace the cap. Adjust the flow rate of argon gas to allow 1 bubble/sec from the bubbler (adjust the argon rate to maintain this bubbling rate throughout the experiment, keeping the pressure fixed at 10.5 PSI).
9. Cover reaction vessel in foil and allow PEG/DCM to stir ~10 min. Check that PEG is completely dissolved before proceeding to addition of NaH.
10. Rinse a scintillation vial with acetone and dry with inert gas line. Open NaH container in hood and then move to balance for weighing.
11. Bring the bottle of dry DCM, a pipette to the balance, and the scint vial to the balance with the NaH. Weigh the NaH (0.1167g NaH) into the vial (never use > 1g in a reaction). Note: there should be a 5-fold excess of NaH with respect to OH

groups. Immediately add a small amount of dry DCM to the NaH. Make sure to rinse off any residual NaH from the spatula while adding the DCM to the vial.

12. Take the container of NaH and the vial of NaH/DCM back to the hood. Flush the bag containing NaH with argon (just disconnect the gas line from the reaction vessel for a few seconds) and move the container of NaH back to the desiccators.
13. Note: reaction vessel should be at room temperature at this point (on ice is also ok). Uncap one arm of the reaction vessel to allow for the introduction of the NaH slurry (due to the positive pressure being applied, opening the vessel for a short period of time will not allow for introduction of appreciable amounts of air). Transfer the NaH/DCM slurry via glass pipette to reaction vessel, watching carefully for the evolution of gas and/or solvent boiling. If either occurs, stop adding the NaH slurry until it calms down a bit, then resume. Rinse vial containing slurry with a little more dry DCM and transfer this also to the reaction (Don't transfer to reaction vessel via cannula techniques, as the slurry can clog the cannula.) Once vial is empty, place it and the glass pipette used to add the NaH/DCM in the back to the hood to allow any residue to react with moisture in the air or, alternatively, quench with MeOH or EtOH.
14. After adding all the NaH restore the inert atmosphere to the reaction vessel (i.e. close top with cap). Cover reaction vessel with foil, keep at room temp, and wait 45 min-1 hr to allow for hydrogen evolution.
15. Go back to balance and clean up, making sure no pyrophoric powder is on the balance, etc. Bring the spatula used to measure out the NaH to the back of the hood where the vial and glass pipette are.

16. Dilute 9.8 mL divinyl sulfone (1 OH: 100 DVS) in 10 mL DCM (for a total of ~20 mL) and add this solution dropwise by syringe (ie. maintaining inert atmosphere) to reaction vessel. Cover reaction vessel in foil and allow reaction to proceed 3 days under inert atmosphere with stirring.
17. Place 4L container of ether in -20^{o}C freezer 1d after starting reaction. Also, remove glassware which contained NaH from back of hood and quench, clean, etc.
18. At day 2 check on reaction completion by taking a small aliquot and performing a mini work-up (obviously stop earlier if mini work-up suggests reaction has reached completion):
    a. Use syringe to take small aliquot of reaction solution (10 mL, should contain ~0.125g PEG) and filter off salts (using syringe filter) into a clean scint vial (washed, then rinsed with ddH_2O and acetone).
    b. Dry sample by blasting with air or N_2 for 5 min in scint vial to generate a very viscous solution.
    c. Precipitate viscous/concentrated solution into diethyl ether (scale down volume to 40 mL).
    d. Remove ether by centrifuging and decanting the solvent.
    e. Dry sample in vac oven (overnight) to remove remaining ether and run NMR.
19. Once the reaction is complete, remove the reaction from inert atmosphere. Add 278 uL glacial (ie anhydrous) acetic acid to quench reaction (1 acetic acid: 1 NaH).
20. Then filter the solution, turn off the vacuum, and remove the Buchner funnel. The product we are interested in is the solution which has passed through the filter. (This solution, passed through the filter, should now be clear.) Rinse the funnel with

water then acetone and place the used filter paper in the dry pyrophoric waste container. Place a new piece of filter paper in the funnel for precipitation later.

21. Then concentrate the filtrate down to ~10 mL by attaching to the vacuum line. While doing this, prepare a stir plate with an ice bath for the flask containing ether to rest during precipitation.
22. Once the PEG/DCM product is concentrated, remove 600 mL of ether from the freezer into a clean reaction flask, place a clean, dry stir bar inside, and add the concentrated solution *dropwise* into the ether, while stirring. Once the flask that contained the concentrated product is empty wash it with ~20 mL DCM and pour this into the ether as well. Wait ~5 min for crystallization while mixing (keep in ice bath!).
23. In the meantime, check the flask for residual NaH and quench; then wash as with normal glassware.
24. Place the Buchner funnel over the flask which contained the filtrate, apply vacuum and add the precipitate solution to the funnel. Wash product on filter paper with 100 mL additional diethyl ether. Cover the funnel with foil and allow the precipitate to dry. Take a sample of this product to run on NMR.
25. While allowing precipitate to dry dissolve 5g NaCl in 200 mL ddH_2O. Then dissolve dried precipitate into this NaCl/ddH_2O solution.
26. Add 200 mL DCM to this solution and stir vigorously, then move quickly to separatory funnel. (The PEG product should move to the organic phase, leaving behind impurities).
27. Allow the layers to separate. Then drain off the lower layer (this is DCM and contains the product we want to save!) into a 1L flask. Keep the aqueous layer in

the sep funnel and repeat the extraction 2 more times with 200 mL DCM (2x200=400mL), keeping the organic/lower layer each time.

28. Add sodium carbonate to organic/DCM layer while stirring until the drying agent stops clumping (indicating the solution is dry).
29. Filter solution to remove water-saturated sodium carbonate (or decant to remove solids). Then move DCM/PEG solution to 1L RB flask and reduce volume of solution to ~10 mL under vacuum with stirring.
30. Precipitate this 10 mL solution into ~600 mL diethyl ether while stirring. Rinse RB flask with a small aliquot of DCM and precipitate this rinse into the ether as well.
31. Filter the ether/ppt solution under vacuum to recover the solid multi-arm PEG-VS. Dry the product overnight in the vacuum oven (NO HEAT). Store the dry multi-arm PEG-VS under argon at -20C.
32. Check product functionalization via NMR.

A1.4 NMR Characterization

1. Weigh 5 mg of product into a scintillation vial and dissolve in 0.6 ml of deuterated DMSO. Transfer to 5mm NMR tube- the solvent should reach 3 fingers in height.
2. Use the Gallium machine to acquire the NMR. Login with UM uniqname and Kerberos password and open VNMRJ application
3. Insert sample: ‘e’ to eject (or use eject button): turns on air, put spinner into top, place sample on air flow in spinner, and ‘i’ to insert (or button): turns off air, lowers sample
4. Standard window → pick solvent (DMSO) (middle-bottom window)

5. Type ‘Setlock’ into command line. This is a macro for lock parameters and shim, should see setup complete message
6. On the lock window adjust power (can increase up to 4 units) and gain (amplify signal using gain after increasing power). If you don’t automatically get lock (i.e. lock is below 20): turn lock off and perform lock scan. Look for a step; if it is too low you will see a sinuosoidal pattern. Use ‘setlock’ to restore defaults. Once you have a step hit lock and the electronics will fine tune. A good lock will show the status ‘regulated’.
7. Go to the shim window. The shim represents currents around main field, you want a homogenous field, i.e. narrow lines. To shim: ignore x and y, on 400 use z1, z2 and on 500 use z3, z2, z1, ignore z4, z5, z6. Primarily use z1. Keep clicking until the shim increases. Want to max out at 100, then lower gain, and keep going until you find the max. Alternately, you can do an automated shim using ‘gradient shim’. This runs 1-5 iterations and takes 30sec-1min. Avoid using ‘find z0’
8. Go to the experiment pulldown tab and select nuclei. Click start and then go back to standard and add sample information to the comments field.
9. Go to the ‘acquire’ tab and choose the spectral window (-2 to 14) and number of scans (any multiple of 8). Click the green ‘acquire’ button to generate spectra. This should run the pro-tunes first. After the first acquisition type ‘ga’ (autogain). The bottom middle window will turn blue an count down. When the green ‘idle’ note shows up the scan is done. Review the data and type ‘svf’ to save if it looks good. To remove the spinner type ‘e’ to eject, retrieve sample, and place spinner next to keyboard. Log out of linux

Appendix 2 : Characterization of Endothelial Cells and Fibroblasts Encapsulated in PEG Hydrogels

A2.1 Introduction

The *in vitro* portion of the work outlined in Chapter 3 primarily focuses on the organization of ECs into tubule networks in a vasculogenesis assay. Prior to completing these studies, we characterized cell behavior within the PEG gels using several other assays. In the process of optimizing the gel formulations, we assessed the viability of ECs and fibroblasts. Additionally, we monitored the response to MMP inhibition of fibroblasts encapsulated with ECs for the vasculogenesis assay in PEG gels.

A2.2 Materials and Methods

A2.2.1 Cell Isolation and culture

Human umbilical vein endothelial cells (HUVECs, or ECs) were harvested from fresh umbilical cords according to a previously established protocol [1]. ECs were cultured in supplemented Endothelial Growth Medium (EGM-2, Lonza, Walkersville, MD) at 37^{o}C and 5% CO_2 and used at passage 3. Normal human lung fibroblasts (NHLFs, Lonza) were cultured in M199 (Invitrogen Corporation, Carlsbad, CA) with 10% fetal bovine serum (FBS), 1% penicillin/streptomycin (Mediatech, Manassas, VA), and

0.5% gentamicin (Invitrogen) at 37^{o}C and 5% CO_2 and used prior to passage 15. Cells were cultured in monolayers until reaching 80% confluency and passaged with 0.05% trypsin-EDTA (Invitrogen).

A2.2.2 PEG Hydrogel Formation

Hydrogels were formed via a Michael-type addition reaction of 4-arm PEG vinyl sulfone (henceforth termed PEG-VS) (20 kDa, JenKem USA, Allen, TX) with a combination of thiol-containing adhesive and protease-sensitive peptides by modifying a published protocol [2]. To prepare the gels, PEG-VS was dissolved in HEPES (50 mM, pH 8.4, supplemented with growth factors from endothelial medium bullet kit) at the appropriate concentration to produce gels of 3.5% or 5% (w/v) total solids content. The adhesive peptide (CGRGDS, Genscript, Piscataway, NJ) was added to the PEG solution at 10 µg/ml in HEPES to yield a final adhesive site density upon gelation of 500 µM and the solution was reacted 30 minutes at room temperature. Following conjugation of RGD, bis-cysteine-containing crosslinking peptides were added in HEPES such that -SH and -VS groups were present at a 1:1 molar ratio. Gels were polymerized with 1 of 2 peptides, Ac-GCRD-GPQG↓IWGQ-DRCG-NH_2 or Ac-GCRD-VPMS↓MRGG-DRCG-NH_2 (cleavage site indicated by↓). After mixing, precursor solutions were polymerized for 1 hour at 37^{o}C in sterile 1-ml syringes with the needle end cut off [3]. After polymerization gels were transferred to medium, as appropriate. All gels were formed under aseptic conditions from precursors that were filtered through a 0.22 um syringe filter.

A2.2.3 EC and NHLF Viability in PEG Hydrogels

Hydrogels were formed as described above with either ECs or NHLFs, encapsulated at 1 million cells/ml. After 7 days in culture, cells were stained with Calcein AM and Ethidium homodimer-1 using a kit from Invitrogen (LIVE/DEAD Viaibility/Cytotoxicity Kit for mammalian cells, Invitrogen). The interior of each gel was imaged using an Olympus IX81 spinning disk confocal microscope (Olympus, Center Valley, PA) with a Hammamatsu (Bridgewater, NJ) camera.

A2.2.4 Assessment of Cell Morphology in Vasculogenesis in the Presence of GM6001

Gel constructs (3.5%G, 5%G, 3.5%V, and 5%V; each with and without GM6001) were polymerized in 50 µl aliquots using cut off syringes. A broad-spectrum MMP inhibitor, GM6001 (EMD Chemicals, San Diego, CA), was added at 10 µM, as in previous work from our lab[4]. Cell mixtures in a 1:1 ratio of ECs and NHLFs were added for a total of 10^5 cells/gel. Following polymerization, cell-seeded constructs were cultured in fully supplemented EGM-2 in a 12-well plate with the media changed every other day. Inhibitor was replenished with each media change. At 7 days post-fabrication, gels from each condition were washed several times with PBS and then fixed with formalin. Following permeabilization and TBS-T washes, constructs were incubated 4 hours with rhodamine phalloidin to allow visualization of the actin cytoskeleton of encapsulated endothelial cells and fibroblasts. Low magnification fluorescent images were obtained of vessel network formation in each gel.

A2.3 Results and Discussion

A2.3.1 EC and NHLF Viability in PEG Hydrogels

EC and NHLF viability exceeds 80% in all PEG gel formulations (3.5%G, 5%G, 3.5%V, 5%V), even after 7 days in culture post-polymerization (Figure A2-1 shows 5%G gels). The viability studies confirmed that PEG hydrogels support viability of encapsulated ECs and fibroblasts. Despite high viability, however, ECs remain rounded in 5% gels even after 7 days.

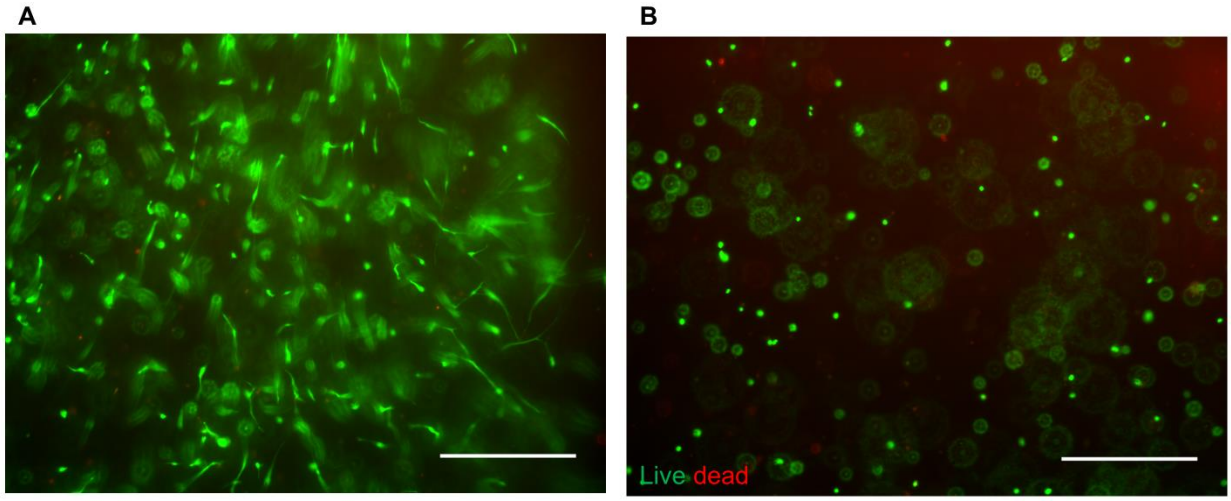

Figure A 2-1. Cell viability in PEG gels. LIVE/DEAD staining on gels 7 days after encapsulation of NHLFs (A) or ECs (B). Green indicates live cells, red are dead. Scale = 100 μm.

A2.3.2 Morphology of Fibroblasts upon MMP Inhibition

Staining for the actin cytoskeleton of fibroblasts and ECs encapsulated in PEG hydrogels demonstrated notable differences between PEG hydrogels with and without the addition of GM6001 (Figure A2-2). The phalloidin stain does not distinguish between ECs and NHLFs. Nonetheless, it is clear that MMP inhibition eliminates NHLF spreading in the gel constructs. Both endothelial cells and fibroblasts remain rounded in PEG gels incubated with GM6001; these results parallel the attenuation of vasculogenesis in GM6001-treated gels (Figure 3-4). These data also demonstrate

that, despite minimal EC network formation, fibroblasts still spread in 5%G and 5%V gels that do not contain GM6001. Thus, fibroblast morphology cannot predict the ability of the gel constructs to support vasculogenesis- fibroblasts spread in gels with increased solids content, but EC network formation is still attenuated.

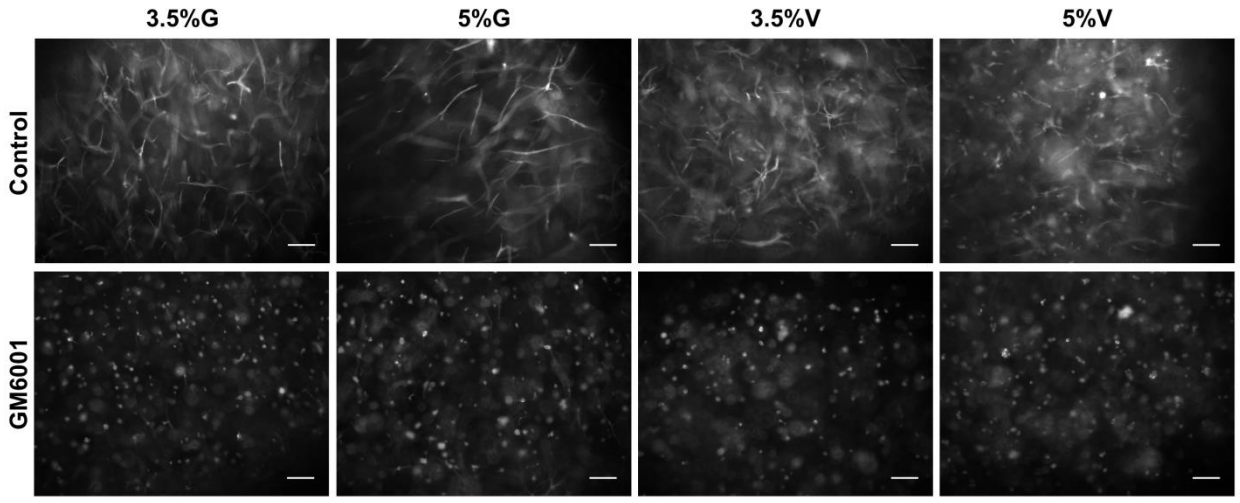

Figure A 2-2. Phalloidin staining of EC and NHLF co-cultures with and without MMP inhibition. Both EC and fibroblast morphology is notably constrained in gels treated with GM6001. Scale = 200 μm.

A2.4 References

[1] Ghajar CM, Blevins KS, Hughes CC, George SC, Putnam AJ. Mesenchymal Stem Cells Enhance Angiogenesis in Mechanically Viable Prevascularized Tissues via Early Matrix Metalloproteinase Upregulation. Tissue engineering. 2006;12:2875-88.
[2] Lutolf MP, Hubbell JA. Synthesis and Physicochemical Characterization of End-Linked Poly(ethylene glycol)-co-peptide Hydrogels Formed by Michael-Type Addition. Biomacromolecules. 2003;4:713-22.
[3] Khetan S, Burdick J. Cellular encapsulation in 3D hydrogels for tissue engineering. Journal of visualized experiments : JoVE. 2009.
[4] Ghajar CM, Kachgal S, Kniazeva E, Mori H, Costes SV, George SC, et al. Mesenchymal cells stimulate capillary morphogenesis via distinct proteolytic mechanisms. Experimental cell research. 2010;316:813-25.

Appendix 3 : Role of Exogenous Fibronectin in Modulating Vasculogenesis

A3.1 Introduction

Translation of tissue engineering and therapeutic angiogenesis approaches to the clinic has been slow, in part due to significant technical hurdles in creating functional vascular networks. Substantial research aims to understand angiogenesis and recapitulate the process *in vitro* and *in vivo*. Several approaches have been utilized to this end, but in this study we investigate vasculogenesis *in vitro* in bioengineered PEG gels supplemented with fibronectin which deliver ECs and supportive fibroblasts. Several natural materials have been used to this end [1-10], but recent effort has focused on the development of proangiogenic synthetic materials. These materials aim to bypass the several limitations of natural materials, including variability associated with material sourcing and processing, possible concerns regarding immunogenicity, and poorly defined biological functionality. Nonetheless, these materials suffer from limitations as well, including concerns regarding the ability of small peptides to provide sufficient cues to direct cell behavior.

In this work specifically, we investigate the ability of peptide-functionalized poly(ethylene glycol) (PEG) hydrogels, further modified with exogenous fibronectin, to

support vascular morphogenesis *in vitro*. In our system, PEG is typically functionalized with RGD, a minimal integrin-binding domain derived from fibronectin, and then crosslinked with peptides susceptible to cleavage by cell-derived matrix metalloproteases. RGD supports cell adhesion [11-14], but does not fully replicate the dynamic signaling triggered by native ECM proteins [15]. Beyond simple adhesive cues, the native ECM presents signals in the form of proteolytically-cleaved ECM fragments [16], matrix-tethered growth factors, and "cryptic" binding sites that are exposed in response to force-mediated changes in protein conformational states [17]. By utilizing gels which contain both adhesive peptides and full ECM-derived proteins, we aim to assess the extent of vascular network formation in constructs containing and lacking adhesive signals relevant in physiology.

Fibronectin was chosen for encapsulation into PEG hydrogels based on data demonstrating a role for fibronectin-binding integrins $\alpha_5\beta_1$ and $\alpha_v\beta_3$ in the migration of endothelial cells during angiogenesis [18-21]. Specifically, the interaction of $\alpha_5\beta_1$ with fibronectin facilitates cell migration; this response is potentiated by vascular endothelial growth factor (VEGF)-bound fibronectin [22, 23]. Despite the ubiquity of RGD on several ECM proteins, fibronectin's RGD site interacts uniquely with the PHSRN synergy site to facilitate engagement of the $\alpha_5\beta_1$ integrin [24, 25]. RGD and the synergy site both are typically required to support $\alpha_5\beta_1$ coupling [15, 26-29]. The RGD motif alone, which is typically incorporated into synthetic biomaterials, does not possess the same nuanced bioactivity as intact fibronectin, binding $\alpha_v\beta_3$ primarily when displayed as a shorter peptide motif [30, 31]. This is highly relevant for biomaterial design for vascular engineering because, while not required in all contexts, $\alpha_5\beta_1$ interactions with

fibronectin are critical for angiogenesis under certain conditions. The importance of α_5 integrin [32] and fibronectin [33] are further evident from on the defects in vascular development seen in null mice, which lead to embryo deterioration within 10 or 11 days of gestation. RGD alone may not adequately recapitulate native cell binding. In this work, vasculogenesis is compared in hydrogels containing exogenous fibronectin and the RGD peptide and in gels containing RGD alone, to better assess the role of more nuanced cell binding cues.

A3.2 Materials and Methods

A3.2.1 Cell Isolation and culture

Human umbilical vein endothelial cells (HUVECs, or ECs) were harvested from fresh umbilical cords according to a previously established protocol [34]. ECs were cultured in supplemented Endothelial Growth Medium (EGM-2, Lonza, Walkersville, MD) at 37^{o}C and 5% CO_2 and used at passage 3. Normal human lung fibroblasts (NHLFs, Lonza) were cultured in M199 (Invitrogen Corporation, Carlsbad, CA) with 10% fetal bovine serum (FBS), 1% penicillin/streptomycin (Mediatech, Manassas, VA), and 0.5% gentamicin (Invitrogen) at 37^{o}C and 5% CO_2 and used prior to passage 15. Cells were cultured in monolayers until reaching 80% confluency and passaged with 0.05% trypsin-EDTA (Invitrogen).

A3.2.2 PEG Hydrogel Formation

Hydrogels were formed via a Michael-type addition reaction of 4-arm PEG vinyl sulfone (henceforth termed PEG-VS) (20 kDa, JenKem USA, Allen, TX) with a

combination of thiol-containing adhesive and protease-sensitive peptides by modifying a published protocol [35]. To prepare the gels, PEG-VS was dissolved in HEPES (50 mM, pH 8.4, supplemented with growth factors from endothelial medium bullet kit) at the appropriate concentration to produce gels of 3.5% or 5% (w/v) total solids content. The adhesive peptide (CGRGDS, Genscript, Piscataway, NJ) was added to the PEG solution at 10 μg/ml in HEPES to yield a final adhesive site density upon gelation of 500 μM and the solution was reacted 30 minutes at room temperature. Immediately prior to gelation, fibronectin was added to select precursor solutions to yield a final concentration of 90 μg/ml upon gelation. Following conjugation of RGD and addition of fibronectin, bis-cysteine-containing crosslinking peptides were added in HEPES such that -SH and -VS groups were present at a 1:1 molar ratio. Gels were polymerized with 1 of 2 peptides, Ac-GCRD-GPQG↓IWGQ-DRCG-NH_2 or Ac-GCRD-VPMS↓MRGG-DRCG-NH_2 (cleavage site indicated by↓). After mixing, precursor solutions (3.5%G, 5%G, 3.5%V, and 5%V, each tested with and without fibronectin) were polymerized for 1 hour at 37^{o}C in Teflon molds for rheology or in sterile 1-ml syringes with the needle end cut off for vasculogenesis [36]. After polymerization gels were transferred to PBS for rheology and medium for vasculogenesis. All gels were formed under aseptic conditions from precursors that were filtered through a 0.22 um syringe filter.

A3.2.3 Mechanical Characterization of PEG Gels

Bulk mechanical properties were characterized via parallel plate rheology on pre-swollen gels. Following polymerization in Teflon molds, 5% gels of 100 μl were swollen overnight in PBS at 37^{o}C. Measurements were obtained on an AR G2 rheometer (TA

Instruments, New Castle, DE) equipped with a Peltier stage and an 8 mm geometry. Both surfaces were coated with P800 sandpaper (3M, St. Paul, MN) and the gap was adjusted to apply a constant 0.1 N force to prevent slip during measurement. For each gel, a 5 minute time sweep was followed by a frequency sweep from 0.1 to 10 Hz at 5% strain and then a strain sweep from 0.1 to 50% at 1 Hz. Reported shear storage modulus (G') values are the average over the linear viscoelastic region of the frequency sweep.

A3.2.4 Vasculogenesis Assay in PEG Hydrogels

ECs were fluorescently labeled via retroviral transduction with a gene encoding mCherry (Clonteck, Mountain View, CA) as previously described [2]. Lipofectamine 2000 (Life Technologies) was used to transfect Phoenix Ampho cells (Orbigen, San Diego, CA) with a plasmid encoding for mCherry. Viral supernatant was collected after 48 hours, passed through a 0.45 μm syringe filter and supplemented with 5 μg/ml Polybrene (EMD Millipore, Billerica, MA) prior to incubation with EC for 6 hours. The medium was changed to EGM-2 and cells were cultured overnight. Transduction was repeated via another round of viral infection the following day, and the ECs were then grown to confluence and used directly in the vasculogenesis assay. Constructs (conditions outlined above) were polymerized in 50 μl aliquots using cut off syringes. Cell mixtures in a 1:1 ratio of ECs and NHLFs were added for a total of 10^5 cells/gel. Following polymerization, cell-seeded constructs were cultured in fully supplemented EGM-2 in a 12-well plate with the media changed every other day. At 7 days post-fabrication, gels from each condition were washed several times with PBS and then

fixed with formalin prior to imaging. Low magnification fluorescent images were obtained of vessel network formation in each gel. Each gel was imaged at 5 locations in the interior of the gel using an Olympus IX81 spinning disk confocal microscope (Olympus, Center Valley, PA) with a Hammamatsu (Bridgewater, NJ) camera. Average total network length was determined as described previously [37] for each condition using the automated Angiogenesis Module in Metamorph Premier Software (Molecular Devices Inc., Sunnyvale, CA).

A3.3 Results and Discussion

Bulk mechanical properties of gels containing and lacking fibronectin were not significantly different. These data demonstrate the PEG hydrogel crosslinking was ostensibly equivalent in the presence of fibronectin compared to control gels. Still, no data was collected to characterize the microstructure of the gel constructs, and the local environment experienced by cells in the different gel formulations is not necessarily equivalent.

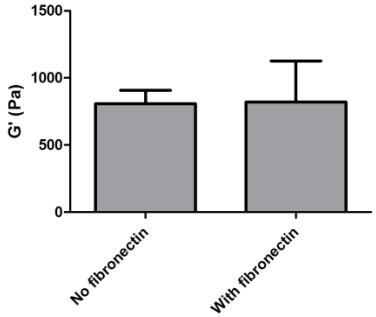

Figure A 3-1. Bulk gel mechanical properties, as assessed by shear rheology, do not differ between 5% gels containing and lacking fibronectin.

The vasculogenesis assay was performed to assess whether the addition of adhesive signals presented in a more physiologic way modulated vascular organization.

The data demonstrate qualitative differences in network formation in the presence of fibronectin, but no statistically significant differences were found upon quantification. Soluble fibronectin is encapsulated within the gel, and not tethered to the matrix. Thus, cells may not be able to generate traction or deform fibronectin on binding; in a physiologic context remodeling of soluble fibronectin into a fibrillar network modulates vascularization [38]. Nonetheless, at 7 day qualitative differences are seen in network formation between gels containing and lacking fibronectin. Perhaps, at later time points statistically meaningful differences would be seen between these conditions.

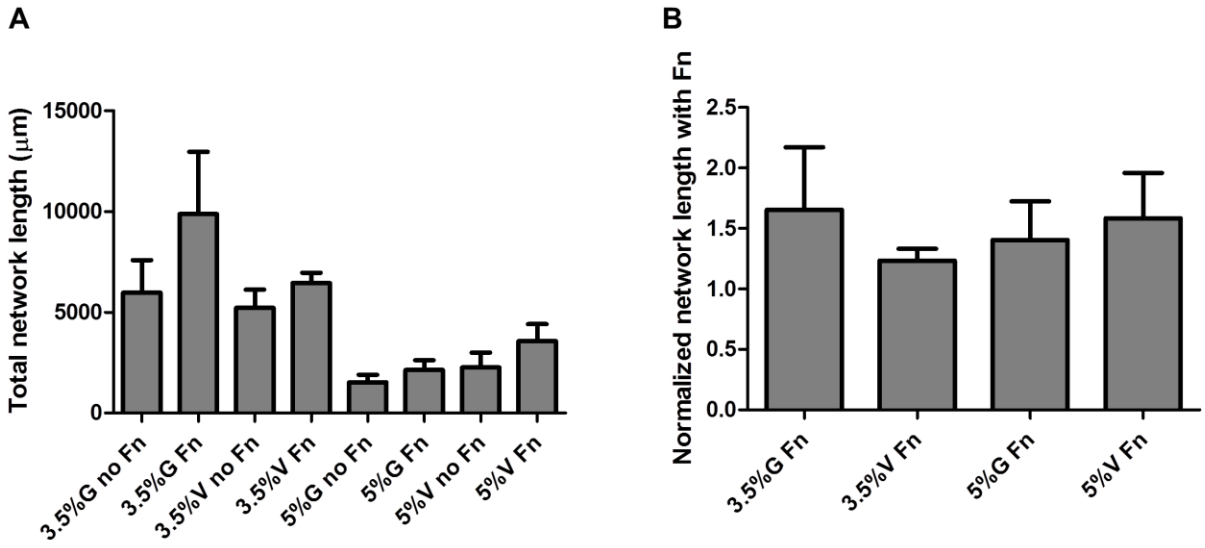

Figure A 3-2. Network length with and without fibronectin. Total network length (A) is not statistically different between gels treated with fibronectin and controls at day 7. Network length of gels with fibronectin is normalized to controls of the same w/v% and crosslinking peptide in B. Qualitative differences suggest significant differences may be present at 14 or 21 day time points.

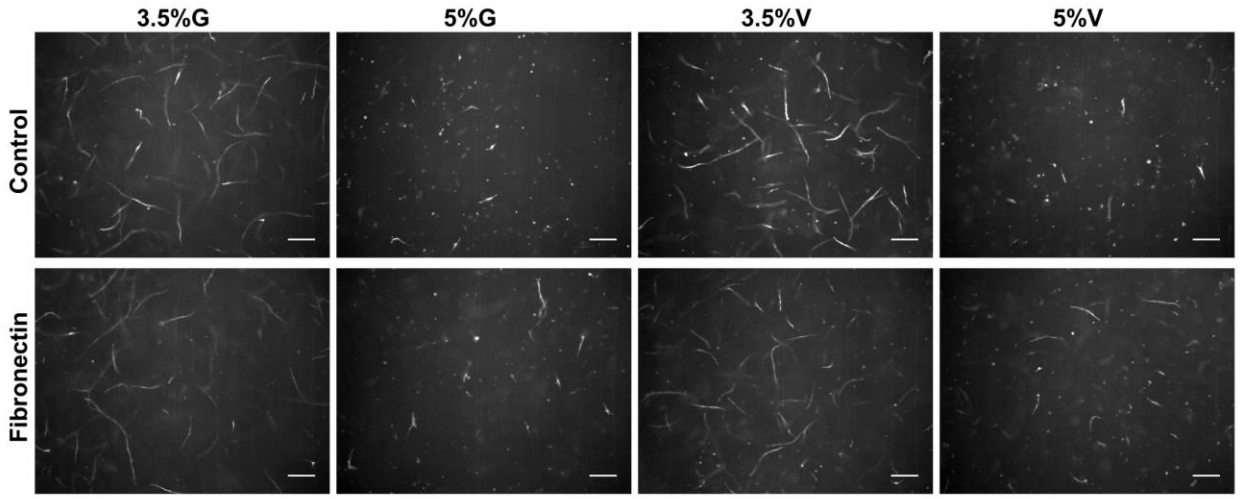

Figure A 3-3. Labeled ECs organize into vascular networks with and without fibronectin. Scale = 200 μm. See quantification in Figure A3-2.

A3.4 References

[1] Chen X, Aledia AS, Ghajar CM, Griffith CK, Putnam AJ, Hughes CC, et al. Prevascularization of a Fibrin-Based Tissue Construct Accelerates the Formation of Functional Anastomosis with Host Vasculature. Tissue engineering Part A. 2009;15:1363-71.
[2] Ghajar CM, Chen X, Harris JW, Suresh V, Hughes CC, Jeon NL, et al. The effect of matrix density on the regulation of 3-D capillary morphogenesis. Biophysical journal. 2008;94:1930-41.
[3] Ghajar CM, Kachgal S, Kniazeva E, Mori H, Costes SV, George SC, et al. Mesenchymal cells stimulate capillary morphogenesis via distinct proteolytic mechanisms. Experimental cell research. 2010;316:813-25.
[4] Kachgal S, Putnam AJ. Mesenchymal stem cells from adipose and bone marrow promote angiogenesis via distinct cytokine and protease expression mechanisms. Angiogenesis. 2011;14:47-59.
[5] Kachgal S, Carrion B, Janson IA, Putnam AJ. Bone marrow stromal cells stimulate an angiogenic program that requires endothelial MT1-MMP. Journal of cellular physiology. 2012.
[6] Melero-Martin JM, Khan ZA, Picard A, Wu X, Paruchuri S, Bischoff J. In vivo vasculogenic potential of human blood-derived endothelial progenitor cells. Blood. 2007;109:4761-8.
[7] Morin KT, Tranquillo RT. In vitro models of angiogenesis and vasculogenesis in fibrin gel. Experimental cell research. 2013;319:2409-17.
[8] Koike N, Fukumura D, Gralla O, Au P, Schechner JS, Jain RK. Creation of long-lasting blood vessels. Nature. 2004;428:138-9.

[9] Au P, Daheron LM, Duda DG, Cohen KS, Tyrrell JA, Lanning RM, et al. Differential in vivo potential of endothelial progenitor cells from human umbilical cord blood and adult peripheral blood to form functional long-lasting vessels. Blood. 2008;111:1302-5.
[10] Au P, Tam J, Fukumura D, Jain RK. Bone marrow-derived mesenchymal stem cells facilitate engineering of long-lasting functional vasculature. Blood. 2008;111:4551-8.
[11] Hern DL, Hubbell JA. Incorporation of adhesion peptides into nonadhesive hydrogels useful for tissue resurfacing. J Biomed Mater Res. 1998;39:266-76.
[12] Lutolf MP, Lauer-Fields JL, Schmoekel HG, Metters AT, Weber FE, Fields GB, et al. Synthetic matrix metalloproteinase-sensitive hydrogels for the conduction of tissue regeneration: engineering cell-invasion characteristics. Proceedings of the National Academy of Sciences of the United States of America. 2003;100:5413-8.
[13] Burdick JA, Anseth KS. Photoencapsulation of osteoblasts in injectable RGD-modified PEG hydrogels for bone tissue engineering. Biomaterials. 2002;23:4315-23.
[14] Mann BK, West JL. Cell adhesion peptides alter smooth muscle cell adhesion, proliferation, migration, and matrix protein synthesis on modified surfaces and in polymer scaffolds. J Biomed Mater Res. 2002;60:86-93.
[15] Bellis SL. Advantages of RGD peptides for directing cell association with biomaterials. Biomaterials. 2011;32:4205-10.
[16] Integrins and Angiogenesis.
[17] Barker TH. The role of ECM proteins and protein fragments in guiding cell behavior in regenerative medicine. Biomaterials. 2011;32:4211-4.
[18] Kim S, Harris M, Varner JA. Regulation of integrin alpha vbeta 3-mediated endothelial cell migration and angiogenesis by integrin alpha5beta1 and protein kinase A. The Journal of biological chemistry. 2000;275:33920-8.
[19] Kim S, Bell K, Mousa SA, Varner JA. Regulation of Angiogenesis in Vivo by Ligation of Integrin α5β1 with the Central Cell-Binding Domain of Fibronectin. The American Journal of Pathology. 2000;156:1345-62.
[20] Lamalice L, Le Boeuf F, Huot J. Endothelial cell migration during angiogenesis. Circ Res. 2007;100:782-94.
[21] Zeng ZZ, Yao H, Staszewski ED, Rockwood KF, Markwart SM, Fay KS, et al. Alpha5 Beta1 Integrin Ligand PHSRN Induces Invasion and Alpha5 mRNA in Endothelial Cells to Stimulate Angiogenesis. Trans Onc. 2009;2:8-20.
[22] Martino MM, Hubbell JA. The 12th-14th type III repeats of fibronectin function as a highly promiscuous growth factor-binding domain. FASEB journal : official publication of the Federation of American Societies for Experimental Biology. 2010;24:4711-21.
[23] Wijelath ES. Novel Vascular Endothelial Growth Factor Binding Domains of Fibronectin Enhance Vascular Endothelial Growth Factor Biological Activity. Circulation Research. 2002;91:25-31.
[24] Koivunen E, Gay DA, Ruoslahti E. Selection of Peptides Binding to the alpha5 beta1 integrin from Phage Display Library. The Journal of biological chemistry. 1993;268:20205-10.
[25] Hood JD, Cheresh DA. Role of integrins in cell invasion and migration. Nature reviews Cancer. 2002;2:91-100.
[26] Garcia AJ, Schwarzbauer JE, Boettiger D. Distinct Activation States of Alpha5 Beta1 Integrin Show Differential Binding to RGD and Synergy Domains of Fibronectin. Biochemistry. 2002;41:9063-9.

[27] Krammer A, Craig D, Thomas WE, Schulten K, Vogel V. A structural model for force regulated integrin binding to fibronectin's RGD-synergy site. Matrix Biology. 2002;21:139-47.
[28] Singh P, Carraher C, Schwarzbauer JE. Assembly of fibronectin extracellular matrix. Annu Rev Cell Dev Biol. 2010;26:397-419.
[29] Wierzbicka-Patynowski I, Schwarzbauer JE. The ins and outs of fibronectin matrix assembly. The Journal of cell biology. 2003;116:3269-76.
[30] Massia SP, Hubbell JA. An RGD Spacing of 440 nm Is Sufficient for Integrin Alphav Beta3-mediated Fibroblast Spreading and 140 nm for Focal Contact and Stress Fiber Formation. The Journal of cell biology. 1991;114:1089-100.
[31] Ruoslahti E. RGD and Other Recognition Sequenes for Integrins. Annu Rev Cell Dev Biol. 1996;12:697-715.
[32] Yang JT, Rayburn H, Hynes RO. Embryonic mesodermal defects in alpha5 integrin-deficient mice. Development. 1993;119:1093-105.
[33] George EL, Georges-Labouesse EN, Patel-King RS, Rayburn H, Hynes RO. Defects in mesoderm, neural tube and vascular development in mouse embryos lacking fibronectin. Development. 1993;119:1079-91.
[34] Ghajar CM, Blevins KS, Hughes CC, George SC, Putnam AJ. Mesenchymal Stem Cells Enhance Angiogenesis in Mechanically Viable Prevascularized Tissues via Early Matrix Metalloproteinase Upregulation. Tissue engineering. 2006;12:2875-88.
[35] Lutolf MP, Hubbell JA. Synthesis and Physicochemical Characterization of End-Linked Poly(ethylene glycol)-co-peptide Hydrogels Formed by Michael-Type Addition. Biomacromolecules. 2003;4:713-22.
[36] Khetan S, Burdick J. Cellular encapsulation in 3D hydrogels for tissue engineering. Journal of visualized experiments : JoVE. 2009.
[37] Grainger SJ, Putnam AJ. Assessing the Permeability of Engineered Capillary Networks in a 3D Culture. PloS one. 2011;6:1-9.
[38] Zhou X, Rowe RG, Hiraoka N, George JP, Wirtz D, Mosher DF, et al. Fibronectin fibrillogenesis regulates three-dimensional neovessel formation. Genes & development. 2008;22:1231-43.

Appendix 4 : Induction of Hindlimb Ischemia via Femoral Artery Ligation and Preliminary Data with Different Stromal Cells

A4.1 Introduction

In Chapter 4 we demonstrate induction of ischemia in a mouse hindlimb via FAL and the reperfusion of the ischemic tissue via delivery of ECs and fibroblasts in PEG or fibrin gels. In this section, we delineate the details of the surgical procedure and present preliminary data with different stromal cells in this model.

As discussed at length in Chapter 4, the extent of ischemia resulting from femoral artery ligation varies widely, depending both on the mouse strain [1-4] as well as ligation site [5-7]. Total loss of flow to the hindlimb results when the femoral artery is ligated and excised proximal to the bifurcation of the deep femoral. In this model collateralization is attenuated due to removal of the pre-existing arteriole network. Additionally, necrosis of the toes and limb paralysis are more profound when the first ligation is placed proximally [8]. Additionally, T cell deficient mice undergo impaired recovery in response to FAL [9]. Our choice of the more distal model of hindlimb ischemia was motivated by poor results seen in even immune competent animals following proximal FAL, arguments regarding the superior physiologic relevance for

PAD of the distal model, and concerns regarding poor recovery following ischemia in the mice population we used- CB15/SCID mice- due to the lack of T and B cells in this strain. Accordingly, the full procedure is outlined below.

Additionally, different stromal cells were explored in our pilot studies using the model of hindlimb ischemia.

A4.2 Materials and Methods

In all conditions, unilateral ligation of hindlimb blood vessels was performed and the unligated, contralateral limb served as a control. See chapter 4 for the protocol overview; details can be found below. Images are shown in Figure A4-1.

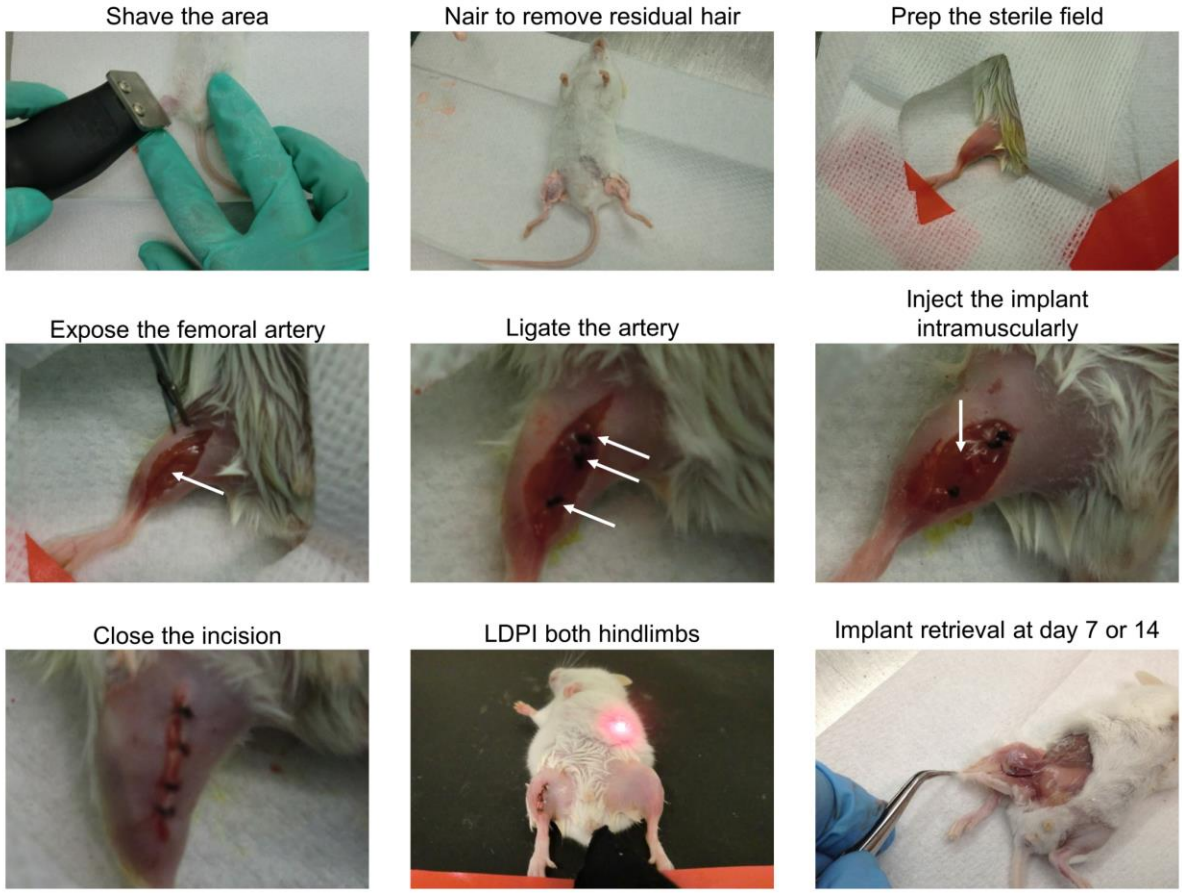

Figure A 4-1. Hindlimb ischemia induced in SCID mice via femoral artery ligation.

In our pilot studies, all animals were delivered fibrin gels. All gels contained ECs, and the response in animals was determined for constructs delivering various stromal cells- specifically NHLFs and ASCs- with the ECs. Cells were resuspended at 10 million total cells/ml in gel precursors for implantation post-FAL.

1. At the initiation of the surgical procedures, transfer mice to a biological safety cabinet. Perform all procedures in a sterile laminar flow hood. This area must be routinely cleaned and sprayed down with alcohol then wiped with an anti-bacterial disinfectant, prior to and after use.
2. Use sterile gloves when performing animal surgery. The surgeon must also wear a gown, booties, cap, and face mask during all procedures. All instruments must be sterilized prior to surgery by autoclaving.
3. Weigh mice and return to cages in animal room. The remaining procedures will be performed for 1 mouse at a time.
4. Anesthetize the mouse with ketamine plus xylazine applied via intraperitoneal injection. Administer prophylactic analgesia when dosing with the ketamine/xylaxine cocktail by addition 0.06 mg/kg buprenorphine to the drug cocktail. Apply ophthalmic ointment to the eyes of the mouse following administration of the anesthetic. Check the depth of anesthesia by monitoring the breathing rate and lack of withdrawal reflex after gently squeezing hind toes.
5. After the animal is anesthetized, shave the entire hindlimb, apply Nair hair removal cream, wait 1 minute, and then remove the Nair with a soap solution.

6. Sterilize the entire surgical site prior to making an incision by 2 applications of betadine and then alcohol to the surgical site.
7. Next, using surgical scissors and curved fine forceps, make an incision 5 mm in length through the dermis and the muscle layers starting from the level of the inguinal ligament. Identify the deep femoral branch and ensure the incision reaches the saphenous-popliteal bifurcation distally.
8. Dissect the connective sheath surrounding the muscle with spring scissors and fine forceps. Carefully isolate the femoral artery and vein from the surrounding muscle at a location distal to the deep femoral branch, again use forceps and fine spring scissors.
9. Use 5-0 Ethilon sutures to tie off the femoral artery and vein at 3 locations: immediately distal to the deep femoral, immediately distal to the first ligation, and just proximal to the saphenous-popliteal bifurcation. Before proceeding with gel delivery, snip the femoral artery and vein segments between ligations 2 and 3. Flood the region with sterile saline to remove remaining blood or loose tissue and dab away excess fluid with sterile gauze.
10. Prior to closing the surgical field, prepare the gel precursor solution, with cells as dictated by the experimental conditions. Transfer the precursor to a syringe and quickly deliver intramuscularly to 3 locations equidistant along the ligated region.
11. Wait 5 minutes for the solution to gel then close the surgical field and suture the wound. Cover the sutures with Mastisol.
12. Return the animal to a fresh cage for recovery. Keep the mouse warm and hydrated and monitor during recovery. To stabilize body temperature, keep the cage on a

heating pad during recovery from anesthesia. Monitor animals until they show normal behavioral signs (i.e. feeding, drinking, grooming, mobile).

A4.3 Results and Discussion

LDPI was used to assess reperfusion to the ischemic limb following delivery of fibrin gels with ECs and the stromal cells outlined above. Our pilot studies suggested implants delivering ECs and NHLFs promote improved recovery following ischemic insult compared to gels delivering other or no stromal cells (Figure A4-2). As discussed in Chapter 4, LDPI is not a perfect metric for revascularization and measures perfusion to a limited depth of tissue. Further studies investigating the role of different stromal cells in modulating revascularization should be conducted to fully parse their role in recovery after ischemic insult.

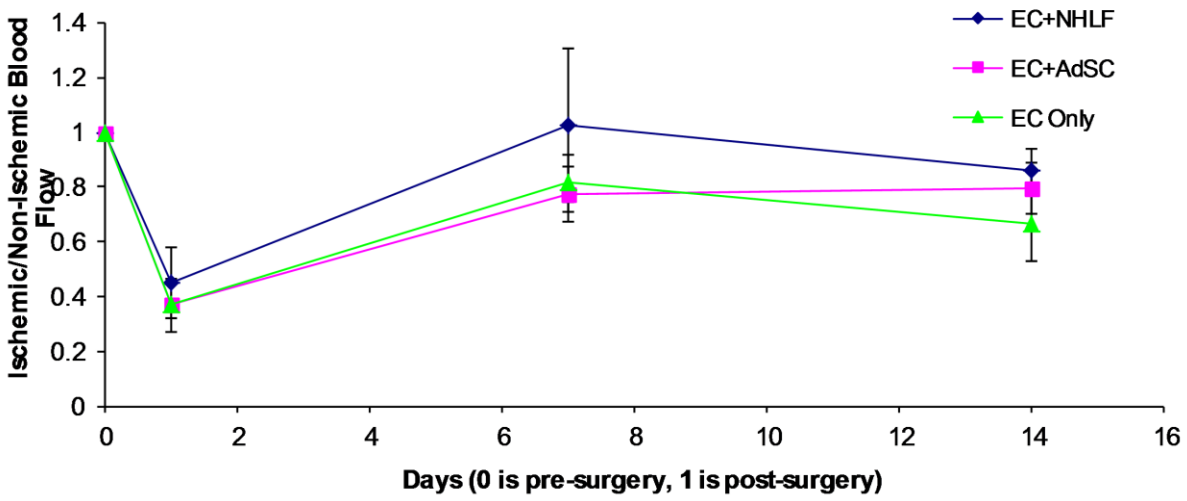

Figure A 4-2. Restoration of perfusion to ischemic limb following delivery of endothelial cells in a fibrin gels with no stromal cells, or with NHLFs or AdSCs.

A4.4 References

[1] Chalothorn D, Faber JE. Strain-dependent variation in collateral circulatory function in mouse hindlimb. Physiol Genomics. 2010;42:469-79.
[2] Scholz D, Ziegelhoeffer T, Helisch A, Wagner S, Friedrich C, Podzuweit T, et al. Contribution of Arteriogenesis and Angiogenesis to Postocclusive Hindlimb Perfusion in Mice. J Mol Cell Cardiol. 2002;34:775-87.
[3] Helisch A, Wagner S, Khan N, Drinane M, Wolfram S, Heil M, et al. Impact of mouse strain differences in innate hindlimb collateral vasculature. Arterioscler Thromb Vasc Biol. 2006;26:520-6.
[4] Greenberg JI, Suliman A, Barillas S, Angle N. Mouse Models of Ischemic Angiogenesis and Ischemia-Reperfusion Injury. Methods in Enzymology. 2008;444:159-74.
[5] Lotfi S, Patel AS, Mattock K, Egginton S, Smith A, Modarai B. Towards a more relevant hind limb model of muscle ischaemia. Atherosclerosis. 2013;227:1-8.
[6] Brenes RA, Jadlowiec CC, Bear M, Hashim P, Protack CD, Li X, et al. Toward a mouse model of hind limb ischemia to test therapeutic angiogenesis. Journal of vascular surgery. 2012;56:1669-79; discussion 79.
[7] Limbourg A, Korff T, Napp LC, Schaper W, Drexler H, Limbourg FP. Evaluation of postnatal arteriogenesis and angiogenesis in a mouse model of hind-limb ischemia. Nature protocols. 2009;4:1737-46.
[8] Madeddu P, Emanueli C, Spillmann F, Meloni M, Bouby N, Richer C, et al. Murine models of myocardial and limb ischemia: diagnostic end-points and relevance to clinical problems. Vascular pharmacology. 2006;45:281-301.
[9] Stabile E, Burnett MS, Watkins C, Kinnaird T, Bachis A, la Sala A, et al. Impaired arteriogenic response to acute hindlimb ischemia in CD4-knockout mice. Circulation. 2003;108:205-10.